Biomedical Engineering Master Thesis

Faculty of Sciences and Technology - University of Coimbra

Development and characterization of chitosan and *N*-carboxybutylchitosan based materials doped with biocompatible ionic liquids for application as stimuli-responsive biopolymers

Supervisor: Hermínio José Cipriano de Sousa, PhD

Co-Supervisor: Ana Maria Antunes Dias, PhD

Student: Ana Alexandra Rebelo Cortez

If I saw further than other men, it was
because I stood on the shoulders of giants.

Sir Isaac Newton

Agradecimentos

A realização deste trabalho nunca teria sido possível se há cinco anos atrás eu não tivesse chorado por ter "sido colocada na Universidade em Coimbra". Não teria sido possível se eu não tivesse conhecido pessoas magníficas nesta cidade dos estudantes, as quais tiveram um papel importantíssimo no sucesso da minha vida académica e motivação, e a quem aqui quero agradecer.

Aos meus avós, pais e irmão, por todo o apoio incondicional e motivação que me deram nesta fase tão importante da minha vida e por terem sempre acreditado em mim. Não posso nunca esquecer o gosto especial pela Engenharia e pelos materiais poliméricos incutido pelo meu pai e irmão.

Aos meus amigos "de sempre" que apesar da distância física, sempre estiveram comigo em todos os momentos. Um carinhoso obrigada à Ana Carina Sá, Catarina Neves, Ana Isabel Araújo e Rita Silva.

Aos meus amigos "de faculdade" por todos os bons momentos que passámos juntos fruto das mais diversas situações, todas elas igualmente produtivas, com ou sem "farra". Um especial obrigada aos meus dois grandes companheiros Leonel Gomes e André Sousa, João Baptista, Ana Margarida Matos, Ana Margarida Martins, Susete Neiva, Marco Costa, Ana Patrícia Silva, Miguel Amaral e "marrõezinhos".

Às maravilhosas pessoas que conheci no DEQ que me ajudaram a adaptar, a crescer e me ensinaram a acreditar mais em mim. Não posso deixar de agradecer em particular ao Professor Doutor Hermínio Sousa por toda a dedicação, conselhos e conhecimentos para o desenvolvimento deste trabalho, à Doutora Ana Dias por toda a "mega" paciência, magnífica dedicação e especial motivação que me trouxeram até aqui e à Doutora Mara Braga por todas as dúvidas esclarecidas e conselhos. Gostava também de agradecer ao Professor Doutor Christopher Brett e à Doutora Madalina Barsan por toda a colaboração neste trabalho. Um especial obrigada à Sofia Marceneiro, Maria de Matos, Rita Chim, Luísa Filipe e Nicolas Gañán pela amizade, ajuda e todos os momentos "awesome" e "de sonho" disfrutados no B18.

A todos aqueles que mesmo não estando aqui referenciados, sabem que tiveram um papel igualmente importante para que eu pudesse concluir com sucesso uma das etapas mais importantes da minha vida, muito obrigada!

Abstract

The emerging need for improved life quality has led industry and academic community to develop new, environmentally and low cost materials for biomedical purposes. This work aims to develop and characterize new stimuli-responsive polyelectrolyte based electroactive polymers (EAPs), by combining the advantageous properties of biopolymers and ammonium based ionic liquids (ILs) in order to obtain EAPs with improved chemical, physical, thermo-mechanical and conductive properties. Chitosan (CS), a cationic polyelectrolyte and its derivative, *N*-carboxybutylchitosan (CBC), an ampholyte, were combined with different amounts (25, 50 and 75% in terms of molar fraction) of two biocompatible ILs (choline chloride ([Ch][Cl]) and choline dihydrogen phosphate ([Ch][DHP])) in order to study their effect on hydrophilic, swelling, thermo-mechanical and impedance properties of the polymer matrices. CBC was synthesized by alkylation of CS according to a method previously described in the literature. Ionic liquid loaded and non-loaded CS and CBC films were obtained by film casting and further characterized by FTIR-ATR, SEM, thermal properties (using thermogravimetric analysis (TGA) and differential scanning calorimetry (DSC)), mechanical properties, water contact angles, water vapor sorption (WVS), water vapor permeability (WVP), water swelling (at different pH) and impedance spectroscopy. The potential of these films to be used as tunable drug delivery systems, was studied by incorporating a charged model drug, sodium phosphate dexamethasone (DXMTNa) into non-loaded and IL ([Ch][Cl] or [Ch][DHP]) loaded CS and CBC films. The kinetic release profiles were studied at pH 7 and pH 10 and at 37 ºC and aimed to evaluate if the presence of the ILs could actuate as an extra parameter (besides pH) to tune the delivery of charged drugs from polyelectrolyte matrices. The results showed that ILs induce different hydrophilicities to both CS and CBC films depending on the IL type and added amount. This has a direct impact on the films WVS capacities and consequently on their WVP and thermo-mechanical properties. These additives rearrange the polymer network, trough hydrogen bonding and electrostatic interactions and lead to higher water absorption capacities which induce plasticization of the films and a clear decrease in the film's stiffness (IL-loaded films are more elastic presenting lower Young Modulus (*E*)). IL-loaded also films presented lower impedance which means that the diffusion of

charged species within the film is promoted when ILs are added to these polyelectrolytes. This effect was more significant for CS based films loaded with [Ch][DHP]. Water swelling measurements in different buffer solutions showed that the film's water swelling capacity is highly dependent on the pH and composition of the buffers. An increase in the IL loaded amount lead to a decrease in the osmotic pressure between the polymer network and the medium and consequently to a decrease in the swelling capacity of the films. The kinetic release profiles of DXMTNa showed different behaviors according to the pH of the release medium with an important effect of the ILs in some specific conditions. Finally physical mixtures of CS and CBCn were also prepared in order to obtain films more resistant to dissolution at neutral pH and they seem to be an alternative to burst release profiles observed at basic pH for CBC. Despite some drawbacks that are discussed along this work the overall results showed that these films have good potential to be used for biomedical purposes as pH-controlled drug delivery systems and actuators due to their pH- and electrical-responsive behavior.

Resumo

A emergente necessidade de melhorar a qualidade de vida do ser humano tem levado a indústria e a comunidade académica a desenvolver novos materiais ecológicos e de baixo custo para fins biomédicos. Este trabalho visa desenvolver e caracterizar novos polieletrólitos de estimulo-resposta baseados em polímeros eletroativos (EAPs), através da combinação de biopolímeros e líquidos iónicos derivados de amónio, com vista a obter EAPs com melhores propriedades químicas, físicas, termo-mecânicas e condutoras. O Quitosano (CS), um polieletrólito catiónico, e o seu derivado, *N*-carboxibutilquitosano (CBC), foram combinados com diferentes quantidades (25, 50 e 75% em termos de fração molar) de dois líquidos iónicos biocompatíveis (cloreto de colina [Ch][Cl] e di-hidrogénio fosfato de colina [Ch][DHP]) com o objetivo de estudar o seu efeito na capacidade de absorção de água e propriedades termo-mecânicas e de impedância das matrizes poliméricas. O derivado foi sintetizado através da alquilação do CS de acordo com um método descrito anteriormente na literatura. Os filmes de CS e CBC com e sem líquido iónico foram obtidos por evaporação de solvente e de seguida caracterizados por FTIR-ATR, microscopia eletrónica de varrimento (SEM), propriedades mecânicas (usando análise termogravimétrica (TGA) e calorimetria diferencial de varrimento (DSC)), propriedades mecânicas, ângulos de contacto, sorção de vapor de água (WVS), permeabilidade ao vapor de água (WVP), absorção de água a diferentes pHs e espectroscopia de impedância. O potencial destes filmes para sistemas de libertação de fármaco foi estudado, adicionando um fármaco-modelo, a dexametasona sódica (DXMTNa), aos filmes de CS e CBC com e sem líquido iónico. Os perfis de libertação foram estudados a pH 7 e 10 e a 37 ºC com o objetivo de avaliar se a presença do líquido iónico poderia atuar como um parâmetro extra, para além do pH, de modo a ajustar a libertação de fármacos carregados a partir de polieletrólitos.

Os resultados demonstraram que os dois líquidos iónicos induzem hidrofilicidades diferentes aos filmes de CS e CBC consoante a quantidade adicionada. Isto leva a um impacto direto na capacidade de sorção de vapor de água dos filmes e consequentemente na sua WVP e propriedades termo-mecânicas. Estes aditivos provocaram o rearranjo das redes poliméricas, através de pontes de hidrogénio e interações eletrostáticas, levando a maiores capacidades de absorção

responsáveis pela plasticização dos filmes e consequente diminuição da sua rigidez (filmes com líquido iónico são mais elásticos e portanto apresentam menor Módulo de Elasticidade (*E*)). Os filmes contendo líquido iónico apresentam valores mais baixos de impedância o que significa que a difusão das espécies carregadas no interior dos filmes é facilitada quando estes aditivos estão presentes nos polieletrólitos. Este efeito foi mais significativo nos filmes de CS contendo [Ch][DHP].

As medidas da capacidade de absorção de água em diferentes tampões salinos demonstraram que esta propriedade é altamente dependente do valor de pH e da composição das soluções tampão. O aumento da quantidade de líquido iónico leva à diminuição da pressão osmótica entre o interior do filme e o meio levando, consequentemente, à diminuição da capacidade de absorção de água. Os perfis das cinéticas de libertação da DXMTNa mostram que existem diferentes comportamentos, que estão de acordo com o pH do meio de libertação e onde a presença do líquido iónico é importante em algumas condições específicas. Após a adição de CBC a CS, com o intuito de obter um complexo de polieletrólitos (PEC), foram obtidos filmes compósitos de CS e CBC (CS/CBC). Estes filmes foram estudados como uma alternativa ao *burst* verificado em algumas curvas de libertação dos filmes de CBC em pH básico. Apesar de algumas desvantagens que são discutidas ao longo deste trabalho, no geral os resultados demonstram que estes filmes têm potencial em aplicações biomédicas, como sistemas de libertação controlada dependentes do pH ou como atuadores devido ao seu comportamento sensível ao pH e ao campo elétrico.

Table of Contents

Figure Index

Table Index

List of Abbreviations

[Ch][Cl]	choline cloride
[Ch][DHP]	choline dihydrogen phosphate
CBC	*N*-carboxybutylchitosan
CBCa	acidic *N*-carboxybutylchitosan
CS	chitosan
DD	degree of deacetylation
DS	degree of substitution
DSC	differential scanning calorimetry
DSSC	dye sensitive solar cells
DXMT	dexamethasone
DXMTNa	sodium phosphate dexamethasone
EAP	electroactive polymer
EB	elongation at break
ECM	extracellular matrix
EIS	electrochemical impedance spectra
EMIM-BF_4	1-ethyl-3-methylimidazolium tetrafluoroborate
EMImSCN	1-ethyl-3-methylimidazolium thiocyanate
EMI-Tf	1-ethyl-3-methylimidazoliumtrifluomethanesulfonate
FDA	food and drug administration
FTIR	fourier transformed infrared spectroscopy
H-NMR	proton nuclear magnetic resonance
IL	ionic liquid
LbL	layer-by-layer
LCST	lower critical solution temperature
MPC	5-methylpyrrolidinone chitosan
MW	molecular weight
MWCO	molecular weight cut off
Na_2CO_3	sodium bicarbonate
$Na_2HPO_4x2H_2O$	disodium hydrogen phosphate dihydrate
NaCl	sodium chloride
$NaH_2PO_4x2H_2O$	sodium dihydrogen phosphate dihydrate
$NaHCO_3$	sodium bicarbonate

NaOH	sodium hydroxide
PAA	poly(acrylic acid)
PDLLA	poly(D, L-lactic acid)
PEC	polyelectrolyte complex
PEG	poly(ethylene glycol)
pH*	critical pH
pKa	dissociation constant ratio
PMAA	poly(methacrylic acid)
PNIPAAM	poly(*N*-isopropylacrylamide)
PPy	polypyrrole
PVP	poly(vinylpyrrolidone)
RH	relative humidity
RTIL	room temperature ionic liquid
SEM	scanning electron microscopy
Tdeg	degradation temperature
Tg	glass transition temperature
TGA	thermogravimetric analysis
UCST	upper critical solution temperature
WVP	water vapor permeability
WVS	water vapor sorption
WVTR	water vapor transmission rate

Introduction

In recent years biomedicine has become a field of special interest both for academy and industry aiming to provide better health conditions for general population and to decrease health care costs. The possibility to develop new biomedical devices has lead to a new generation of principles based on diagnostic and treatment facilities (Reis et al, 2007; Holzapfel et al, 2012). Ideally these devices must be simple, non-invasive, easy to perform and at low costs, with rapid responses and safe, so that any person can benefit, even in the absence of a doctor or other health technician. In this way, human and material resources can be spared and monetized, and more attention can be given to critical illness cases. Therefore, besides financial purposes, biomedical devices help to improve patient's life quality through the development of non- or less- invasive and accurate diagnostic, treatment and monitoring techniques. Nowadays biomedicine considers the use of materials in contact with biological matter, including cells, tissues/organs, physiological fluids and biomolecules. Thus there is a clear need of synergistically and interdisciplinary scientific approaches that combine the most recent advances in material sciences and technology with biocompatibility and biofunctionality requirements/issues (Reis et al, 2007).

Biocompatible materials are attracting attention worldwide because of their desirable properties and potential applications in biomedicine, biocatalysis and bioelectronics. They are environmentally benign materials, composed of natural biomolecules and thus present low toxicity, good biocompatibility and, in some cases, they are biodegradable (Lu et al, 2006). Biomaterials can be defined as natural or synthetic materials intended to interact with biological systems to treat, evaluate, replace or mimic any function, tissue or organ of the body (Holzapfel el al, 2012). According to the Clemson University Advisory Board for Biomaterials the term biomaterial stands for *a systemically and pharmacologically inert substance designed for implantation within or incorporation with living cells* (Park and Bronzino, 2003). These materials are generally further classified as biopolymers, bioceramics, biometallics, composite biomaterials and nanomaterials, according to its physico-chemical composition and properties.

The first generation of biomaterials was developed during the sixties and included materials such as artificial joints, dental implants or ocular lenses. The goal of these early developed biomaterials was the appropriate combination of chemical and physical properties to mimic the injured/replaced tissue with minimal foreign body response from the host, which is still a valid paradigm nowadays. However, in the case of permanent implants, resistance to abrasion, durability, fatigue strength, permeability and stability against small molecules may be also critical leading to an increased interest in materials presenting tunable degradation rates and even resorption properties. Over the last years, advances on cellular and molecular sciences provided great developments on the third-generation biomaterials, characterized by their biocompatibility and biodegradability. This knowledge significantly affected biomaterials synthesis processes, their use and design, leading to the emerging fourth generation of biomaterials, the so-called "smart" biomaterials (Holzapfel el al, 2012) also known as 'stimuli-responsive', 'stimuli-sensitive', 'intelligent' or 'environmentally sensitive polymers'. These materials are defined as polymers that undergo large and abrupt, physical and/or chemical modifications in response to small changes in local environmental (Tokarev et al, 2009).

The basic components of living organic systems are biopolymers such as polysaccharides, proteins or nucleic acids (Gil and Hudson, 2004). These polymers react to different stimulus in order to maintain their structure and/or functionality. Cell membranes, more precisely their extracellular matrix (ECM), are a natural example of intelligent barriers that present unique stimuli responsive properties which include accommodation and selectivity of molecules, interactions with the external environment and signaling, among the most important (Tokarev et al, 2009; Holzapfel el al, 2012). The above mentioned fourth generation of biomaterials are a new active research trend that intends to develop synthetic or modified biological materials that mimic the behavior of body own biopolymers in order to substitute or complement their action. The obtained materials are able to mimic the high selectivity and capacity to adapt and respond, by significant driving forces, to a small change in the surrounding environment (Tokarev et al, 2009). According to Holzapfel et al, smart or biomimetic biomaterials represent the main challenge to the biomaterials community in the 21st century and interesting studies have already been done in order to develop multiple-stimuli responsiveness and drug delivery systems based on these biomaterials (Holzapfel et al, 2012). As an example, studies to attach dual

responsiveness to temperature and pH have recently been developed by combining thermo-sensitive polymers like Poly(*N*-isopropylacrylamide) (PNIPAAM) with natural pH-responsive polymers like alginate and chitosan (carrying ionic groups). Perez et al developed chitosan microspheres coated with the synthetic polymer in order to deliver two different drugs with selective sensitivity to pH and temperature, demonstrating dual-stimuli responsiveness of the composites (Perez et al, 2012).

Stimuli-Responsive Polymers

Stimuli-responsive polymers may be defined as polymers that present a large and abrupt response, which can be physical or chemical, when subject to small external changes in their environment (Gil and Hudson, 2004). Special attention has been given to macromolecular systems sensitive to changes in pH, temperature and electrolyte concentration, due to the fact that these systems can be controlled and applied *in vivo* (Roy et al, 2010). Smart materials may have the ability to present the most important characteristics of synthetic- and bio-polymers, such as mechanical and chemically stability, electrical, optical and magnetic properties, wetting, swelling and adhesion (Tokarev et al, 2009).

The biggest challenge when developing these materials consists in obtaining materials with reversible properties meaning that the responsive material should be able to recover its original properties/characteristics after the external stimulus is stopped or disappear and should actuate if stimulus if trigged again. To make that happen it is crucial to understand how the responsiveness takes place. The first step of this process consists in a high selectivity mechanism for signal/stimulus recognition in order to initiate specific conformational transitions at molecular level. Then, it is necessary to amplify the conformation change or signal, to enable the transduction and signal measurement (Tokarev et al, 2009; Wandera et al, 2010).

These materials have clear opportunities in different biomedical applications such as controlled drug delivery systems, artificial muscles and organs, smart matrices for tissue engineering, biosensors, diagnostic systems, actuators, coatings capable of interacting and responding, microelectrochemical systems and many others (Gil and Hudson, 2004; Roy et al, 2010; Stuart et al, 2010). Through a controlled design it is possible to potentiate the response of the polymer by changing polymer's

conformation, solubility, degradability, biocompatibility, self assembly behavior as well as its physical properties such as wettability, permeability and adhesive, adsorptive, mechanical and optical characteristics, depending on the desired application (Roy et al, 2010; Stuart et al, 2010).

Stimuli-responsive polymers have been applied in different forms that include: permanently cross-linked hydrogels, reversible hydrogels, micelles, modified interfaces and 2D and 3D films (Stuart et al, 2010). An interesting kind of stimuli-responsive thin film consists in layer-by-layer complexes of polyelectrolytes, comprising deposited layers of oppositely charged polymers that permit to obtain structures that are sensitive to salt concentration and pH changes (Tokarev et al, 2009). Most common stimulus include changes in temperature, pH, ionic strength, light, biological, electrical charge, magnetic field and ultra sounds (Roy et al, 2010; Peres et al, 2012), being the first two the most studied by far. Despite of the efforts done so far to improve actual applications, the main challenge still remains the development of stable systems with capacity to respond to two or more of the above referred stimuli simultaneously, as already referred (Tokarev et al, 2009; Stuart et al, 2010; Perez et al., 2012).

Temperature-responsive polymers

Temperature is the most common stimulus used in environmentally responsive polymers or systems (Gil and Hudson, 2004). These temperature-sensitive polymers present reversible transition between different physical forms (expanded or collapsed) in response to changes in temperature (Felber et al, 2011). This change is not driven by a typical swelling behavior but mostly by intermolecular and intramolecular interactions. The most common characteristic of these materials is the presence of hydrophobic side groups (mostly propyl, ethyl and methyl groups) and its ability for controlled drug delivery systems based on temperature (Schwartz, 2008). The temperature-sensitivity, conferred by those groups, is usually due to the crossing of a transition temperature in the polymer that may be the glass transition temperature or the melting point of crystalline segments (Crespy et al, 2007). PNIPAAM is the most known thermo-responsive polymer presenting a lower critical solution temperature (LCST) in the physiological range, near 32°C, which is ideal for biomedical

applications. Moreover, this thermo-responsive polymer and its derivatives are easily prepared and homogeneous (Crespy et al, 2007, Gil and Hudson, 2004).

Thus, one of the main properties of temperature-responsive polymers is its critical solution temperature. This parameter represents the temperature at which phase separation of solution-polymer or polymer-polymer mixtures is observed (depending on mixture's composition) (Gil et al, 2004). Polymer solutions that present just one phase below this specific temperature, and that are insoluble above it, have a LCST. Beyond this temperature the polymer becomes insoluble in water. Such behavior is typical for the polymers that form hydrogen bonds to water (Dormidontova, 2002). In the opposite situation, when phase separation occurs below a specific temperature, polymer solutions present an upper critical solution temperature (UCST). For temperatures lower than LCST, polymer-polymer interactions are weaker than polymer-solvent interactions while above LCST polymer-polymer interactions prevail and thus polymeric structures collapse leading to phase separation due to volume phase transition caused by the coil-to-globule transitions (Dautzenberg et al, 2000). According to the literature, the LCST of a specific polymer can be modified for a particular application by changing the polymeric chain hydrophobic and/or hydrophilic co-monomer content (Gil and Hudson, 2004; Schwartz, 2008; Shakya et al, 2010; Heras et al, 2005).

Besides polymer-solvent interactions, intermolecular interactions (mainly hydrogen bonding and hydrophobic interactions) may also lead to hydrogel shrinkage, micelle aggregation or the physical cross-links and therefore those interactions also play an important role on the response due an external stimulus and they should be considered when *designing* a thermal-responsive material (Gil and Hudson, 2004).

pH-responsive polymers

Polymers with capacity to react or respond to pH changes present either basic or acidic functional groups. Thus, they can be defined as polyelectrolytes that can accept and/or release protons (H^+ ions), due to pH changes on the surrounding environment. The ability to donate or accept protons is possible because these polymers present ionizable structures, such as basic amino groups and carboxylic or sulfonic acids (Gil and Hudson, 2004; Carreira et al, 2010; Shakya et al, 2010; Heras et al, 2005).

Variations on pH and/or slight variation on the ionic strength of the solution lead to reversible phase transitions and solubility changes caused by the disturbance

of the hydrodynamic volume that results from the osmotic pressure generated to neutralize the network charges. In fact, the continuous ionization and deionization of acid and alkaline parts of the polymer structures are the main cause of variations in those electrostatic interactions.

It is observed that the ionization level of functional groups changes intensively for a pH value near pK_a, which is directly related to changes in polymer chains' solubility. pK_a is defined by the specific pH value at which the degree of ionization of the weakly ionizable groups present in the polymeric network is dramatically changed (Gil and Hudson, 2004). Thus, it may be possible change the pH at which the response occurs by including specific ionizable moieties with pKa matching the desired pH. Conformational changes usually take place at a critical pH (pH*) which are followed by phase transition. The pK_a is related to pH*, but conformal transition does not take place at the exact pK_a value. The transitions are controlled by a balance between hydrophobic interactions and electrostatic repulsions. In this way, the introduction of hydrophobic groups will increase the pH*, and consequently the pH value at which a conformational change (as swelling or deswelling) takes place, due to higher electrostatic interactions that require more ionizable groups (Gil and Hudson, 2004, Wandeta et al, 2004).

Typically pH-responsive polymers are classified as polyacids or polybases, considering the presence of weak acidic or basic groups in the polymer's backbone, respectively. Polyacids present a considerably number of carboxylic groups with pK_a around 5-6, and, in these conditions, they are considered as weak polyacids. Carboxylic groups accept protons at acidic pH and donate at higher pH. Therefore, at basic pH the number of electrostatic repulsions will increase and the polyacid will swell. The opposite happens at lower pH, when the pendant groups are protonated and non-ionized leading to hydrogen bond interactions that decreases the swelling capacity of the matrix. On the contrary, polybases usually present amine groups as pendant functional groups. Unlike polyacids, these groups accept protons under low pH and release under basic pH and therefore their swelling behavior will be opposite to that described for polyacids (Kost and Langer, 2001).

Several applications for pH-responsive polymers are mentioned in the literature, especially in the development of controlled drug delivery systems. These systems are able to bypass drug resistance and deliver sufficient amount of drugs into specific

body locations, preventing the toxicity of certain pharmaceuticals in specific organs (Schwartz, 2008).

Electro-responsive polymers

Electrically-responsive polymers are usually prepared from polyelectrolytes. They are pH-responsive and electro-responsive structures, since they contain high concentrations of ionizable groups (Murdan, 2003). Even if most of these responsive polymers are polyelectrolytes, it is possible to observe electric field sensitivity in some neutral polymers, by the addition of a charged component (Roy et al, 2010). Polypyrrole (PPy) and Nafion are well-known examples of neutral conducting polymers used in biomedical applications. The final form of PPy is a long conjugated backbone which has resonance structures that resemble the aromatic form being conductive only when it is oxidized. The charge associated to the oxidized state is usually delocalized over several PPy units and can form a radical cation that promotes conductivity (Saville, 2005). However, the high oxidation potential limits PPy-cells interactions (Guimard et al, 2007). Nowadays, Nafion® from DuPont is the most commonly used material for proton conducting membranes (Schwenzer et al, 2011). Nafion® is produced by the co-polymerization of unsaturated perfluoroalkyl sulfonyl fluoride with tetrafluoroethylene. Proton conduction occurs through the ionic channels formed by micro or nano phase separation between the hydrophilic proton exchange sites and the hydrophobic regions, and is highly dependent on water content of the membrane (Sahu et al, 2009).

When an electric field is applied to electric-sensitive materials it might cause changes on the polymer ionization state, hydration, swelling or deswelling and permeability leading to actuation of the material (Kost and Langer, 2001). The magnitude of the response is related to the intensity of the stimulus. Many advantages are associated with the use of electrical sensitive polymers, being the most important the tunable versatility of the response that can be done by controlling the magnitude of the applied current, if it is continuous or pulsatile and, in the last case, by controlling the duration of the electric pulses and the intervals time between them (Murdan, 2003).

The response of electric-responsive materials has become an interesting field of study. The most common experimental set-ups consider the polymer in contact and fixed to one or two electrodes, or placed in an electro-conducting medium. When an

electric field is applied to an electric-sensitive polymer, normally hydrogels, it promotes swelling/deswelling (shrinkage) or erosion of the material (Murdan, 2003). An anisotropic swelling or deswelling on polyelectrolyte gels happens when the gel is fixed to one of the electrodes: protons migrate to the cathode and anions move to the anode, and a unixial stress along the structure is verified creating an anisotropic deformation (mechanical actuation) (Roy et al, 2010; Murdan, 2003). Other examples referred in the literature describe gel's deswelling when immersed in a conducting medium to which an electrical field is applied. Changes in local pH near the electrodes are detected due to electrolysis of water promoted by the electrical current: local pH value is lower at the anode and increases at the cathode since water suffers oxidation at the anode and reduction in the cathode. As a result, the charge density on the polymer chains, polymers water content and the repulsions between polymer chains are reduced and gel deswells at the anode (Murdan, 2003). Polymer swelling promoted by an electric field is a much rarer occurrence than deswelling, and thus, more difficult to explain. Electro-induced gel swelling is observed when the gel is placed at a fixed position without electrodes contact, unlike gel deswelling. As an example, a polymer gel prepared from a weak polyacid, immersed in aqueous medium, expand when two electrodes face each other at a fixed distance from the gel. To explain this behavior it was suggested that upon electrical stimulation, the cations (mobile ions) in aqueous medium migrate towards the cathode, penetrating the gel network. Their entrance induces ionization of acidic groups on the gel network and makes the gel to swell on the anode side as the ionized groups become hydrated. In the case of a gel prepared from a polybase, anions travel towards the anode and ionize specific groups on the gel (amino groups for example), which induces gel swelling at the cathode side (Murdan, 2003). The swelling behavior caused by electrical stimulation is therefore due to the increase in the electrostatic potential present on the macromolecules (Osada and Khokhlov, 2005). Erosion is another electro-induced phenomenon that is common in polyelectolyte gels that experience disintegration due to the erosion of the gel surface in contact with the electrode that composes the experimental setting (Murdan, 2003).

Due to this characteristics, electro-responsive materials find their most promising applications on the biomedical field as: i) drug delivery systems because their swelling/deswelling behavior, and consequently their drug release profiles can be tuned and ii) organ actuators, as artificial muscles, since they have the ability to

convert electrical information into mechanical actuation (Figure 1) (Kost and Langer, 2001; Murdan, 2003; Roy et al, 2010; Stuart et al, 2010; Li et al, 2011). Intelligent drug carriers would be useful to create new drug delivery systems with the ability of pulsatile and local release that mimic the natural release of many molecules such as insulin (for instance to treat *Diabetes Mellitus* using an electro-conducting patch applied in the skin), hormones and others. Besides that, some of these hydrogel based materials are biodegradable and may be injected into the body therefore being minimally invasive (Schwartz, 2008; Murdan, 2003).

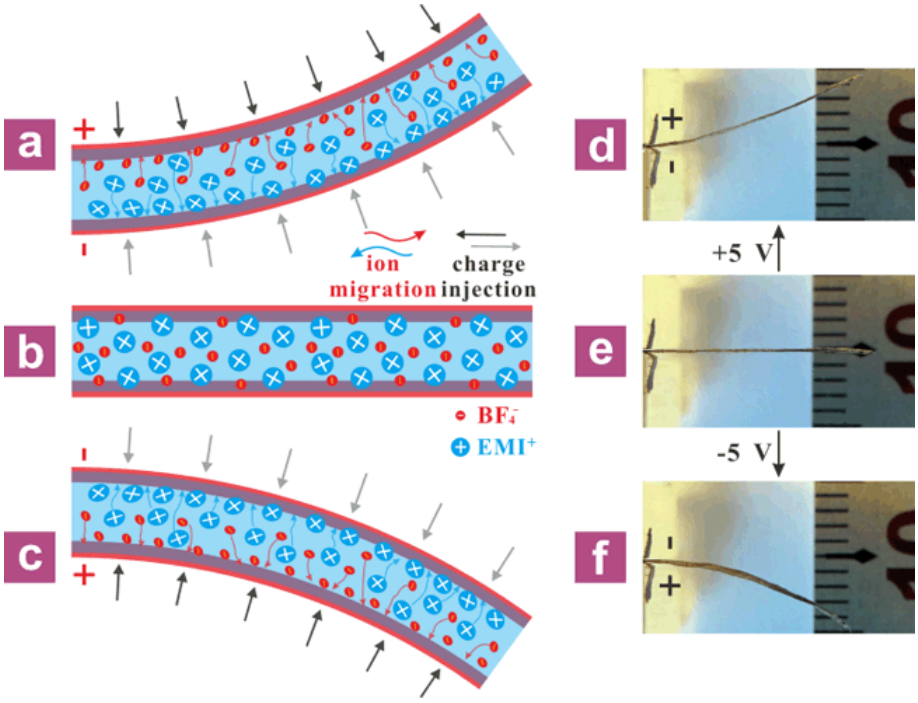

Figure 1. Electrochemical actuation mechanism of a double electrode layers separated by a chitosan electrolyte layer consisting of an 1-ethyl-3-methylimidazolium tetrafluoroborate (EMIM-BF_4) ionic liquid actuator: actuation illustration of the bimorph configures actuator under positive (a), negative (c) and no extra electrical field (b). The corresponding photographs of an actuator with a positive (d), negative (f) and no applied voltage (e) confirm the electrochemical actuation mechanism (Li et al, 2011).

Biopolyelectrolytes

In this work, biopolymers containing ionic groups are presented as potential smart materials in biomedical field. These materials can be divided into two groups namely polyelectrolytes and polyzwitterions according to the ionic nature of their characteristic groups: the first contain ionizable (anionic or cationic) groups while the

second contain both anionic and acidic groups. The polyzwitterions that present charged groups in different monomer units are named polyampholytes and these have the ability to behave both as polyelectrolyte and anti-polyelectrolyte depending on the composition of external medium (Martínez et al, 2012). Furthermore, polyampholytes as smart polymers can be able, or not, to respond to changes in pH depending on their anionic/cationic ratio. If both species are present in the same proportion, charges may be neutralized and thus, the polymer will be insensitive to pH changes. When a polyelectrolyte is in contact with polar solvents, those groups may dissociate, leaving charges on the polymer chains with simultaneous release of a counter ion to the solution. Their remarkable physico-chemical properties and electrostatic interactions between charges are the main difference between polyelectrolytes and uncharged common polymers (Dobrynin and Rubinstein, 2005). Many theoretical and experimental techniques try to explain the origin of the special behavior of highly charged polyelectrolytes characterized by "slow" domains or "loose" clusters in semi-diluted solutions. In general terms, this kind of attractive interactions between macro-ions contradicts the standard theory based on the overlap of electrical double layers between charged flat chains. The charge fluctuation forces between several polyanions may be due to: *i)* sharing of their counterions or *ii)* attraction by expansion of the condensed layers between charged surfaces (Radeva, 2001). Polyelectrolytes and polyzwitterions may occur synthetically or naturally and they present advantages in different fields due to their unique structures and properties that are different from other materials (Honarkar et al, 2009; Scraton et al, 1995). Examples of common synthetic-based polyeletrolytes include polymeric acids such as poly(methacrylic acid) (PMAA) or poly(acrylic acid) (PAA), while natural-based polyeletrolytes include proteins, nucleic acids and polysaccharides such as chitosan, carrageenan, pectin, etc (Scraton et al, 1995).

Polysaccharides are widely distributed in nature and the most naturally occurring are cellulose, chitin, dextran, pectin, agar, agarose and carragenans (Kumar, 2000). After cellulose, produced in plants, chitin is the most important biomass resource that can be obtained by different living organisms. It naturally occurs as ordered crystalline microfibrils structures in the exoskeleton and internal holders of arthropods or in the cell walls of fungi yeasts, acting as reinforcement material (Duttar et al, 2004; Jayakumar et al, 2010). Chitin is a hard, inelastic and white polysaccharide of *N*-acetyl-D-glucosamine (2-acetylamino-2-deoxy-D-glucose) units

linked by β-(1-4) glycosidic bonds that is highly hydrophobic and consequently insoluble in water and most organic solvents. It is usually extracted from crustaceans by acid treatment to promote the dissolution of calcium carbonate, followed by an alkaline extraction to solubilize proteins. Finally, there is a decolorization step in order to remove pigments and obtain a non colored product (Honarkar et al, 2009; Kumar, 2000; Duttar et al, 2004). The interest in the use of chitin is not only because it is an under-utilized resource and therefore cheaper and readily available, but also because it can be applied as a new functional biomaterial (Duttar et al, 2004).

The most important derivative of chitin is chitosan which can be obtained through partial deacetylation of chitin (between 50 to 85%) under alkaline conditions (NaOH) or by enzymatic hydrolysis in the presence of chitin deacetylase as shown in Figure 2 (Jayakumar et al, 2010; Arora et al, 2011). Since chitin presents semi crystalline morphology, chitosan obtained by solid-sate reaction has a heterogeneous distribution of acetyl-groups along its chains (Jayakumar et al, 2010).

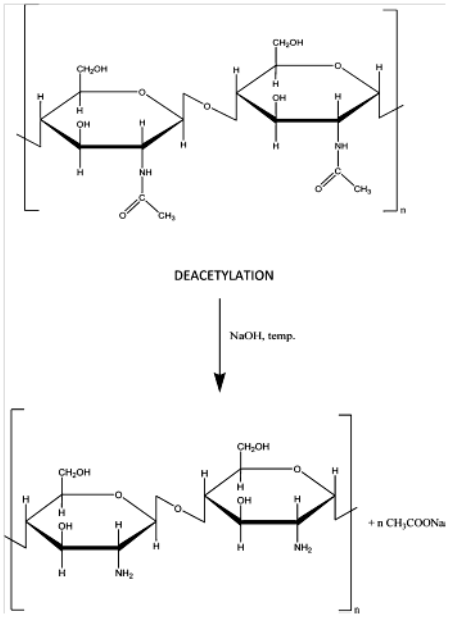

Figure 2. Scheme of the deacetylation process that converts chitin (top) into chitosan (bottom) (Sionkowska et al, 2011).

Chitosan is a linear copolymer of β(1→4)-linked 2-acetomido-2-deoxy-β-D-glucopyranose and 2-amino-2-deoxy-β-D-glucopyranose, available in different grades depending upon the degree of acetylated moieties. The conditions used for the deacetylation define the molecular weight (MW) and the degree of deacetylation

(DD) of the polymer and both parameters are known to significantly influence the chemical and biological properties of the polymer, as well as some of its specific structural changes (Mash et al., 2011).

This biopolymer is insoluble at high pH values, but it becomes a polyelectrolyte that is water-soluble at acidic media after protonation of the amino groups (NH_2 to NH_3^+) in the C-2 position of the D-glucosamine repeating unit. This leads chitosan to be more soluble than chitin, and thus more suitable for useful biomedical applications (Mash et al, 2011). In fact, there are relatively few solvents for chitin, but chitosan dissolves in aqueous acidic media of acetic and formic acids. Due to the protonation of amino groups, the multiple sites formed by acids along the chitosan's chain increase the solubility of the biopolymer by increasing both the degree of electrostatic repulsion and the polarity of the chains (Mourya et al, 2008). Therefore, chitosan is readily soluble in diluted acidic environments below pH 6.0, but above that value, chitosan amines become deprotonated and the polymeric structure loses its charge and becomes insoluble. The transition between soluble-insoluble states occurs at its pKa value around pH values between 6.0 and 6.5. On the vicinity of pKa values, chitosan charges are substantially altered and consequently the polymer's properties. Furthermore, it may be possible the attachment of other reactive groups at mild reaction conditions. Since pKa directly depends on DD, the solubility of chitosan is highly affected by DD and molecular weight as previously mentioned (Mash et al, 2011).

Both chitosan and chitin present amino and hydroxyl groups but the first can show crystallinity and polymorphism depending on chitin's origin, on the treatment during the extraction process and on the deacetylation process. Crystallinity is maximum for chitin (0% deacetylated chitosan) and polymorphism increases with DD. Thus, chitosan is less crystalline and more accessible to reagents **(**Mash et al, 2011; Mourya et al, 2008). Other properties that vary depending on DD are the polymer chain stiffness and thermal stability. The first decrease when DD increases, due to local intra-chain hydrogen bonding (Rinaudo, 2006), while chitosan decomposition is an exothermic process and the activation energy values are highly dependent on DD. After heating, chitosan decomposes before melting, and thus it has no melting point (Arora et al, 2011; Mourya et al, 2008). Depending on deacelylation conditions, the viscosity of chitosan is affected by changing the inter- and intra-molecular repulsion forces. The viscosity of chitosan increases with concentration and

decreases with temperature and DD. According to the literature, viscosity has great influence in chitosan biological properties as wound-healing capacity and biodegradation (Mash et al, 2011). Biodegradation plays the most important role in the metabolic fate of chitosan, and other biopolymers, in the body mainly if drug delivery systems and scaffolds for tissue engineering are envisaged. Chitosan degradation kinetic is highly affected by DD, cristallinity, MW and acetyl groups' distribution. Biodegradation increases as DD, cristallinity, MW and homogenous distribution of those side specimens decrease (Mash et al, 2011). The degradation in physiological environment may be chemical (acid catalyze in the stomach) or enzymatic (degradation of glucoseamine linkages in chitosan's structure by lysozymes and specific enzymes present in the colon) and must guarantee that degradation fragments suitable for renal excretion are obtained (Kean, 2009). Fast degradation rates of chitosan may be undesirable since it may cause accumulation of amino saccharides that can promote an inflammatory response. Higher DD leads to a lower chitosan degradation ratio, and thus, to minimal inflammatory response (Mash et al, 2011). Besides biodegradability, other important biological characteristics of chitosan, that dependent on its physicochemical properties, and that justify the great interest in the use of this polymer include its biocompatibility, low or non-toxicity, its ability to bind and aggregate cells, its regenerative effect on connective tissue, permeability and cell interaction capacity (for proliferation for different cell types) and hemostatic, antitumor, fungistatic, analgesic, hypochlolesterolemic, antimicrobial and antioxidant properties (Duttar et al, 2004; Mash et al, 2011).These properties make chitosan a biomaterial with excellent properties to be used for surgical sutures, for tissue engineering structures, as biomaterials for drug delivery systems (prepared in the form of films, foams, microspheres, microcapsules, etc) and as wound dressings for the treatment of wounds, ulcers and burns (Carreira et al, 2010).

Due to its abundant amino and hydroxyl active groups, chitosan can be easily modified. Many derivatives can be prepared by chemical and physical modification of the chitosan's structure, in order to obtain chitosan derivatives with enhanced properties. Recently, many techniques such as crosslinking, blending, irradiation γ-ray and grafting have been studied to modify chitosan (Dash et al, 2011; Carreira et al, 2010). Among all, chitosan alkylation is one of the most common grafting modification technique which has been used to prepare hydrophobic modification of chitosan with alkyl halides bearing different alkyl chain lengths for fast drug release

(Li et al, 2005). Liu et al. studied *N*-(aminoalkyl) chitosan microcapsules as carriers for gene delivery (Liu et al, 2003) and poly(D, L-lactic acid) (PDLLA) with improved biocompatibility was reported with *N*-(aminoalkyl) chitosan-modified PDLLA (Cai et al, 2002).

N-Carboxybutylchitosan (CBC) is another example of an amphoteric chitosan derivative that has as main advantage the fact that it may be soluble under basic, neutral and acidic conditions, unlike chitosan, that is only soluble at low pH, as discussed before (dos Santos et al, 2005). CBC is presented as a biodegradable and biocompatible natural-based polymer characterized by its highly hydrophilic networks. In this way, and besides its higher solubility in water, CBC also presents higher water vapor swelling capacity (Dias et al, 2010).

Structurally, the main difference between chitosan and CBC is the introduction of a butyl group that will replace part of the amino groups present in chitosan (Figure 3).

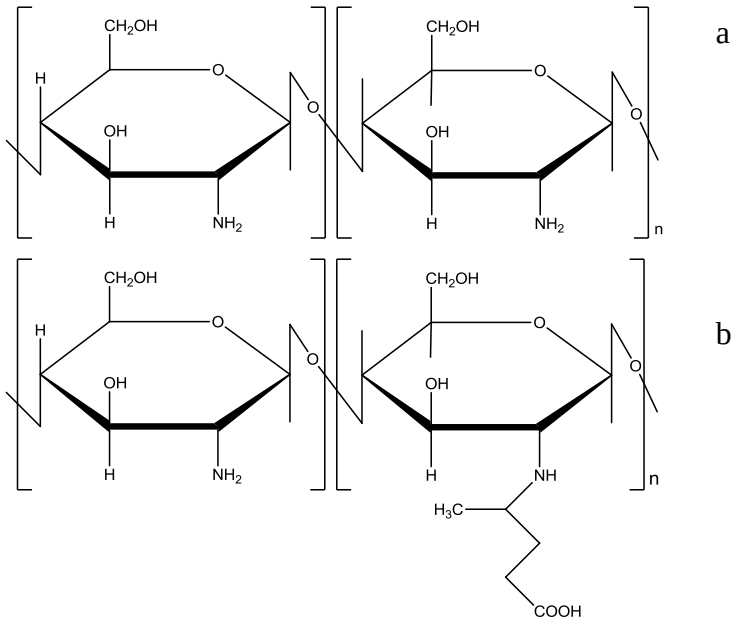

Figure 3. Esquematic representation of the chemical structures of chitosan (a) and *N*-carboxybutylchitosan (b).

N-Carboxybutylchitosan is obtained after reaction of chitosan with levulinic acid under reducing conditions. Levulinic acid or 4-oxo-pentanoic acid ($CH_3COCH_2CH_2COOH$) is obtained from fructose and is also a metabolic product of the human body (Muzzarelli et al, 1989). The reaction of chitosan in the presence of levulinc acid and reducing agent, commonly sodium borohydride, may results in the

formation of three main compounds, depending on mixing ratios and which are: *N*-carboxybutylchitosan (mono- or disubstituted forms) and/or 5-methyl-pyrrolidinone chitosan (MPC). Thereby, there is an optimum molar ratio for levulinic acid/chitosan/reducing agent to obtain the best substitution degree for CBC (dos Santos et al, 2004; Rinaudo et al, 2001). CBC may have some advantages when compared with other chitosan's derivatives or with chitosan itself. In fact, it presents prevailing cationic character due to a major proportion of free glucoseamine units, and lack of side reaction products due to mild synthesis chemical conditions (Riccotti et al, 1991). Moreover, CBC presents good gel- and film-forming properties, moisturizing effect, wound-healing capacity, bacteriostatic effects and bioadhesive properties enabling its use for several biomedical applications (Dias et al, 2010; Biagini et al, 1991; dos Santos et al, 2005).

Ionic Liquids

Ionic liquids (ILs) are generally defined as molten salts composed by organic/inorganic cations and/or anions and with a melting point below 100°C. When their melting point is below room temperature they are called "Room Temperature Ionic Liquids" (RTILs) (Marsh et al, 2004). The use of these specimens has received a lot of attention during the last few decades due to their negligible vapor pressure, wide liquid-phase range, low flammability, outstanding solvation ability, good thermal, chemical and electrochemical stability and high ionic conductivity (Mecerreyes, 2011; Jia et al, 2012; Petkovic et al, 2010). Commonly, ILs are composed of organic or inorganic anions and organic cations of low symmetry (Pernak and Chwala, 2003; Kirchner, 2009) with a number of possible cation/anion combinations estimated to be 10^{18} (Pernak and Chwala, 2003) (Figure 4).

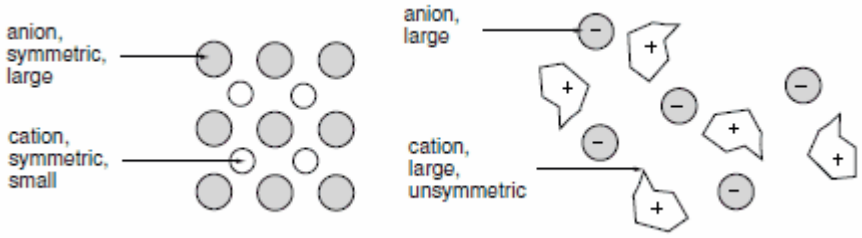

Figure 4. Symmetry differences between common salts and ionic liquids (Sigma-Aldrich).

The cationic centre typically presents a positively charged nitrogen or phosphorous and depending on its basis, ILs can be divided into six different groups: (a) five-membered heterocyclic cations, (b, c) six-membered and benzo-fused heterocyclic cations, (d) ammonium, phosphonium, sulphonium based cations, (e) functionalized imidazolium cations and (f) chiral cations (Marsh et al, 2004; Kirchner, 2009) (Figure 5).

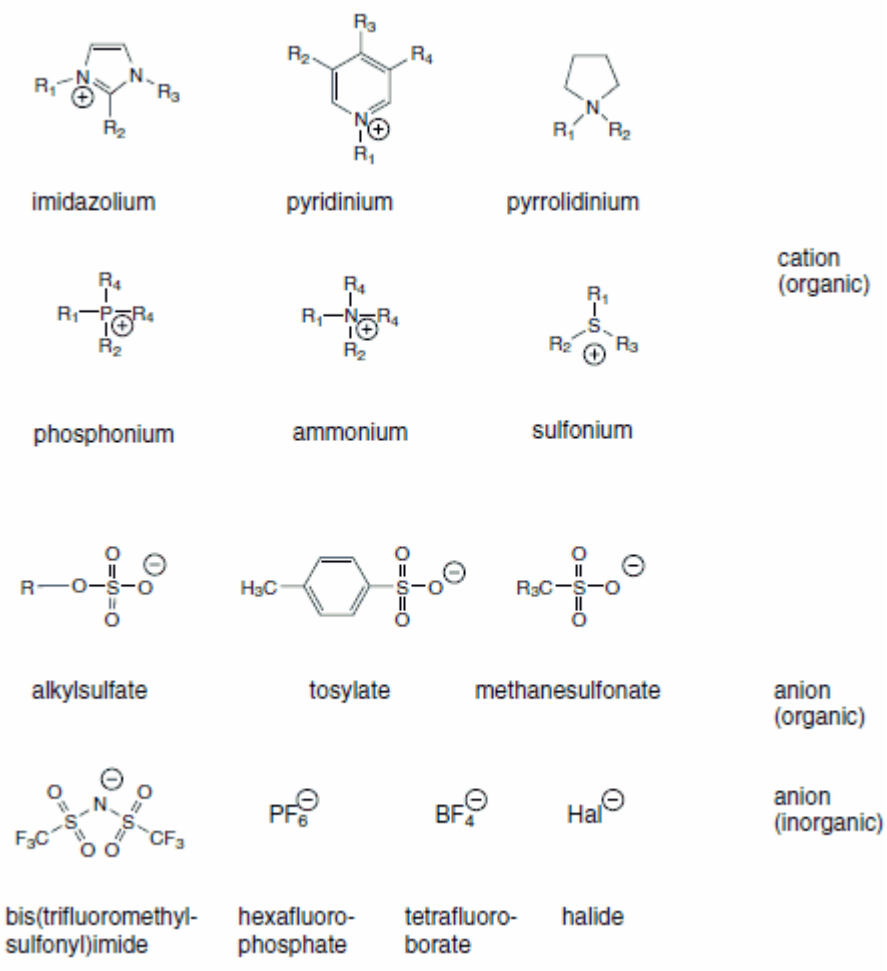

Figure 5. Examples of the most common ionic liquids (Sigma-Aldrich, 2004).

The physico-chemical properties of ILs or RTILs are determined by the nature, structure and interaction of the cation and anion that constitute the IL (Marsh et al, 2004). The charge distribution, hydrogen bonding, Van der Waals interactions and symmetry of the ions are presented as the main factors that largely influence the melting point of these salts. Furthermore, several reports have proved the influence of alkyl chain on their properties (Marsh et al, 2004). Most RTILs are denser than water with values between 1 and 1.6 g.cm^{-3}. Generally, this might be due to the increase of

the length of the alkyl chain, meaning that ILs present a major number of atoms per volume unit (Marsh et al, 2004). ILs may present a disadvantage due their relatively high viscosity which can negatively affect mass transfer and thus hamper the mixing in heterogeneous liquid systems. It has been reported that viscosity is mainly dependent on the type of cation and anion and it is higher compared to common organic solvents (Rooney et al, 2009). However, unlike density or melting temperature, the increase of length of alkyl chains on the cation does not result in a direct increase in viscosity (Marsh et al, 2004). Moreover, ILs are soluble with many polar substances and may dissolve organic and inorganic substances (Marsh et al, 2004) as well as natural polymers such as chitin, cellulose or starch (Armand et al, 2009; Izawa and Kadokawa, 2010; Prasad et al, 2010; Silva et al, 2011). The solubility of ILs is directly affected by the nature of the counter-anion (Mecerreyes, 2011). The nature of the side group may also influence IL's solubility according to its hydrophlicity and polarity (Liying, 2011). The interactions existing in conventional organic solvents, commonly hydrogen bonding, dipole-dipole and Van der Waals interactions do not enhance the solubility of polar substances as ILs do. Indeed, ILs present ionic interactions (electrostatic attraction or repulsion of charged particles) and hydrogen bonding is expected to exist between an oxygen or halide atom (F^-, Cl^-, Br^-, I^-) on the anion and the hydrogen atom of the cation (Marsh et al, 2004) and this may justify the observed higher solubility for complex molecules.

Due to this unique combination of properties, ILs present several advantages when compared to common solvents. Most materials are processed/synthesized by chemical processes that make use of volatile organic solvents. The emissions and disposal resulting from its usage are an important source of environmental pollution. In order to overcome this issue, ILs are being proposed as alternative *grenner* solvents, mainly because of their negligible vapor pressure (that decreases solvent evaporation) and their broad liquid range (up to more than 400K) and high density (compared to water).

Despite of the advantages of using Ils as non-volatile solvents, recent intensive research on the toxicity of these solvents has shown that they can be toxic than common organic solvents, specially the pyridinium and imidazolium based (Haerens et al, 2009). Here again toxicity has been related with the type of cations/anios that constitute the IL. It was reported that the head group of the cation has an important role on the toxicity of the IL and that longer side chains have a more severe impact on

living cells (Petkovic et al, 2010). However, the anion is responsible for some of the physico-chemical properties of these salts that can indirectly affect their toxicity. Therefore researchers have been working on the development on friendlier ILs that are less toxic and more biodegradable and that can even be applied to the development of biomedical based materials (Pernak et al, 2003; Armand et al, 2009). Some examples show that the anion toxicity is defined by its lipophilicity, as a consequence of the length of the linear chain and its branching. Chain branching is generally considered to increase resistance to aerobic biodegradation (Petkovic et al, 2010).

ILs are also well known in electrochemistry for their conductive properties and more recently they are being intensively studied to improve the conductivity of several materials, especially polymers (Kubisa, 2005; Armad et al, 2009; Prasad et al, 2009; Singh et al, 2010; Mecerreyes, 2011). The presence of a large cation is favourable to achieve highly conductive ionic liquids because the surface charge becomes weaker as the cation size increases and therefore a decrease in the interaction between cation and anion is observed (Egashira et al, 2005; Armand et al, 2009). As an exception, salts based on small quaternary ammonium cations are basically solid at room temperature and thus, an increase on cation size decreases its mobility. In these cases small cation size may improve ionic conductivity since it improves ions mobility (Egashira et al, 2005).

In the context of this work, especial focus will be given to ammonium-based ILs more particularly to cholines whose properties will be briefly detailed in what follows. Tetraalkylammonium salts are known since 1890 (Pernak and Chwala, 2003) and longer alkyl chains were required in order to obtain room temperature melting points of these specimens typically prepared by alkylation of the parent amine (Kirchner, 2009). Among all the IL types, this class is assumed to be one of the most promising for battery electrolytes due its wider electrochemical window, especially along cathodic direction (Egashira et al, 2005).

Choline based ILs

In general terms, the use of ILs in numerous applications aims for cost-efficiency and sustainability. The growing potentiality of these molten salts for biomedical purposes require the knowledge of their toxicity, biocompatibility and

their behaviour concerning biosorption, bioaccumulation and biodegradation pathways (Petkovic et al, 2010). Most studies with ILs refer to imidazolium-based salts, but pyridinium, phosphonium and quaternary ammonium salts are being investigated as well. Quaternary ammonium salts are a promising class of ILs for medical applications due to their very low (eco)-toxicity in aqueous solutions (Nockemann et al, 2007). When used in commercial preparations they may present several parallel functions such as surface activity, anti-microbial and anti-electrostatic activity (Pernak et al, 2003). Vijayaraghavan and co-authors synthesized and studied a number of novel ammonium salts based on the choline cation and several anions generally recognized as safe which included lactate, levulinate and tartarate. They concluded that these ILs have potential to replace glutaraldehyde (the most commonly used chemical crosslinker for collagen) in order to reduce the toxicity on collagen based biomaterials (Vijayaraghavan et al, 2010). Petkovic and co-authors studied the combination of choline with alkanoates with different elongated alkyl chains, in order to better understand the influence of the anion on the ILs toxicity against filamentous fungi. This study showed that choline alkanoates are environmentally benign, biodegradable and extraordinarily good solvents for plants biocomposites (Petkovic et al, 2009).

Choline may be found as a dietary compound in foods as free choline and other esterified forms such as phosphocoline, sphingomyeline and phosphatidylcholine. It works as a precursor for acetylcholine or phospholipids playing an important role on the structural integrity of cell membranes, nerve transmission, cellular signalling and lipid transport and metabolism (Pernak et al, 2007; OECD SIDS, 2004). Dietary choline is highly absorbed in intestine and it can be obtained from other nutritional sources as phosphatidilcholine, by enzymatic cleavage in pancreas. Fasting plasma choline concentrations are known to vary between 9 and 20 μmol/L and thus its presence is crucial for organism equilibrium (OECD SIDS, 2004).

Choline chloride [Ch][Cl] and choline dihydrogenphosphate [Ch][DHP] (Figure 6) are quaternary ammonium salts that despite being solid at room temperature they are considered as molten salts because they liquefy at high relative humidity or when mixed with a small amount of water (Egashira et al, 2005; Vijayaraghaven et al, 2010). The presence of a hydroxyl group on the cation provides an excellent hydrophilic character. Their use is being suggested for several applications mostly due to their biocompatibility. Choline is produced in large

quantities as a vitamin supplement (vitamin B complex) (Pernak et al, 2007) and thus is readily and easily available at relatively low cost and easy to prepare, water and air stable and thus suitable for large scale applications (Haerens et al, 2009; Jia et al, 2012). Furthermore, choline chloride is presented as being highly biocompatible, with low-toxicity, non-mutagenic and biodegradable (OECD SIDS, 2004), being therefore suitable for food, pharmaceutical and biomedical applications. Abbott and co-authors successfully showed that a mixture of an IL analogue based on [Ch][Cl] and urea acts both as reagent and solvent in the effective cationic functionalisation of cellulose to obtain new materials more hydropholic than cellulose (Abbott et al, 2006). Haerens and co-authors also referred this IL as an environmentally friendly compound to enhance metal deposition processes as it is easy to prepare and easily biodegradable when compared to other ILs (Haerens et al, 2009). More recently, Maugeri and de María presented deep eutectic solvents formed by the complexion of quaternary ammonium salts, including [Ch][Cl], with hydrogen bond donors such as amines or carboxylic acids in order to decrease the freezing point of the mixture. These deep eutectic solvents were reported as cheaper and biodegradable and can be applied in electrochemistry, electrodeposition and biocatalysis (Maugeri and de María, 2012).

Choline dihydrogenphosphate [Ch][DHP] is called a hydrated ionic liquid that has been reported as an excellent solvent for cytochrome and other proteins (Armand et al, 2009). Although the two cholines have the same cation, the hydrogen bonding between the cation and the anion is markedly different in each case as well as the possible interactions that those anions may establish with other solvents and/or matrices. Their different structures, shown in Figure 6, may induce different hydrophilicities (due to the presence of hydroxyl groups on the dihydrogenphosphate anion) and consequently differentiated behaviour in aqueous media. Moreover, dihydrogenphosphate can generate protons and thus it has been used to synthesize as a new class of proton-conducting materials (Yoshizawa-Fujita et al, 2007).

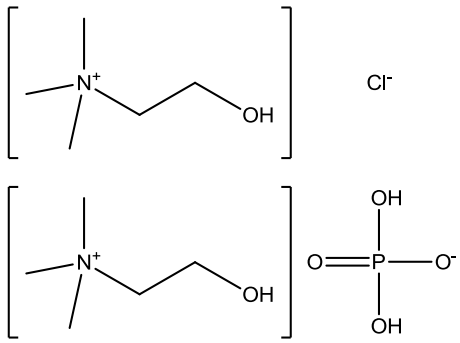

Figure 6. Choline chloride, [Ch][Cl] (above) and choline dihydrogenphosphate, [Ch][DHP] (below).

Polymers doped with Ionic Liquids

Ionic liquids have been conjugated with different polymer systems for the most diverse applications that include biopolymers dissolution, development of alternative renewable energy sources, fuel cell, battery, sensor, photovoltaic and medical applications since they fulfill requirements like relatively low cost and high efficiency (Prasad et al, 2009; Singh et al, 2010; Izawa and Kadokawa, 2010). Prasad and co-authors prepared a weak gel of chitin with 1-allyl-3-methylimidazolium bromide and proved the capacity of the IL to dissolve the chitin (Prasad et al, 2009). Other studies showed that the nature of the anion may influence the dissolution of cellulose and that hydrated ILs were excellent solvents for proteins (Armand et al, 2009). Singh and co-authors reported the development of a solid polymer electrolyte film of chitosan doped with a low viscosity IL (1-ethyl-3-methylimidazolium thiocyanate (EMImSCN)) to prepare dye sensitive solar cells (DSSC) for photovoltaic applications. The observed enhanced ionic conductivity was attributed to the presence of the IL with a maximum value of 2.60×10^{-4} S.cm^{-1} (Singh et al, 2010) which is still lower than the one previously reported for Nafion® equal to 0.16 S.cm^{-1} (Slade et al, 2002). Another important emerging area for ionic liquids is the development of electrochemical actuators, pioneered by Lu and co-authors, which showed that ILs could indeed provide a huge increase in the performance of these biomedical devices through the improvement of their operational life up to 10^6 cycles (Lu et al, 2002; Armand et al 2009).

Recently the mixing of stable, soluble, highly polar, highly conductive and non volatile ILs with polymer electrolytes (polyelectrolytes) lead to a remarkable improvement in their performance. In this way, a new generation of polyelectrolytes

may be obtained as flexible membranes or films with excellent mechanical and electrochemical properties (Kubisa, 2005). As an example, Shen and co-authors immobilized ILs into solid supports through various methods such as electrophoresis, layer-by-layer (LbL) assembly and casting and noticed that ILs could be linked to the polyelectrolyte surface (Shen et al, 2005). Another example of the addition of ILs to polyelectrolytes was presented by Lin co-authors that aimed to obtain short flexible side chains in Aquivion® to provide better mechanical coupling between the ions and membranes backbones and, thus, more efficient electrochemical transducers. Authors investigated the charge dynamics of 1-ethyl-3 methylimidazoliumtrifluomethanesulfonate (EMI-Tf) in Aquivion® membranes swelled with different uptakes of IL. The results obtained showed a more successful electromechanical performance of this electroactive polymer EAP membrane when compared with commercial Nafion® (Lin et al, 2011).

Despite the increasing interest in this research area and the increased number of publications related with IL loaded polymers, there is not much information concerning the interactions between ILs and biopolyelectrolytes and the influence of the external medium on their responsiveness. Moreover, most studies have been performed using imidazolium based ILs that present higher toxicity and may limit biomedical applications of the prepared materials. Therefore, the aim of this thesis is the preparation and characterization of biopolyelectrolyte films (chitosan which is a polycation and *N*-carboxybutylchitosan which is a polyzwitterion) loaded with biocompatible quaternary ammonium molten salts at different amounts that can be used as enhanced stimuli responsive materials to drug delivery systems and/or bioactuators. This work intends to better understand the influence of the ILs presence on the physico-chemical, mechanical and thermal behaviour of the IL loaded films as well as on its ionic conductivity and drug release properties when subjected to different external conditions.

Materials and Methods

Synthesis of non-loaded and loaded chitosan films

Chitosan 1% w/v (MW=145 000 g/mol, 73% deacetylated) (Sigma-Aldrich, Portugal) was dissolved in bi-distilled water containing 1% (v/v) glacial acetic acid (Panreac, Spain), and stirred over night. The pH of the mixture was adjusted to 3.5 using additional glacial acetic acid. 15 ml of chitosan solution was casted on polystyrene petri dishes and evaporated at 50°C for 2 days.

Chitosan films loaded with choline choline, [Ch][Cl], or choline dihydrogenphosphate, [Ch][DHP], (both from Io-li-tec, Germany) were obtained by adding three different amount of each ionic liquid (25, 50 and 75% in a molar basis) (further details are presented on Appendix A) to 15 ml chitosan solution and further mixed vigorously for approximately 12 hours. Each mixture was casted on polystyrene petri dishes at 50°C for 2 days.

For the drug release measurements, sodium phosphate dexamethasone (DXMTNa, MW=516.40 g/mol from Edol, Portugal) was chosen as a charged test model. The drug (5 mg per 15ml of polymer solution) was added to solutions of non-loaded and 75% IL ([Ch][Cl] or [Ch][DHP]) loaded CS and the solution was vigorously stirred for 24 hours at room temperature, away from light (to avoid DXMTNa degradation), and casted on polystyrene petri dishes at 50°C for 2 days. In the case of the IL loaded solution, the drug and the IL were added simultaneously to avoid preferential interaction with the positively charged groups of chitosan.

Synthesis of non-loaded and loaded carboxybutylchitosan films

The synthesis of carboxybutylchitosan was done following the methodology previously presented in the literature (dos Santos et al, 2005). 1 g of chitosan (MW=145 000 g/mol, 73% deacetylated) was dissolved in bi-distilled water in the presence of 0.932 ml of levulinic acid (98%) (Sigma-Aldrich, Portugal) and stirred vigorously for 12 hours at room temperature. The solution was then heated until 80°C using a thermal bath under reflux for 2 hours. After cooling, 0.06 g of sodium borohydride (Sigma-Aldrich, Portugal) was added as a redutor agent and the solution was further stirred for 30 minutes at room temperature. The system was again heated

until 80°C for 1 hour and under reflux. After cooling the final solution was directly recovered for a wet cellulose dialysis membrane that was immersed in bi-distilled water for 4 days, replacing dialysis water 3 times per day. The degree of substitution was determinate by H-NMR as described latter. In this work, the experimental conditions and the reagents molar ratios were optimized in order to achieve the maximum degree of substitution of chitosan into mono-carboxybutylchitosan and the lowest amount of other possible derivatives, such as 5-methylpyrrolidinone chitosan (MPC) (dos Santos et al, 2004). The optimum molar ratios of levulinic acid/chitosan/sodium borohydride were (3/1/0.5). After 4 days the pH of the solution was checked and it ranged between 4.6 and 5.3. From the original solution two different CBC systems were prepared: *i)* an acidified CBC solution, identified as CBCa, which was acidified with acetic acid to a final pH between 3-3.5 and *ii)* a neutral solution, identified as CBCn, with no pH adjustment (pH between 4.6-5.3 as in the original solution, due to the dialysis process).

As in the case of chitosan, CBC films were also loaded with three different amounts of each ionic liquid (25, 50 and 75% in terms of molar fraction) and the solutions were vigorously stirred for approximately 12 hours and further casted on polystyrene petri dishes at 50°C for 2 days. The molar fraction of ionic liquid added was calculated after H-NMR analysis of the modified chitosan in order to determine the real substitution degree of amino groups. As an example, and in the case of the CBC, 25% of IL correspond to an IL loaded amount of 0.25×(number of the remaining amino groups) that were calculated based on the total substitution degree (including *N*-carboxybutylchitosan and other derivatives as obtained by H-NMR). In the case of CBCa the remaining amino groups are considered to be completely protonated (since the pH solution was adjusted to 3.5) while in the case of CBCn they co-exist in both protonated and neutral forms.

For the DXMTNa release experiments, 5 mg of the drug were added to non-loaded and 75% loaded CBCn films and stirred for approximately 24 hours at room temperature and protected from light. The mixture was casted on polystyrene petri dishes at 50°C for 2 days.

Synthesis of non-loaded and loaded chitosan/carboxybutylchitosan composites

The CBC/CS composites were prepared using a CBC solution with pH adjusted to 7.7, adding small drops of NaOH solution (0.1 M), and a CS solution with pH 3.5. CS was added slowly, drop by drop, to the CBC solution under vigorous stirring at room temperature, in order to avoid CS precipitation and using equal volumes of CS and CBC. The mixture was stirred for 48 hours and casted on polystyrene petri dishes at 50°C for 2 days.

As before, 75% (molar fraction) [Ch][Cl] or [Ch][DHP] loaded CS/CBC films were prepared by the addition of 47.59 mg and 68.57 mg of [Ch][Cl] and [Ch][DHP], respectively, into 15 mL of CS/CBC solution. The total amount of IL added was considered to be the same for 75% loaded CS films. For the DXMTNa release experiments, 5 mg of the drug were added to non-loaded and films and the solutions were mixed vigorously for approximately 12 hours. Films were further casted on polystyrene petri dishes at 50°C for 2 days.

Characterization tests

Films' thickness

The thickness of each film was measured using a digital paquimeter, *Electronic Outside Micrometer*, at room temperature. The values are presented as the average of at least five measurements and the respective standard deviation.

Scanning electron microscopy analysis (SEM)

The morphologies of the surfaces and cross sections of the films were examined by Scanning Electronic Microscopy (SEM) on a Jeol, model JSM 5310 microscope (Japan) with an operating voltage of 10 kV. Samples were cryo-fracturated on liquid nitrogen and stored at 20% RH and room temperature before analysis. Then the surface and the cross sections were sputter-coated with gold for 40 seconds, before being observed under the microscope.

Attenuated total reflection Fourier transform infrared (FTIR-ATR)

Fourier transform infrared spectrometer (Jasco FT/IR-4200, Japan), was used, in the reflection mode at 4 cm^{-1} resolution using 128 scans between 500 and 4000 cm^{-1}, to identify the functional groups of CS and CBC, as well as their possible interactions with the tested ILs. Three replicates of each sample, previously stored at room temperature and 20% relative humidity (RH) were used.

Proton nuclear magnetic ressonance analysis (H-NMR)

The H-NMR spectrum of synthesized CBC was recorded on a Bruker Avance III 400 MHz spectrometer, with a 5-mm TIX triple resonance detection probe, in D_2O at room temperature with tetramethylsilane (TMS) as an internal standard. Conversion of CS into CBC was determined by integration of the peaks using MestRenova software version: 6.0.2-5475. The signal used for the integration was the one that corresponds to the $–CH_2$ group closest to the carboxyl group of the butyl substituent, at approximately 2.1 ppm. A small amount of the 5-methylpyrrolidione chitosan derivative was also identified and its substitution degree was calculated from the peak corresponding to $–CH_3$ group of the cyclic element at 1.1ppm (further details will be presented latter on the discussion section).

Water contact angles

Static contact angles of non-loaded and loaded (25, 50 and 75%) CS and CBCn films were measured using a *Dataphysics Contact Angle System OCA 20* on *Laplace Young method*, normal sliding drop type and 10μL water drops. All samples were maintained at 20% RH for 48 hours before measurement. Data is presented as an average of at least three measurements.

Water swelling (WS)

Squared samples with 1 cm^2 were kept at 20% RH and room temperature for 24 hours before swelling measurements. After initial weighing, each sample was immersed into buffer solutions at different pH (4, 7 and 10) at fixed ionic force (0.1M) and into bi-distilled water, at 37ºC. The following buffer solutions were used: pH 4 (0.23 mL of acetic acid (Panreac, Spain), 0.07 g of sodium acetate and 2.87 g of

NaCl (both from Sigma-Aldrich, Portugal)), pH 7 (0.31 g of $NaH_2PO_4x2H_2O$ (M & B), 0.52 g of $Na_2HPO_4x2H_2O$ (Riedel-de Haen) and 2.29 g of NaCl (Sigma-Aldrich, Portugal)) and pH 10 (0.23 g of $NaHCO_3$ (BDH) and 0.07 g of Na_2CO_3(Merk)) all for 500 mL of bi-distilled water. The pH values were checked precisely by a pH-meter (Standard pH Meter, MeterLab). After 30 minutes the films were taken out from the buffer solutions and weighed after removing the excess surface water with a filter paper. After that, they were placed back into the same buffer solution. The procedure was repeated at regular time intervals up to 8 hours. The water swelling (WS) of each film was calculated using the following equation:

$$WS\ (\%) = \frac{m_t - m_0}{m_0} \times 100 \quad (1)$$

where m_t is the weight of the film at time t and m_0 is the initial weight (before immersion, $t = 0$).

Water Vapor Sorption (WVS)

The water vapor sorption of each film (squared samples with 1cm^2, previously stored at 20% RH and room temperature) was measured by keeping the samples in small flasks inside a desiccator containing a potassium sulfate saturated solution to create a RH of ≈90% at 37°C. Each sample+flask system was weight before they were stored at controlled atmosphere. Each system was weighted during 8 hours, at regular time intervals of 1 hour. A control empty flask was also used. The water vapor sorption (WVS) was calculated using the following equation:

$$WVS\ (\%) = \frac{m_t - m_0}{m_{dry\ sample}} \times 100 \quad (2)$$

where m_t is the weight of the sample film at time t, m_0 the initial weight at $t = 0$ and $m_{dry\ sample}$ is the initial weigh of the film before it is placed at controlled temperature and RH. All weights are expressed in grams and the results presented are the average of three replicates.

Water Vapor Permeability (WVP)

Test samples were firmly fixed on the top of vials containing 1 ml of water with a transmission exposed area of ~0.64 cm^2. Vials were then placed into a desiccator containing lithium chloride (Sigma-Aldrich, Portugal) at 37°C and 10% RH (atmosphere created with a saturated lithium chloride solution). The water vapor rate

transferred through the films was determined by measuring the water weight loss at regular time intervals (every hour during the first 8h and then every 24 hours) until a constant weight decrease was achieved. The slope of water weight loss (change in the weight of the vials) over time, at steady state conditions was used to calculate the water vapor transmission rate (WVTR) by dividing the calculated slope by the exposed area according to the following equation:

$$WVTR = \frac{\Delta w}{\Delta t \times A_{\odot}} \quad (3)$$

where $\Delta w/\Delta t$ is the amount of water lost per unit of time (g/h) and $A_{\odot}$ is the exposed water vapor transmission area (m^2). The water vapor permeability was then calculated as:

$$WVP = WVTR \times \frac{l}{P_{H_2O(37°C)} \times \Delta RH_{in-out}} \quad (4)$$

Where l is the film's thickness (mm), $P_{H_2O(37°C)}$ is the water vapor pressure at 37°C (6.28 kPa) and ΔRH_{in-out} is the relative humidity difference between the inside of the permeability cell (assumed to be equal to 100 %) and in the desiccator (10 %). The calculated WVP expressed in ($g.h^{-1}.m.kPa$) resulted from the average of three replicates that were performed for each film.

Mechanical properties

The tensile strengths, tensile stress (σ) and strain (ε), and elastic or Young's modulus (E) of the films were measured at room temperature using a universal electronic tensile testing machine (Stable Micro Systems Company). Before measuring the films were stored in a desiccator with a saturated potassium sulfate solution (Sigma-Aldrich, Portugal) at 80% RH and at room temperature. Two replicates were performed for each film. The initial gauge length was 15 mm and the testing speed was 0.1 mm/s for a test distance of 10 mm and 0.1 g trigger force. Tensile strength and elongation properties were determined from the stress-strain curves. σ (MPa) was calculated by the following equation:

$$\sigma = \frac{F}{A} \quad (5)$$

where F is the maximum load applied to the film before failure in (g) and A is the initial cross sectional area (mm^2), considering the thickness of the film and its width on the rupture zone. The strain, ε, representative of the ratio of total deformation to

the initial dimension of the film (L_0), was determined considering the variation on the gauge length (L):

$$\varepsilon = \frac{\Delta L}{L_0} = \frac{(L - L_0)}{L_0} \quad (6)$$

The elastic modulus, E (MPa) was obtained directly by the slope comprehended between 0.05% and 0.25% of the stress-strain relation:

$$E = \frac{\sigma}{\varepsilon} \quad (7)$$

Thermal characterization – TGA and DSC

Thermogravimetric analysis (TGA) were performed using a TGA-Q500 (TA Instruments) equipment. Measurements were conducted by heating the samples from room temperature to 600°C at a heating rate of 10°C/min under flowing nitrogen atmosphere. Differential scanning calorimetry (DSC) analyses were performed using a DSC-Q100 (TA Instruments) equipment. Samples were sealed in aluminum pans and heated at constant rate (10°C/min), over a temperature range from -40 to 300°C. An inert atmosphere was maintained by purging nitrogen at the flow rate of 50 ml/min. In both cases samples were maintained in a desiccator at room temperature and 20% RH before analysis to achieve better reproducibility. Two replicates were performed for each film and for each analysis using samples that weighted between 7 and 10 mg.

Impedance measurements

Electrochemical impedance spectroscopy (EIS) experiments were carried out using a PGSTAT 30 potentiostat-galvanostat with Frequency Response Analyser (FRA2) module controlled by FRA software version 4.9 (EcoChemie, Utrecht, Netherlands). A r.m.s. perturbation of 350 mV was applied over the frequency range 1.0 MHz to 0.1 Hz with ten frequency values per decade. The spectra were recorded at 0.1 V and were fitted using electrical equivalent circuits with ZView 3.2 software (Scribner Associates Inc., USA). The samples were placed on the maximum RH achieved at room temperature (≈ 85%) 48 hours before measurements. The dry membranes were then sandwiched between two steel (Steel s 136) blocking electrodes in the measurement cell with 1 cm^2. The potential was applied between the reference and the working electrode (0.1V). The *counter* electrode was used to minimize the

possible effects of redox reactions on the cell's surface, and thus, minimize the background noise.

Drug release experiments

Sodium phosphate dexamethasone (DXMTNa) release kinetic studies were performed using a spectrophotometer (Jasco model V550, Japan) by monitoring the maximum absorbance at 242 ± 2 nm. Two different release media were used, pH 7 and pH 10 buffers, both with fixed ionic strength (0.1 M). Squared film samples with 1 cm^2, previously stored at 20% RH, were introduced in a dialysis membrane (Spectra/Por® Dialysis membrane, MWCO 8000) which was sealed with teflon on both side. Each sample was immersed in 20 ml of release media and the release took place at 37°C under orbital stirring (100 rpm). The loaded polymer weight/volume release solvent ratio was previously optimized in order to avoid saturation of the release solution. The analysis consisted in the removal of an aliquot from the released solution (approximately 3 ml) that was analyzed and returned into the release medium. Measurements were carried out until a constant release profile was achieved. Released DXMTNa concentrations were calculated using previously determined calibration curves (using pH 7 and pH 10 buffer solutions at 37°C). Samples of IL loaded and non-loaded polymers, without DXMTNa, were also measured at the same wavelength to study the influence of the polymers dissolution on the release profiles. All release assays were carried out in duplicate.

Diffusion coefficients (calculation procedure)

Release kinetic coefficients were estimated from DXMTNa release profiles using the Korsmeyer-Peppas equation:

$$\frac{M_t}{M_\infty} = kt^n \quad (8)$$

In Eq. (8), M_t and M_∞ are the absolute cumulative amounts of bioactive substance at time t and at infinite release time, respectively, n is the release exponent (characteristic power for the drug release) and k is the so-called kinetic constant. This equation was applied for M_t/M_∞ values within the range 10 to 60% or for linear relation. The most common release mechanisms can be divided into diffusion-controlled, degradation-controlled or a combination of both (Siepmann and Peppas,

2001; Zuleger and Lippold, 2001). Diffusion-controlled release profiles are commonly divided into two periods: short-time and long-time approximations that are described by Eq. (9) and Eq. (10), respectively;

$$\frac{M_t}{M_\infty} = 4\left(\frac{tD_1}{l^2\pi}\right)^{1/2} \quad (9)$$

$$\frac{M_t}{M_\infty} = 1 - \frac{8}{\pi^2} exp\left(-\frac{t\pi D_2}{l^2}\right) \quad (10)$$

where t is the release time, l is the thickness of the sample and D_1 and D_2 are the short-time and the long-time diffusion coefficients for each of the considered release periods and which are considered constant. Theoretically, both equations are just valid for cumulative percentages of delivered drug between 10-60% and 40-100%, respectively.

Results and discussion

Synthesis and characterization of chitosan (CS) and *N*-carboxybutylchitosan (CBC)

pH adjustment of CS

Chitosan applications are limited due to its low solubility in aqueous solutions being only soluble in acidic media. Recently many authors have discussed the influence of various acid solutions to dissolve CS in order to improve its physiological activities, chemical reactivity and biocompatibility (Kittur et al, 2002). In this work, the dissolution of CS was achieved using acetic acid aqueous solution (1% v/v). The amine groups (NH_2) of CS become protonated in acidic medium (NH_3^+) and thus, the dissolution is promoted. In this context, the polymer deacetylation degree (DD) and MW play an important role in the dissolution behavior of CS as these parameters influence the number of amino groups present in the polymer structure.

Modification of CS into CBC

The presence of free amine groups in the CS structure is an essential feature to obtain different CS derivatives through physical and chemical modification originating derivatives with different physico-chemical-mechanical properties (Li et al., 2005).

The CS derivative studied in this work, *N*-carboxybutylchitosan was obtained by the reaction of levulinic acid with chitosan using a reducing agent (dos Santos et al, 2005; Rinaudo et al, 2001). According to these authors, the reaction of CS can produce two main compounds: *N*-carboxybutylchitosan (CBC) and 5-methylpyrrolidinone chitosan (MPC) as schematized in Figure 7. The experimental conditions used in this work (described before) to synthesize the CS derivative aimed to maximize the substitution degree of CBC and to minimize it for MPC.

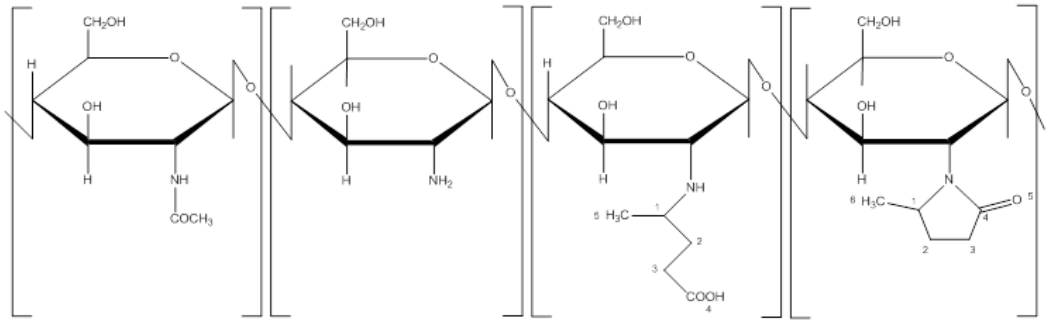

Figure 7. Chitosan derivative structures which represent the acetylated monomer, deacetylated monomer, *N*-carboxybutyl derivative (CBC) and 5-methylpyrrolidinone derivative (MPC), from the left to the right.

The H^1-NMR spectrum of the CS derivative allowed the determination of the substitution degree (SD) induced into CS using the obtained peak integrals (Figure 8). This technique, as well as FTIR-ATR, showed the effective modification of CS into CBC.

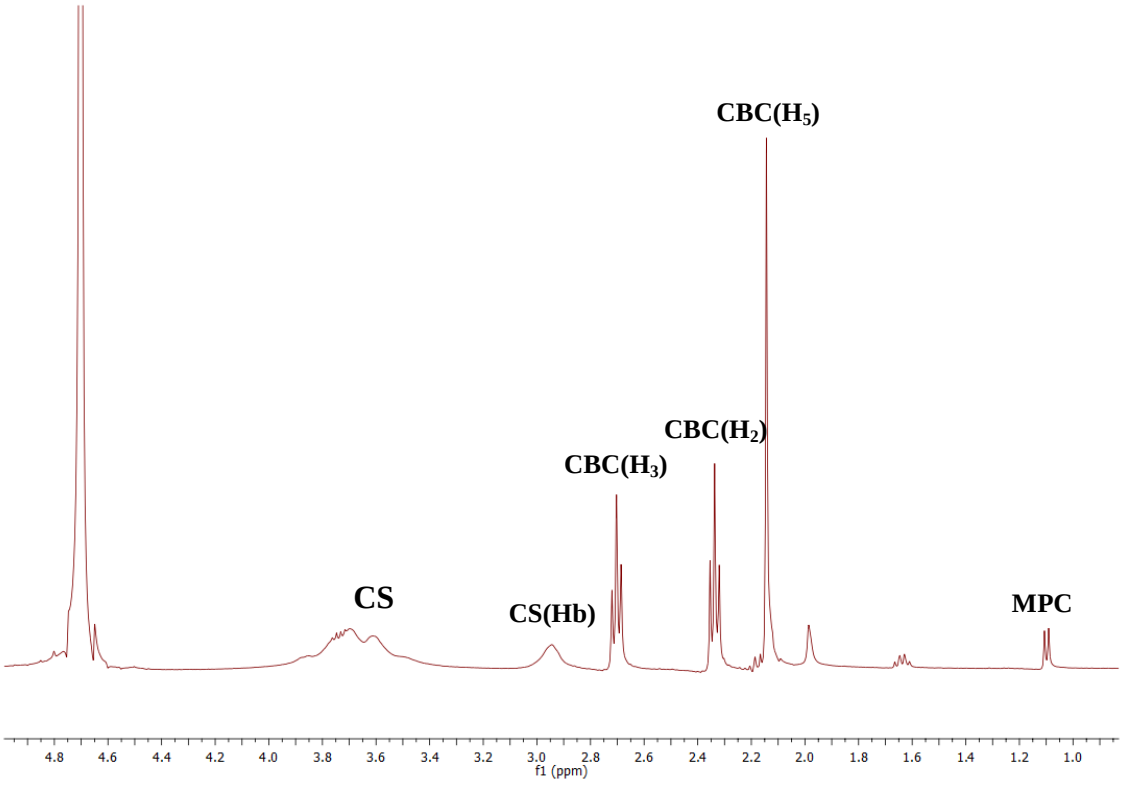

Figure 8. H^1-NMR spectrum for CS derivatives.

The SD of CBC was calculated from the signal integral at 2.1 ppm, corresponding to the $–CH_3$ group of the butyl substituent (H_5 in Figure 8). On the other hand, the SD of MPC was determined from the peak relative to the $–CH_3$ group

of the cyclic compound at 1.1 ppm (H_6 in Figure 8). H_b at 2.9 ppm corresponds to a hydrogen atom that is common to all portions of the CS derivative, working as the reference peak. The remaining integral peaks correspond to non-modified CS.

The integral peaks corresponding to H_b and H5 allowed the determination of the SD obtained for CBC, by the following equations:

$$SD_{CBC} = \frac{H_5 integral}{H_b integral} \times \frac{number\ of\ hydrogens\ H_b}{number\ of\ hydrogens\ H_5}$$

$$\Leftrightarrow SD_{CBC} = \frac{1{,}84}{1} \times \frac{1}{3} \cong 61\%$$

The substitution degree achieved for *N*-carboxybutylchitosan (CBC) was 61%, which is higher than the values previously described in the literature (dos Santos et al, 2005). For further interpretation of the results, it was considered that approximately 61% of the 73% deacetalyted CS was modified into CBC. The substitution degree for the cyclic derivative (MPC) was nearly 10%. Thus, the remaining 30% corresponds to non-modified NH_2 groups of CS.

CBC may be classified as a polyampholyte because it has both amino and carboxylic acid ionisable groups in its structure that show different ionization states depending on the external environment being consequently classified as a pH-responsive material. In order to evaluate the pH-dependent ionization degree of CBC, two potentiometric titrations were performed to determine the pKas of CBC. The titration curves are presented in Figure 9 and they show that CBC has two pKa values at 3.2 and 7.7. The first pKa value corresponds to the pH at which amino groups become protonated (NH_2/NH_3^+) while the second corresponds to the pH at which carboxylic groups become ionized ($COOH/COO^-$).

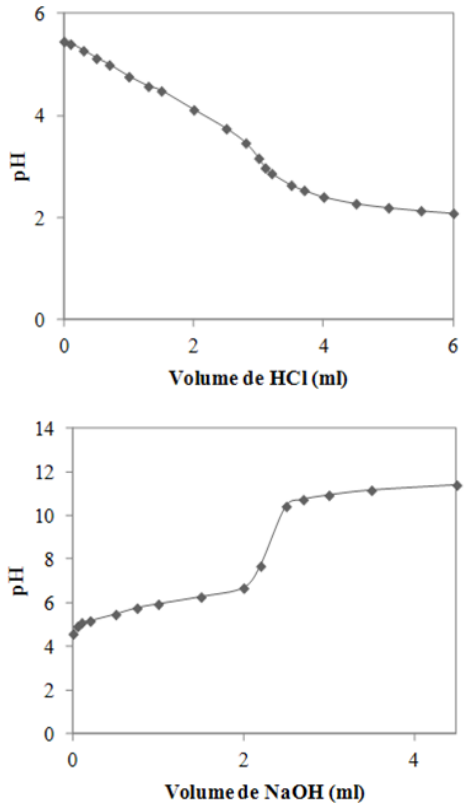

Figure 9. Potentiometric titrations of CBC with HCl (on top) and NaOH (at the bottom).

FTIR-ATR

FTIR-ATR analysis was performed to identify the characteristic peaks of CS and CBC and to confirm the modification of CS into CBC (Figure 10). This analysis is also important to identify possible interactions between the polymer matrices and the ILs. In the case of CS (Figure 10 (a)), a characteristic band between 3650 and 2800 cm^{-1} is attributed to O-H and N-H groups stretching (typical absorption bands exhibited by polysaccharides) and C-H vibrations (peaks at 3243 and 2851 cm^{-1}) and also include the O-H stretching characteristic of water, very common in hydrophilic materials (Singh et al, 2010; Dias et al, 2011). The peak observed at 1634 cm^{-1} is assigned to the C=O stretching of the acetylated unit of CS and the peak at 1536 cm^{-1} represents the overlapping of the N-H bending vibration and C-N stretching of the amide II (Coimbra et al, 2011). The peak at 1404 cm^{-1} is attributed to C-H and O-H bending vibration while the peaks at 1151, 1062, 1019 and 897 cm^{-1} are characteristic of the oxygen bridge (C-O-C) stretching bands (Silva et al, 2008).

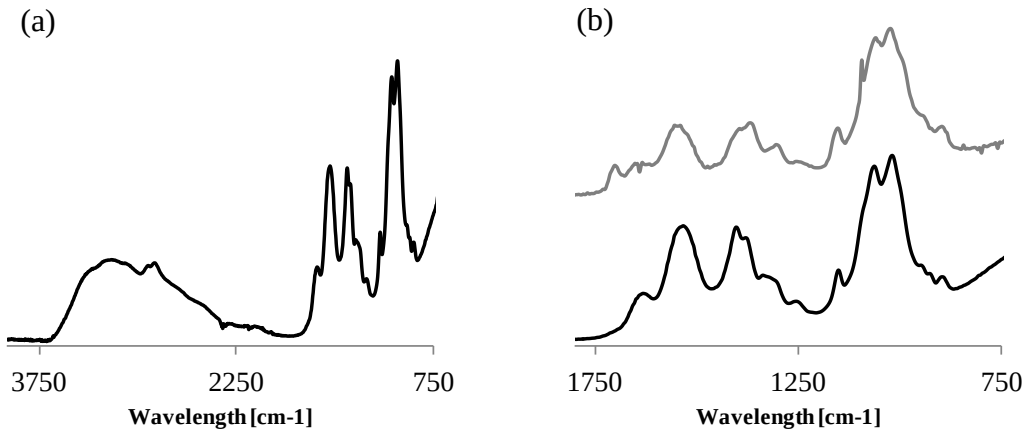

Figure 10. FTIR-ATR spectra of chitosan (CS) films (a) and comparison with CBC films (grey lines) (b).

The FTIR-ATR spectra of CBC films (Figure 10 (b)) shows an intense peak at 1701 cm^{-1} assigned to C=O stretching of the COOH groups (from levulinc acid), confirming the modification of CS in CBC. Peaks observed at 1600-1680 cm^{-1} where previously attributed to protonated amine and acetamine groups (intermiediate specie formed during the modification reaction) (Muzzarelli et al, 1989). The evident peak at 1096 cm^{-1} represents the C-N stretching of the tertiary amine.

Characterization of IL loaded CS and CBC films

FTIR-ATR

The FTIR-ATR spectra of pure ionic liquids ([Ch][Cl] and [Ch][DHP]) and IL loaded CS and CBC polyelectrolyte films are shown in Figure 11.

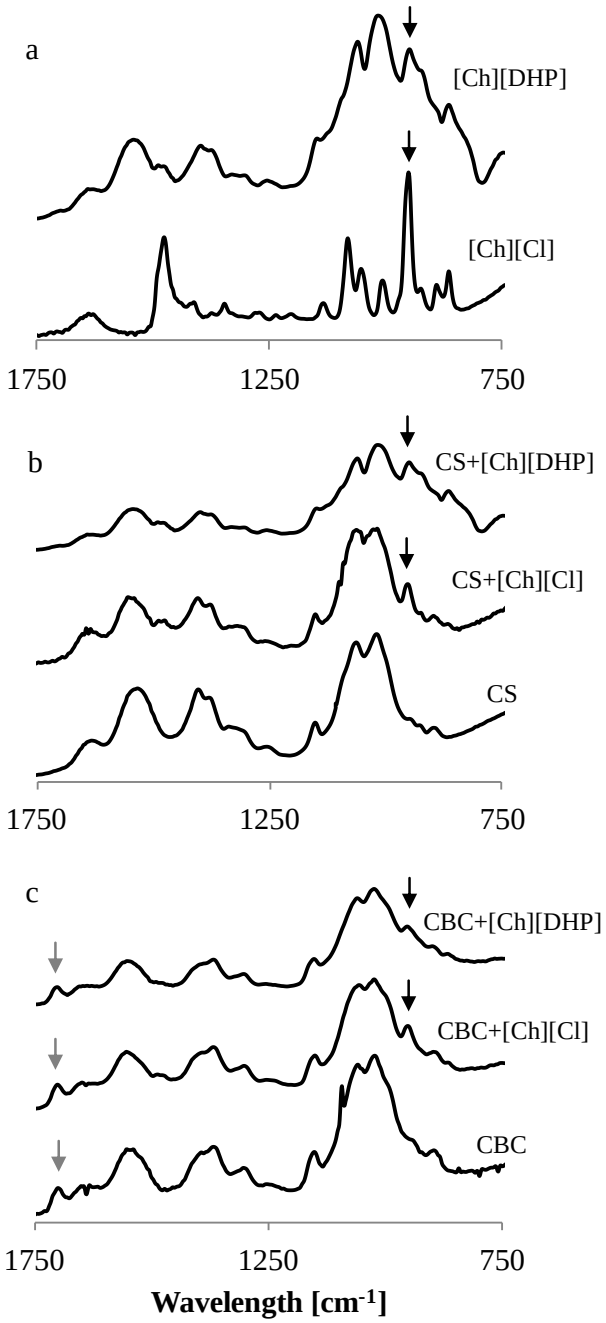

Figure 11. FTIR-ATR spectra of: pure [Ch][Cl] and [Ch][DHP] (a); non-loaded and IL loaded (75%) CS films (b) and non-loaded and IL loaded (75%) CBC films (c).

The spectra of [Ch][Cl] presents two characteristic peaks: one at 1479 cm^{-1} assigned to the CH_3 rocking and to harmonious movements of Cl (Yue et al, 2012) and the other at 952 cm^{-1} that represents the C-N stretching in the cation. In the case of [Ch][DHP], the peak at 1479 cm^{-1} is also identified and the peaks at 1122, 1079 and 1051 cm^{-1} are assigned to the C-O, C-N and C-C stretching maybe promoted by the dihydrogen phosphate anion (PO_4^-). The last characteristic peak of [Ch][DHP]

appears at 930 cm^{-1} and represents the C-O stretching of CH_2-O-P-O of the IL, that may be related to anion-cation interactions.

The ILs characteristic peaks are easily identified in the CS and CBC loaded films as also shown in Figure 11 (b and c). In the case of [Ch][Cl] the characteristics peaks at 952 cm^{-1} and 1479 cm^{-1} appear at the same wavelengths however in the case of [Ch][DHP], beside the characteristic peak at 952 cm^{-1} (from the IL cation), the peaks between 900 and 1100 cm^{-1} present deviation compared to CS non-loaded films. This may indicate stronger interactions between [Ch][DHP] and the polymer chains. The same effect seems to be verified for CBC films loaded with the same IL, but the deviation is less pronounced and only a small narrow on those bands is observed. On CBC films loaded with [Ch][DHP] the peak at 952 cm^{-1} is assigned to the cation choline, has happens with CS films doped with this IL, and there are not any other interactions between the polymer and the IL detectable by this technique.

Scanning electron microscopy (SEM)

Loaded and non-loaded CS and CBC films matrices were analyzed using SEM to infer about any possible structural changes that may occur due to addition of 75% of [Ch][Cl] or [Ch][DHP] into neat films. Surface and cross section images are shown in Figure 12. No significant differences were found between the surfaces of CS and CBC loaded and non-loaded films that were very homogenous (figures not shown). The structure of CS seems to be denser than that of CBC (Figure 12 (a and d)). The rugosity that is seen in the cross section bottom results from the cut of the freeze dried samples. The presence of the ILs does not seem to have a significant effect on the morphology of the films and loaded CS and CBC also present a dense structure. From the figure (mainly Figure 12 (c)) it could be said that [Ch][DHP] is somehow affecting the bulk structure of CS, however it is not clear if the observed non-homogeneity is due to the presence of the IL or due to the fracture process of the films. Further studies should be performed, including SEM-EDX analysis in order to conclude about the homogeneous distribution of the IL through the matrices.

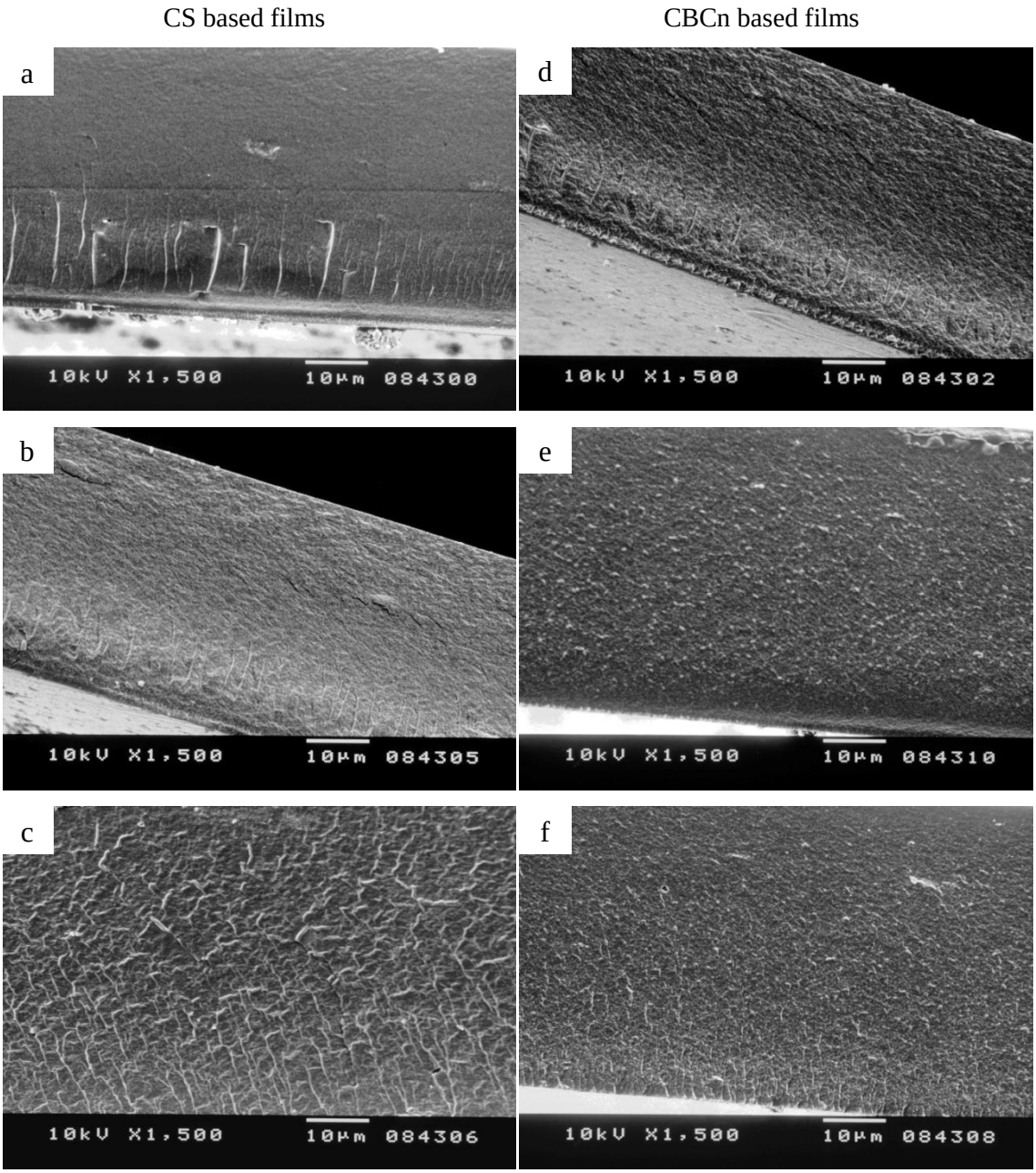

Figure 12. Cross section SEM micrographs for non-loaded and loaded CS (column from the left) and CBCn (column from the right) films, corresponding to: (a) non loaded CS, (b) 75% [Ch][Cl] and (c) 75% [Ch][DHP] loaded CS films and (d) non loaded CBC, (e) 75% [Ch][Cl] and (f) 75% [Ch][DHP] loaded CBCn films.

Thermo-mechanical properties

Thermal analysis methods, such as thermogravimetry (TGA) and differential scanning calorimetry (DSC) are powerful thermo-analytical techniques that can give important information about the physico-chemical properties of natural and synthetic

based polymers, mainly in terms of their thermal stability, composition, phase transition on heating/cooling, endothermic and exothermic events, etc. In this work these analyses were performed to study the effect of the IL type and loaded amount on the thermal stability and plasticization capacity of the films. Polysaccharides normally have a strong affinity towards water since in solid state these macromolecules present disordered structures which can be easily hydrated (Kittur et al, 2002). In order to normalize the residual water present in the samples all of them were kept in a desiccator (20% RH, room temperature) before TGA and DSC analysis. It was decided to analyze all the films at similar low hydration state instead of completely dry because it is very difficult to guarantee dryness during sample manipulation for these hydrophilic materials.

Thermogravimetric profiles were measured for pure ILs and for non-loaded and loaded CS and CBCn films. Figure 13 presents the thermograms for [Ch][Cl] and [Ch][DHP]. Both ILs were stored at 20% RH and room temperature before analysis.

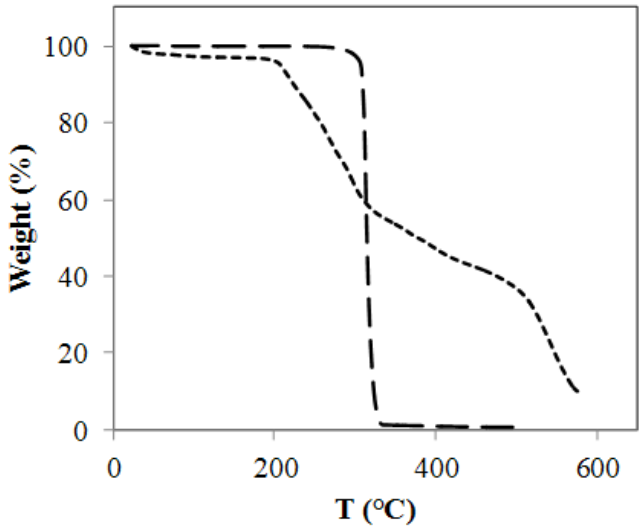

Figure 13. TGA profiles for [Ch][Cl] (dashed lines) and [Ch][DHP] (doted lines).

According to the results presented in Figure 13, [Ch][DHP] present lower thermal stability than [Ch][Cl]. Moreover, and since samples were exposed to similar relative humidity before analysis, [Ch][DHP] is slightly more hydrophilic than [Ch][Cl]: weight losses at 110ºC were equal to 2.91 and 0.075% for [Ch][DHP] and [Ch][Cl], respectively. The results obtained for [Ch][DHP] is in agreement with the one obtained by Rana et al which reported weight losses of 2% at the same temperature (Rana et al, 2010). It can also be observed that [Ch][Cl] presents a

characteristic thermogram for an IL with relatively high thermal stability and a sharp degradation temperature around (315.7 ± 0.2)°C. On the contrary, [Ch][DHP] shows a temperature dependant degradation profile with four main weight loss stages. The first weight loss at lower temperature is due to water evaporation (Prasad et al, 2009; Rana et al, 2010). The second stage between 200 and 320ºC (with weight losses around 40.97%) was reported as due to the dehydration of the [DHP] anion (Rana et al, 2010). According to Sebastião and Canevarolo (Sebastião and Canevarolo, 2005), the third and forth stages may be related to degradation of the inorganic part of the IL. The influence of the addition of different molar amounts of [Ch][Cl] in the thermal stability of CS and CBCn films is presented in Table 1.

Table 1. Influence of the amount of [Ch][Cl] and [Ch][DHP] in the degradation temperatures (Tdegradation °C) of chitosan (CS) and N-carboxybutylchitosan (CBCn) films.

		$T_{degradation}$ (°C)	
Molar % IL		**CS**	**CBCn**
0		287.2 ± 7.3	304.1 ± 1.3
25		271.3 ± 0.1	266.9 ± 1.8
50	[Ch][Cl]	268.2 ± 0.1	264.1 ± 1.3
75		264.6 ± 3.9	259.6 ± 0.4
75	[Ch][DHP]	251.5 ± 1.1	261.9 ± 4.2

Non-loaded CS and CBCn presented similar thermogravimetric profiles with degradation temperatures around 300ºC (287.2ºC for CS and 304.1ºC for CBCn). Arora et al found similar degradation temperature for CS, using this technique (Arora et al, 2011). The higher degradation temperature observed for CBCn is due to the higher reticulation degree of this polymer that induces higher thermal stability. A decrease in the thermal stability of the films is observed when the ILs are loaded into CS and CBCn and this effect is more significant in the case of CBCn with a decrease of ~15% in the maximum degradation temperature compared with ~8% for CS. This may be because the presence of IL decreases the intrinsic reticulation of the polymer structure (due to number of hydrogen bonding and electrostatic interactions) and disrupts its crystalline structure (Suyatma et al, 2005; Prasad et al, 2010).

Differential scanning calorimetry (DSC) analyses were also performed to identify possible phase transitions induced by the ILs to the polymer matrices. DSC

curves were also obtained for pure ILs and the results are shown in Figure 14 (measured at a restricted temperature range to avoid degradation of the material inside the equipment).

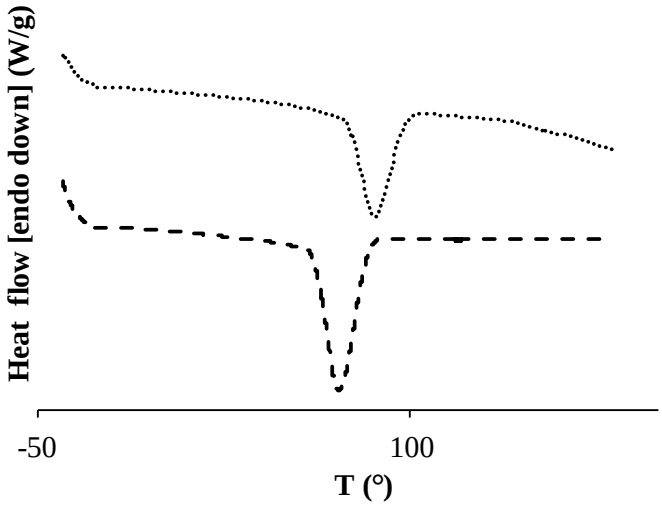

Figure 14. DSC curves for pure [Ch][Cl] (dashed lines) and [Ch][DHP] (doted lines).

The results confirm that both ILs are highly hydrophilic (and hygroscopic) since the DSC curves show sharp endothermic peaks corresponding to water evaporation at 71.2°C for [Ch][Cl] and 85.8°C for [Ch][DHP]. The higher evaporation temperature needed in the case of [Ch][DHP] confirm that water has a stronger interaction with this IL and/or that it is retained inside molecular cavities formed by this IL due to hydrogen bonding and electrostatic interactions (Hossain et al, 2011). The curves measured for non-loaded and loaded CS and CBCn films are presented in Figure 15.

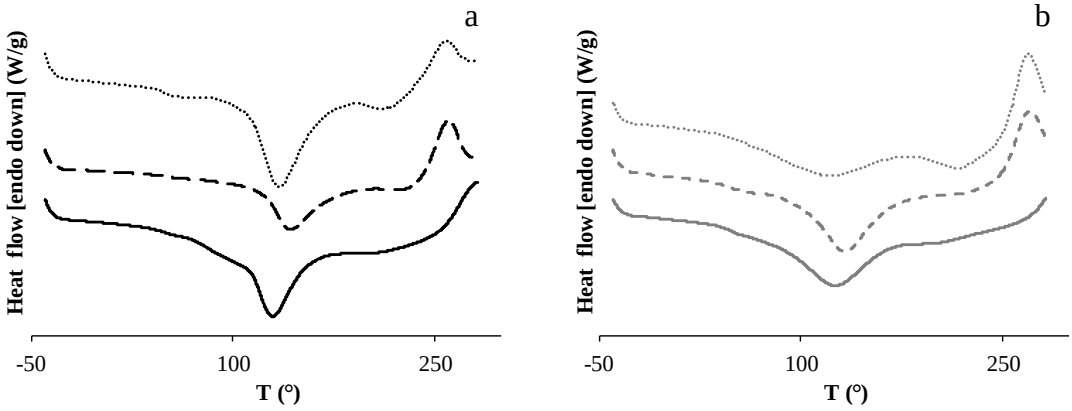

Figure 15. DSC curves for CS (a) and CBCn (b) films: non-loaded (full lines) and 75% [Ch][Cl] (dashed lines) and [Ch][DHP] (doted lines) loaded films.

In both cases, the endothermic peaks centered between 120-140°C are again related to residual water evaporation (Rueda et al, 1999). Differences observed in the vaporization enthalpy as well as in the peak temperature for non-loaded and loaded films are shown in Table 2.

Table 2. Endothermic events of CS and CBCn films doped with 75% [Ch][Cl] and 75% [Ch][DHP] (water evaporation temperature (Twater evaporation) and enthalpy (*ΔH*)).

	CS		**CBC**	
	$T_{water\ evaporation}$ (°C)	**ΔH (J/g)**	**$T_{water\ evaporation}$ (°C)**	**ΔH (J/g)**
0% IL	121.50 ± 11.81	206.70 ± 19.23	130.65 ± 0.78	130.43 ± 6.89
[Ch][Cl]	143.34 ± 1.73	138.65 ± 0.35	131.21 ± 3.56	137.00 ± 8.20
[Ch][DHP]	133.07 ± 1.46	213.90 ± 35.36	122.93 ± 3.86	129.70 ± 13.15

In general terms the results indicate that the presence of the ILs induce different water absorbing capacity and also different water-polymer interacting strengths (Kittur et al, 2002) mainly due to amine, hydroxyl and carboxyl (in CBCn) groups interaction with water molecules (Dong et al, 2004). According to water vaporization enthalpy data, water molecules are strongly associated to non-loaded and [Ch][DHP] loaded CS films, since more energy is necessary to remove them from the matrix.

Most polysaccharides do not present melting temperature due to hydrogen bonding associations, but degrade upon heating above a given temperature (Rueda et al, 1999). The exothermic peak present on the curves shown in Figure 15 corresponds to the thermal decomposition (T_{deg}) of the films (Suyatma et al, 2005). The T_{deg} of non-loaded CS was not determinate due to equipment limitations. Films loaded with [Ch][Cl] and [Ch][DHP] present lower degradation temperatures equal to 260.5°C and 258.9°C, respectively. These results are in accordance with the ones obtained from TGA.

Several authors have used different techniques to determine the glass transition temperature (Tg) of CS however no agreement was found. This may be because in the case of highly hydrophilic materials different amounts of absorbed/retained water induce different plasticization to the films (Suyatma et al, 2005). As mentioned, the presence of hydrophilic ILs induces different water absorption capacities to CS and CBCn films which may affect the water plasticizer effect depending on the IL type

and amount, on the polymer and on the IL-polymer interactions (Kittur et al, 2002; Suyatma et al, 2005). As can be seen in all the curves in Figure 15 (especially the ones for IL loaded films) they present an endothermic thermal event before degradation around 184.6°C for CS and 189.5°C for CBCn films. The value obtained for CS is in good agreement with the values presented by Shanta and Harding and Suyatma and its co-workers (Suyatma et al, 2005; Shanta et al, 2002) which identified this value as a Tg for CS. However in the presence of ILs the peak is deviated for higher temperatures (higher than 200ºC for both CS and CBCn). These results lead to two possible explanations: *i)* the Tg of the loaded films is increased because ILs are working as cross-linking agents that limit chains mobility, also leading to the earlier degradation and decreasing on the thermal stability of these films (Suyatma et al, 2005) or *ii)* this thermal event do not correspond to the Tg of the films, since it is experimentally verified that IL loaded films have a rubber like aspect and therefore they should present lower Tg, but to some polymer structure rearrangement that occur before degradation. Further studies should include dynamic mechanical analysis in order to confirm if the observed endothermic event is indeed related with a plasticization effect.

Mechanical Properties

Owing to their good film forming properties and antimicrobial character, both CS and CBC have potential as wound dressing, coating or packing films materials. The performance of CS and CBC films for these or other biomedical application is strongly dependent on their thermal and mechanical properties which are largely associated with the distribution and number of intramolecular and intermolecular interactions within the polymer network (Leceta et al, 2012).

The tensile strength (σ) and percentage elongation (ε) values of loaded and non-loaded CS and CBC films were calculated to understand the effect of the IL type and added amount on their mechanical behavior. The results are resumed in Table 3. Non-loaded CS films show stress-strain behavior typical of ductile materials, characterized by different regions. At relatively low strains (between 0.05 and 0.25%), the material obeys Hooke's Law and stress is proportional to strain, indicating an elastic behavior of the polymer. The elastic or Young's modulus (E) is calculated in this region. The

elastic limit of the material is reached when Hookes' law is not obeyed anymore and the material is able to return to its original shape if the force is removed. After this point non-loaded CS films experience 'necking' and even thought the stress dramatically increases in this region, the overall stress is decreased until the breaking point is reached. Non-loaded CS films present the highest *E* value (13.01 MPa) when compared to loaded CS and with non-loaded and loaded CBCn films. Its elongation at break (EB), i.e. the strain at which the material can no longer sustain the stress and break (Pocius, 2002) is equal to 1.81 % at 10.73 MPa. Choline chloride loaded CS films show a drastic decrease in the elastic modulus of the films and an increase in the EB, showing that loaded films present significant lower stiffness than non-loaded ones. The effect of the IL depends on the amount of IL added although there is no significant difference between the results obtained at 50 and 75% amount of loaded [Ch][Cl]. In principle the plasticizing effect promoted by the presence of the IL is related with their capacity to improve the water absorption capacity of the films. Therefore it may be said that absorbed water is the plasticizer agent (Suyatma et al, 2005). Moreover the IL may also avoid hydrogen bond interactions between polymer chains which decrease the stiffness of the network. However, and taking into account the WVS capacity results, that will be presented later, the results obtained for the higher IL loaded amounts (50 and 75%) may indicate that at higher concentrations IL may be also reticulating the matrix and therefore there is equilibrium between water absorption capacity and reticulation degree promoted by the IL.

Table 3. Elastic Modulus (*E*), elongation at break (EB) and tensile strength (TS) for non-loaded and loaded CS and CBCn films.

Film		*E* (MPa)	EB (%)	TS (MPa)
CS	0%	13.01	1.81	10.73
	25%	0.75	4.62	2.09
	50%	0.14	6.02	4.24
	75%	0.77	5.97	4.38
CBCn	0%	8.30	2.73	12.21
	25%	0.96	3.65	5.76
	50%	0.99	6.61	9.98
	75%	0.91	5.10	6.50

Note: Deviations are not presented although duplicates were measured for all samples because that was a systematic and consistent deviation between first and second measured samples. This was because the equipment had no temperature and HR control and samples are highly hygroscopic and the effect of water in the mechanical properties of the films is very significant as discussed.

The same analysis was performed for CBCn films at the same experimental conditions (Table 3). Non-loaded CBCn present a lower elastic modulus and higher elongation at break than non-loaded CS most probably because of its intrinsic higher water absorbed capacity, as discussed later. This effect also makes these samples more difficult to measure because films have almost a gel like aspect.

As in the case of CS, and due to the same reasons, the presence of [Ch][Cl] seems to potentiate the plasticization effect however not in a linear IL concentration depend manner. CBCn films loaded with 50% IL present the most pronounced plasticizer effect with higher values for EB (6.61 %) and TS (9.98 MPa). At 75% loaded amount a strong interaction might be occurring between the polymer chains and the IL, producing a "cross-linking" effect, which decreases the free volume and the molecular mobility of the polymer ("antiplasticization" effect). A similar effect was shown by Izawa et al for gels of xanthan gum with ionic liquid, for which tensile modes were dependent on the polymer:IL proportion tested (Izawa et al, 2009).

A comparison between the effect promoted by [Ch][DHP] and [Ch][Cl] on the stress-strain curves of CS and CBCn films is given in Figure 16.

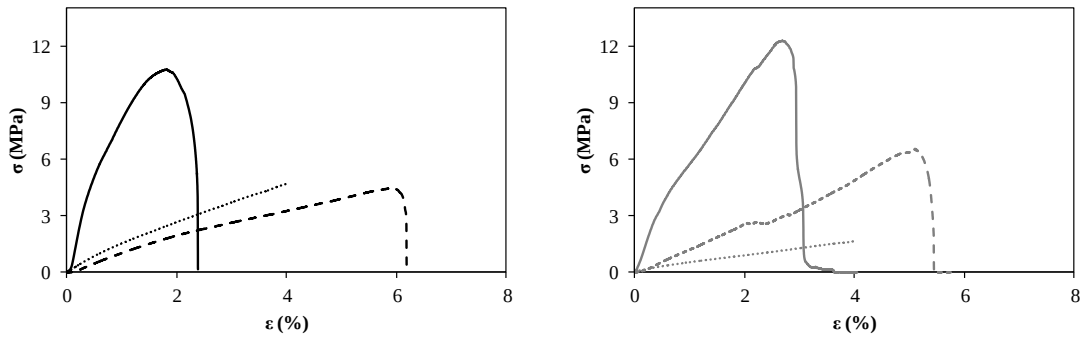

Figure 16. Stress-strain curves for CS (left) and CBCn (right) films: non-loaded (full line) and loaded with 75% [Ch][Cl] (dashed lines) and 75% [Ch][DHP] (doted lines).

Chitosan and CBCn films loaded with [Ch][DHP] no not experience rupture during the tested elongation which was equal to 10cm meaning that they have higher resistance to break than films loaded with [Ch][Cl]. CS films doped with [Ch][DHP] obey to Hooke's Law for a longer period under stress when compared with CS films containing [Ch][Cl] also presenting higher elastic modulus (1.75 MPa). On the other hand, CBCn films loaded with [Ch][DHP] show the lowest *E* values (0.35 MPa) which means that the effect of this IL in the reorganization of the CBCn network is the most important as previously discussed. In principle [Ch][DHP] is interacting with the CBCn chains by both the anion and the cation, which reduces the interaction between the chains and decrease the stiffness of the film.

The strength of biopolymer based films depends on a number of different factors which include the nature of polymer, its crystallinity, cross-linking degree, orientation, ageing, plasticizer type and amount (if used), etc. Comparison between data reported in the literature is difficult since there are a great dispersion associated differences found for composition, degree of acetylation, molecular weight, film preparation methods and conditioning used prior to testing (Pereda et al, 2011). In fact, the storage period may induce recrystallization of chitosan, increasing the rigidity and brittleness of the film. Moreover water evaporation and structure modifications promoted by the IL may also occur (Suyatma et al, 2005) making comparison between results a very difficult task.

In this context, there are many factors that may support the hypothesis that ILs work as indirect plasticizers to these biopolymers. According to the literature, cross-linked chitosan films showed increase on tensile stress and decreased elongation compared to pure films (Kittur et al, 1998). However, the hydrophlicity potentiated by

the IL presence seems to enhance the plasticizing effect of water and not the plasticizer effect of the IL directly. Moreover, the IL may also avoid hydrogen bond interactions between polymer chains which decrease the stiffness of the network. Therefore, the presence of the IL may reticulate the structure, increasing Tg (as given by the DSC results) but also work as indirect plasticizer when the films are stored at the proper RH and temperature conditions.

Hydrophilicity

The surface properties of polymer based materials are extremely important to conclude about their potentiality to be used as cell adhesion and protein adsorption materials since they affect the material's stability and biocompatibility (Caykara et al, 2006). Water contact angle and water vapour sorption measurements are useful tools to determine the hydrophilic/hydrophobic character of a film surface.

The wettability of a surface is highly dependent on the film structure (Leceta et al, 2012; Garneiro-da-Cunha et al, 2010). To understand the effect of the ILs on the films wettability, water contact angles were measured for CS and CBCn films loaded with different contents of [Ch][Cl]. Films loaded with 75% of [Ch][DHP] were also analyzed to conclude about the effect of the IL's anion on this property.

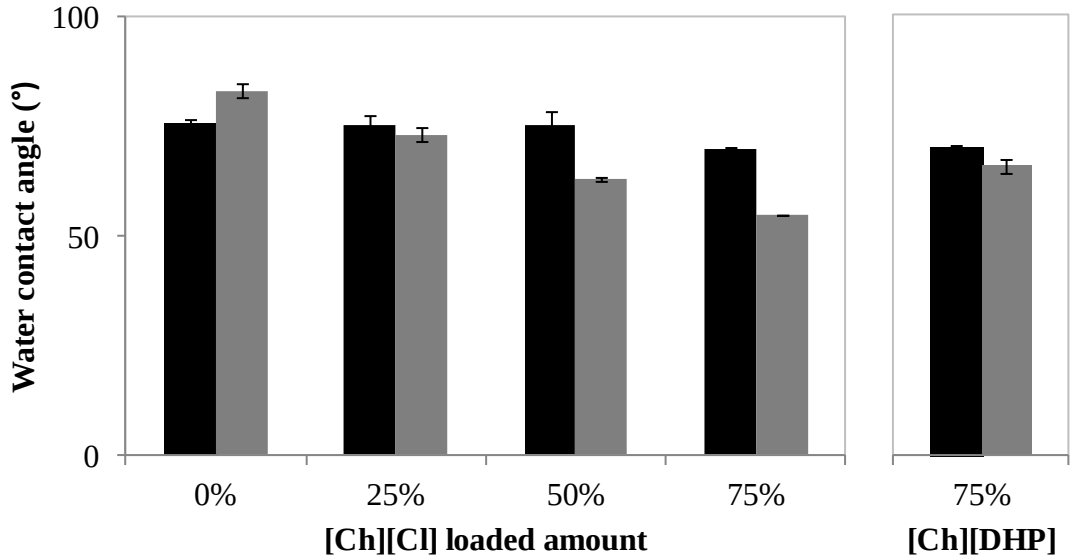

Figure 17. Water contact angle values measured non loaded chitosan, CS (■) and *N*-Carboxybutylchitosan, CBCn (■) films and loaded with different amounts of ILs ([Ch][Cl] on the left and [Ch][DHP] on the right).

As it is shown in Figure 17, water contact angles of pure CS films were around (76.0 ± 0.49)º, in agreement with other values found in the literature (Wanichapichart et al, 2009; de Britto et al, 2007). CBC films were expected to be more hydrophilic than CS, due to the presence of carboxylic, hydroxyl and amino groups. However, CBCn presents slightly higher surface hydrophobicity, which may be due to the presence of the alkyl groups introduced during the CS modification reaction that seems to overlap the influence of the carboxylic groups (Dias et al, 2011, 2). Moreover, the carboxylic acid groups may interact through H-bonding with CBCn hydroxyl and amino groups reducing the number of those groups that are available to interact with water and therefore decreasing the CBCn surface film hydrophilicity. It was also observed that the surface wettability can be affected by pH changes during films synthesis and preparation, since they induce modifications on their structure due to protonation of non-substituted amino groups (Garneiro-da-Cunha et al, 2010; de Britto et al, 2007). This influence was confirmed by comparing water contact angles measured for CBCa and CBCn which were equal to (87.64 ± 0.39)º and (83.15 ± 1.64)º respectively, supporting the evidences presented before.

The addition of [Ch][Cl] originates films that are more hydrophilic, as observed, by a decrease in the water contact angle values. This effect is more pronounced for CBCn than for CS films and it may be due to the hydrophilic character of the IL. When comparing the effect of the IL, at the same added amount, no significant differences were observed between [Ch][Cl] and [Ch][DHP] loaded CS films, although in both cases, the presence of the IL increased the hydrophilicity of the films when compared to non-loaded CS. In the case of CBCn films the water contact angle increases according to the following order: CBCn+[Ch][Cl] (54.90 ± 0.12)º < CBCn+[Ch][DHP] (65.73 ± 0.09)º < CBCn (83.15 ± 1.64)º indicating that both ILs increase the hydrophilicity of CBCn but that effect is more pronounced for [Ch][Cl]. This may be due to the higher reticulation degree promoted by [Ch][DHP] because of the larger number of possible interactions that can exist between this IL and the CBCn matrix that decrease the number of hydrophilic groups that could interact with water (see Figure 37, pp 76).

Water contact angles allow evaluating the hydrophilicity of the film's surface while water vapour sorption (WVS) curves are important to provide a better understanding of the interaction mechanism between water and polymer functional groups. In this work the hydrofilicity of the films is increased since hydrophilic and

hygroscopic IL molecules dispersed trough the matrices are working as "water absorbing" additives, which will consequently affect the physico-chemical and thermo-mechanical properties of the films (Silva et al, 2008).

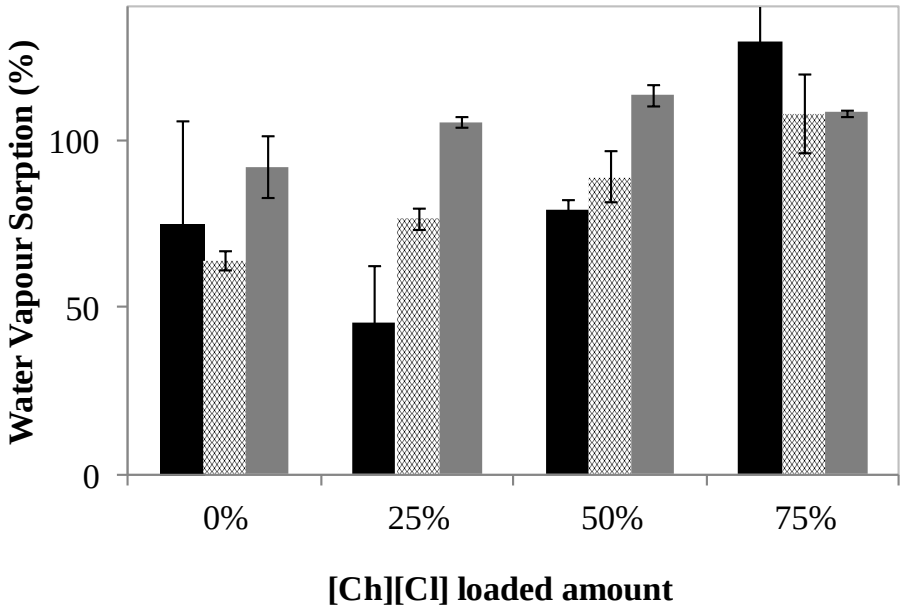

Figure 18. Water vapour sorption capacity of CS (■), CBCn (■) and CBCa (▨) films loaded with different amounts of [Ch][Cl] (measured at 37°C and 90% RH).

The WVS capacity of the films depends significantly on the film´s bulk properties (number of free interaction groups and void volume for instance) and on the interactions of those groups with water molecules. CBCn is expected to have larger void volumes (due to the alkyl chain) and consequently to absorb more water than CS what is evidenced by its relatively large WVS capacity, as can be seen in Figure 18.

The incorporation of [Ch][Cl] increases by a larger extent the WVS capacity of CS when compared to CBCn films. Taking into account that a smaller amount of IL was added to CBCn films (since the IL added ratio took into account only the number of non-substituted amino groups) it means that a larger amount of IL has to be added to CS in order to overcome the WVS capacity of CBCn (0.3409 mmol in CS over 0.1023 mmol in CBCn). By increasing the amount of IL into the CS matrix, the amount of water absorbed in the bulk is increased due to the hydrophilicity and hygroscopic behavior of the IL and also due to electrostatic repulsion that leads to an increase in the free volume and permit that more water molecules are absorbed. When more IL is added to CBCn the intrinsic hydropilicity of CBCn is not affected and the

presence of the IL may even induce higher reticulation degree that may limit the amount of water absorbed. The results obtained for CBCa are between the ones observed for CS and CBCn as can also be seen in Figure 18.

The influence of [Ch][DHP] on the WVS capacity of CS and CBCn films was compared with that induced by [Ch][Cl] for a IL loaded amount of 75%. Figure 19 shows the equilibrium water vapour sorption profiles obtained for a period of 8h. The same profile was observed until 24 hours of swelling but after this period CBCn films start to lose their physical structure and present a gel like aspect conditioned by the higher relative humidity at which films are exposed.

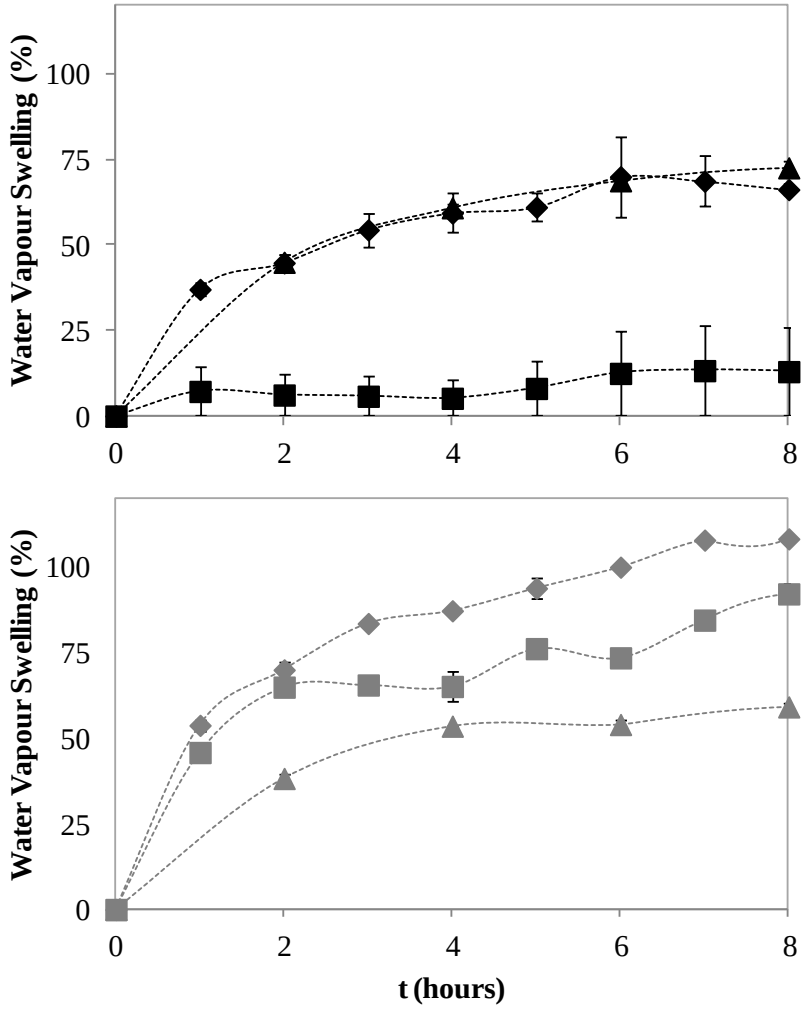

Figure 19. Equilibrium water vapour sorption capacity for non-loaded CS and CBCn films (squares) and for films loaded (75% IL) with [Ch][Cl] (diamonds) and [Ch][DHP] (triangles). Results for CS are presented in black (upper figure) and those for CBCn are presented in grey (bottom figure).

The results show a more sustained water vapour sorption capacity for CBCn films mainly due to the higher amount of hydrophilic sites and larger free volumes

that characterize this structure when compared to CS that promoted the higher capacity of CBCn films to store water needing more time to reach equilibrium. When comparing the difference between each IL it can be seen that in the case of CS both ILs behave in a similar manner and therefore that they interact with the polymer in a similar way. Thus, the nature of the IL's anion seems not to influence the WVS in CS films.

In case of CBC films, the differences between both ILs are more significant. The presence of [Ch][Cl] promoted a more sustained and higher water vapour sorption than non-loaded films while the presence of [Ch][DHP] decreases it. CBCn films containing [Ch][DHP] present a WVS profile divided in two regimes: a first part where the amount of absorbed water increases by 50% within 4 hours and a second one where a plateau is observed and that indicates the saturation of the volume available to accommodate the water molecules (Silva et al, 2008). These results seem to indicate that [Ch][DHP] induce higher reticulation degree of the CBCn matrix (though hydrogen bonding and electrostatic interaction between IL and CBC) and consequently the decrease in the number of hydrophilic groups that interact with water as well as a decrease in the size and number of void volumes that could accommodate water.

Water Vapor Permeability

The knowledge of the moisture permeability through films is of major importance when developing materials for topical drug delivery (wound dressings) or medical supplies packaging applications (Dias et al, 2011, 2; Silva et al, 2008; Garneiro-da-Cunha et al, 2010).

The water vapor permeation through polymeric materials comprehends two main phases. Water vapor firstly penetrates the available void spaces into the polymer structure (absorption) and then condensates. When equilibrium is reached the subsequent water vapor diffusion process starts. In this work the WVTR was calculated using the linear part of the plot of water mass loss against time (Appendix B) where the non-linear part corresponds to the water absorption period. The WVP was calculated from the WVTR data and considering the thickness of the films. The calculated results are presented in Table 4.

Table 4. Water Vapor Transmission Rate (WVTR) and Water Vapour Permeability (WVP) through Chitosan (CS) and N-Carboxybutylchitosan (CBCn) films loaded with [Ch][Cl] (at different molar ratios) and [Ch][DHP] (at 75%). The thickness of the wet films (stored at 90% RH) is also presented.

Film		IL	Thickness (mm)	WVTR ($g/h/m^2$)	WVP (10^{-6}) (g/h.m.kPa)
CS	0%		0.114	43.14 ± 1.87	59.51 ± 1.48
	25%		0.167	54.42 ± 2.50	16.08 ± 0.01
	50%	[Ch][Cl]	0.147	60.74 ± 1.11	15.57 ± 0.01
	75%		0.118	62.00 ± 1.78	12.92 ± 0.04
	75%	[Ch][DHP]	0.108	59.03 ± 1.97	12.80 ± 0.04
CBCn	0%		0.048	58.25 ± 5.06	4.96 ± 0.43
	25%		0.035	65.80 ± 0.11	4.01 ± 0.01
	50%	[Ch][Cl]	0.030	72.87 ± 0.16	3.89 ± 0.01
	75%		0.020	80.11 ± 0.98	2.79 ± 0.03
	75%	[Ch][DHP]	0.062	52.81 ± 0.00	5.97 ± 0.00

The results show that CBC presents higher WVTR than CS which was expected due to the already mentioned higher bulk volume of CBC that facilitates water diffusion through the film. Moreover, it is also observed that the WVTR increases when the [Ch][Cl] loaded amount increases, for both CS and CBCn films and at a similar increasing ratio, meaning that the presence of the IL facilitated the diffusion of water molecules through the film structure. This may occur because the presence of the IL increases the matrix WVS capacity, as discussed, and the absorbed water molecules may act as a plasticizer that favors polymeric chain relaxation thus providing swellability and flexibility to the films that allows an increase in the water flow (which will result in an increase in the WVTR) (Pereda et al, 2009; Olivier and Meinders, 2011). This behavior may be also attributed to weak intra and intermolecular attractive forces in the polymer matrix (Kittur et al, 1998) that lead to a less compact polymeric structure and to higher mobility of the polymer chains that may be reflected on the increase of mechanical flexibility, as presented before (mechanical analysis) (Silva et al, 2008). At high relative humidity as the ones used in this work (90% RH), extensive swelling of polysaccharides occur followed by water absorption that enhances the referred diffusion process (Kittur et al, 1998). Moreover and according to Silva et al, films with higher water content show an increase on their capacity to diffuse water since they already contain intrinsic water (Silva et al, 2008).

On the contrary, the WVP of CS films significantly decreases when [Ch][Cl] is incorporated (73%-78% after IL addition) while a more IL dependent decrease is observed for CBCn (19%-44% after IL addition). This was expected since WVP is a property that is largely dependent on several parameters that include the film's reticulation degree, number of hydrophilic available groups, bulk free volume, thickness, etc. The tendency seems to show that thinner films lead to higher WVTR but lower WVP because thinner films allow fewer interactions between polymer and water molecules. Moreover, they may experience faster saturation.

Finally it is interesting that as before [Ch][DHP] has a higher influence on the WVP of CBCn than in CS for which similar WVP values were obtained. This confirms that the influence of the IL anion is more important in the case of CBCn as it probably induce different levels of reticulation in the film structure that in this case enhances water permeance. No significant differences were found between loaded and non-loaded CBCa and CBCn films and therefore those results are not presented.

Impedance Measurements

The ionic conductivity of a polyelectrolyte is generally related to the number and to the mobility of conducting species (ions) through the polymeric matrix (Xiong et al, 2011). Recently and unlike many other materials, polymers with ability to promote ionic species diffusion may found several applications that range from photovoltaic devices to nerve cell differentiation/regeneration. As previously mentioned CS and CBC are electric-responsive polymers and may be considered as excellent examples of biopolymers suitable for many biomedical applications, as biosensors (electrical transducers), tissue engineering materials (stimuli to enhance tissue regeneration) and neural probes (electrodes) due to their interesting biocompatibility (Guimard et al, 2007).

In this work, the effect of choline based ionic liquids on the electro-responsiveness of CS and CBC films was studied. The ionic conductivity of polyelectrolyte films loaded with [Ch][Cl] (25, 50 and 75%) and [Ch][DHP] (75%) was measured by AC impedance analysis using a symmetrical cell with two steel electrodes as described in the materials and methods section. According to Wan and co-workers, hydrated membranes critically affect the ion permeability through the

polymeric structure. A membrane with high swelling index may allow ions to diffuse more easily in its swollen state (Wan et al, 2003). Therefore all the analyzed films were stored at 80% RH for 48 hours before measurements.

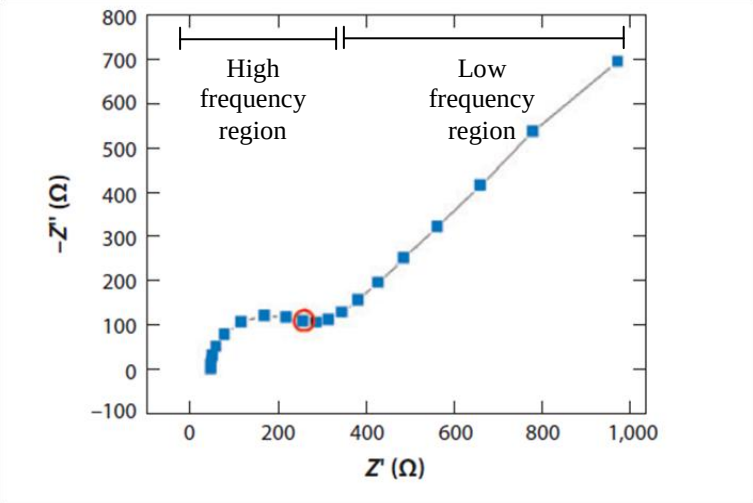

Figure 20. General Nyquist plot obtained by Electrochemical Impedance Spectroscopy (EIS).

Impedance is represented as a complex number, $Z(\omega)$, that is composed of a real (Z') and an imaginary part (Z''). If the real part is plotted on the X-axis and the imaginary part on Y-axis of a chart, a Nyquist Plot is obtained (Figure 20). In this plot, the Y-axis is negative and each point is related to the impedance at one frequency. In Nyquist plots, low frequency values are represented on the right side of the plot and higher frequencies on the left. In the low and intermediate-frequency region, the straight line with a specific slope is related to the diffusional processes inside the material (Chang and Park, 2010). The slope at 45º is representative of the Warburg Impedance (Z_D) that is the effective diffusion resistance at intermediate frequencies (Yamagata et al, 2012), and demonstrates the capacitive character of the material trough the Polarization Capacitance (CPE_{pol}) at lower frequencies. In the high frequency region, the semicircle with a specific radius is representative of the polarization resistance, related to the charge transfer reaction and double layer capacitance. The resistance of a material to the charge mobility may be evaluated by the Nyquist plot according to the slope of the straight line in low frequencies region and to the existence or not of a semicircle in the high frequencies region. A more resistive material will present larger semicircle radius and for slops lower than 45º. In the absence of the semicircle, it is said that the material has low polarization resistance and the capacitive character is privileged (Chang and Park, 2010).

The Electrochemical Impedance Spectra (EIS) of CS based materials were the ones that presented the lowest values of the impedance imaginary part, presenting higher capacitive behavior, as shown in Figure 21. The spectra registered for CS and CS loaded with 25% of [Ch][Cl] presented a small semicircle in the high frequency region (not shown), related to the charge transfer reaction and double layer capacitance, while at higher loaded IL amounts spectra began directly with diffusive lines (≈45°), all of them ending with capacitive lines presenting a angle value that increases with an increase in the IL content.

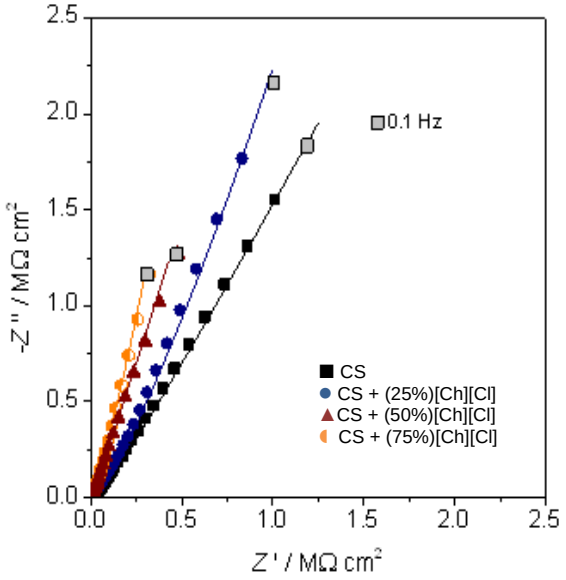

Figure 21. Electrochemical impedance spectra of model cells with CS films loaded with (0, 25, 50, 75%) [Ch][Cl] measured by fixing the perturbation amplitude (Rms voltage) at 0.35 V and applied potential at 0.1 V and varying frequencies from 0.1 to 10^6 Hz.

The equivalent circuit used to fit the spectra (Figure 22) contained a combination in parallel of a charge transfer resistance (R_{CT}) with a double layer non-ideal capacitance, expressed as a constant phase element (CPE_{DL}), in series with a Warburg resistance (Z_w) and a polarization capacitance (CPE_{pol}). The variables that compose this circuit are defined in Table 5.

Figure 22. Model of the equivalent circuit used to describe electrochemical impedance spectra obtained for CS based films.

The Warburg diffusional element, Z_D, is described by the equation: $Z_D = R_D[\text{ctg}(j\omega\tau_D)^{1/2}/(j\omega\tau_D)^{1/2}]$ and is characterized by a diffusional time constant (τ_D), diffusional pseudocapacitance (C_D) and a diffusion resistance ($R_D = \tau_D/C_D$). The constant phase element is expressed by: $\text{CPE} = \{(C\, i\omega)^{\alpha}\}^{-1}$, where C is a constant, i is the imaginary number, ω is the angular frequency and α is the angle of rotation of a purely capacitive line on the complex phase plots.

Table 5. Variables and respective definition of the elements of the equivalent circuit to describe electrochemical impedance spectra obtained for CS based films.

Variable	Definition
$\boldsymbol{R_{ct}}$ ($k\Omega cm^2$)	Charged transferred resistance at the electrode-biopolymer interface.
$\mathbf{CPE_{dl}}$ ($nFcm^{-2}s^{\alpha-1}$)	Double layer non-ideal capacitance (interface electrode-biopolymer).
$\boldsymbol{\alpha_1}$	Homogeneity/porosity of the biopolymer on surface (contact zone with the electrode).
$\boldsymbol{Z_W}$ ($k\Omega cm^2 s^{\alpha-1}$)	Warburg resistance: diffusional resistance values for intermediate frequencies.
$\boldsymbol{\tau_D}$ (s)	Diffusional time constant.
$\boldsymbol{\alpha_2}$	Mathematical parameter with physical meaning (indicates whether the Warburg resistance can be applied).
$\mathbf{CPE_{pol}}$ ($nFcm^{-2}s^{\alpha-1}$)	Polarization Capacitance: quantifies the capacitive character of the biopolymer by charge separation.
$\boldsymbol{\alpha_3}$	Homogeneity within the film.

Table 6 summarizes the resistive and capacitive elements estimated by fitting the Nyquist plots to the equivalent circuit model shown in Figure 22, for CS films.

Table 6. Components of the equivalent circuit fitted using the Nyquist plots for CS films.

Biopolymer	R_{ct} ($k\Omega cm^2$)	CPE_{dl} ($nFcm^{-2}s^{\alpha-1}$)	α_1	Z_W ($k\Omega cm^2 s^{\alpha-1}$)	τ_D (s)	α_2	CPE_{pol} ($nFcm^{-2}s^{\alpha-1}$)	α_3
CS	29.8	0.11	0.93	124.6	0.01	0.43	110	0.60
CS+[Ch][Cl](25%)	20.9	0.20	0.9	3.7	0.001	0.49	150	0.62
CS+[Ch][Cl](50%)	-	-	-	131.3	0.03	0.46	280	0.72
CS+[Ch][Cl](75%)				33.1	0.0042	0.43	280	0.75
CS+[Ch][DHP](75%)	0.015	2400	0.59				403.9	0.83
CS_washed	286.3	0.01	0.96	2390.1	0.098	0.43	27.3	0.68
CS+[Ch][Cl](75%)washed				108.5	0.023	0.49	190.2	0.68
CS+[Ch][DHP](75%)washed	1.4	0.021	0.87				52.5	0.69

The spectra obtained for CS+25%[Ch][Cl] was fitted to the same equivalent circuit used for non-loaded CS and that is represented in Figure 22, while the circuit applied to describe CS+50%[Ch][Cl] and CS+75%[Ch][Cl] systems did not contain the R_{CT} and CPE_{DL} elements, as expected since their spectra do not have the semicircle in the high frequency region.

As can be seen in Table 6, the R_{CT} and Z_w values decrease while CPE_{DL} and CPE_{pol} when comparing CS+25% [Ch][Cl] with non-loaded CS. This means that when the IL is added to the polymer it is possible to observe a decrease in the charge transfer resistance at the electrode-biopolymer interface and an increase in both double layer and polarization capacitance values. Z_w values show an increase when the IL amount changes increases to 50% probably because the circuit did not contained the parallel combination including R_{CT} and CPE_{DL}. However, CS+75% [Ch][Cl] films had the lowest Z_w values that decreased from 125 (for non-loaded CS) to 33 $k\Omega cm^2 s^{\alpha-1}$. This may indicate that there is a specific range for the number of available charges (charges from both polymer and IL), that favours their diffusion within the polymer at intermediate frequencies.

It was also observed that the CPE_{pol} values increase systematically with the increase in the amount of [Ch][Cl] as well as the α_3 values suggesting that the loaded biopolymer becomes more conductive and homogeneous (in terms of charge distribution) with the increase in the IL loaded amount. There are no observed

significant differences in α_1 and α_2 values, suggesting the surface and bulk homogeneity of the polymer.

The spectra measured for the CS+75% [Ch][DHP] system (Figure 23 (a)) showed a very small semicircle in the high frequency region, exhibiting a very low R_{CT} equal to 15 Ωcm^2 and a high CPE_{pol} value equal to 2.4 $\mu F cm^{-2} s^{\alpha-1}$. The polarization capacitance was higher than the one obtained for CS+75% [Ch][Cl] indicating that conductivity is enhanced when using [Ch][DHP]. This may be because this IL is more homogenously dispersed through the film, since it may interact by hydrogen bonding with both the cation and the anion, creating a more uniformly dispersed charge distribution network that enhances conductivity.

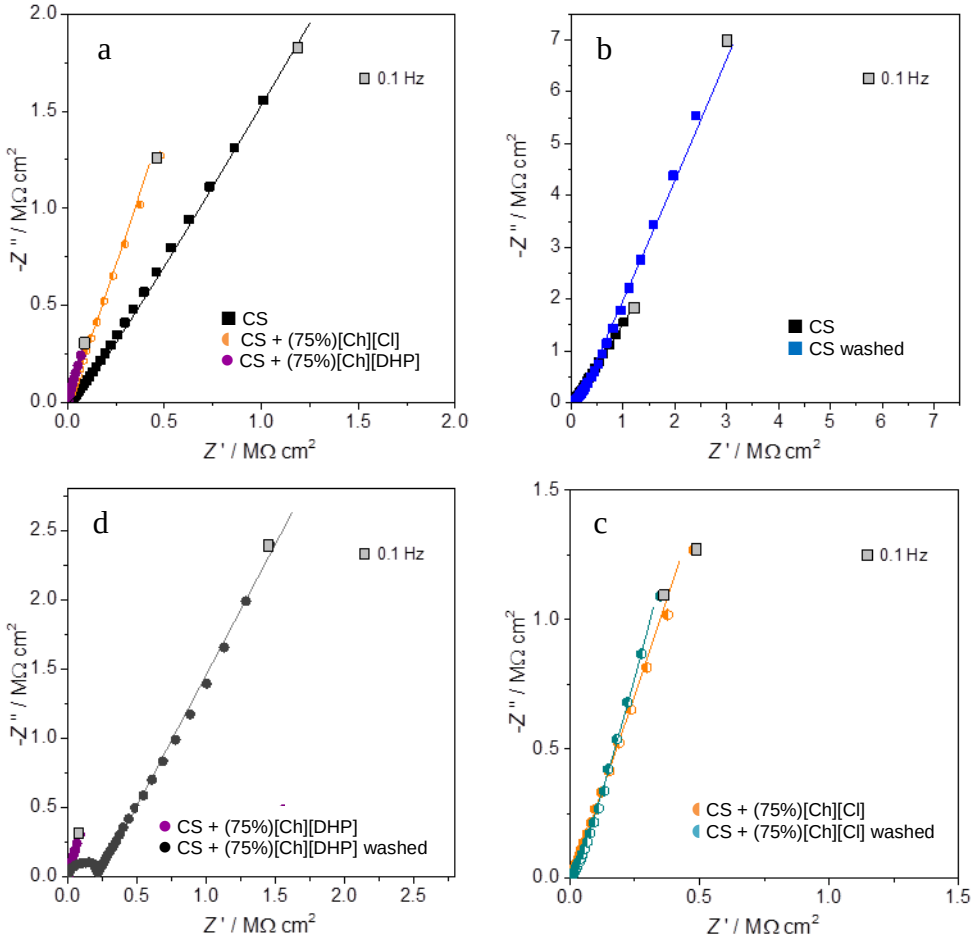

Figure 23. Comparison of the electrochemical impedance spectra of: (a) non-loaded and 75% [Ch][Cl] and [Ch][DHP] loaded CS films; (b) non-loaded CS and non-loaded CS films that were washed with a NaOH solution to neutralize acetic acid; (c) washed and non-washed CS+75% [Ch][Cl] and (d) washed and non-washed CS+75% [Ch][DHP] films.

At this point it was questioned if the acetic acid used to dissolve chitosan and that still remains in the film is having some influence on the overall conductivity of the films. To evaluate this possible influence films of non-loaded CS and 75% [Ch][Cl] and [Ch][DHP] loaded CS films were neutralized with NaOH. Each film was immersed in 20 mL of NaOH solution (0.5 M) for approximately 10 seconds and then washed three times with bi-distilled water. The films were dried for 24 hours at 37ºC. The respective EIS spectra are presented in Figure 23 (b, c and d) and compared with the results obtained for non-washed CS films. Washed CS films lead to a drastically increase in both R_{CT} and Z_w values and also to a decrease in the double layer and polarization capacitance (Table 6) meaning that residual acetic acid was indeed enhancing the conductivity of the films. The same effect was observed for washed films loaded with IL and this effect is more evident for [Ch][DHP]. Therefore it is possible to conclude that acid acetic plays an important role on the overall conductivity capacity of CS loaded and non-loaded films. Among the non-washed CS films, the ones loaded with [Ch][DHP] present the less resistive behaviour. The opposite is found when the acetic acid is removed and in this case, the capacitive behaviour follows the tendency: CS+75%[Ch][Cl] > CS+75%[Ch][DHP] > CS. This is in accordance with data presented in the literature for imidazolium based ILs. Xing and co-authors reported that the incorporation of 1,4-bis(3-carboxymethyl-imidazolium)-1-yl butane chloride ([CBIm][Cl]) into a CS matrix increased the number of ions (H^+ and Cl^-) and the mobility of the conducting species in the polymer and that the small size of Cl^- ions gave the highest mobility compared to other used anions due to their lower molecular weight (Xiong et al, 2011). Recently Yamagata and co-workers proposed a gel electrolyte consisting in chitosan and a hydrophobic ionic liquid to develop a non aqueous electric double-layer capacitor (EDLC). Their results showed that the gel film containing 1-ethyl-3-methylimidazolium tetrafluoroborate ([EMIm][BF_4]) improved the capacitive elements, as reflected on the enhanced ionic diffusion through the gel. Moreover these authors also referred that CS itself presents a capacitive character since it is a charge carrier supplier, through amino and hydroxyl groups (Yamagata et al, 2012), which is in good agreement with the results obtained for non-loaded CS films.

The same study was performed for non-loaded and loaded CBCn films and the results are presented in Figure 24. As can be seen all spectra present a small semicircle in the high frequency region, related to the charge transfer reaction and

double layer capacitance, followed by a 45° line for CBCn and CBCn+25%[Ch][Cl] due to diffusion within the polymer. These films end with capacitive lines in low frequencies, while CBCn loaded with 50 and 75% of [Ch][Cl] present capacitive behavior at high frequencies which is related to the intrinsic capacitive properties of the films that is enhanced when the IL is added to the matrix.

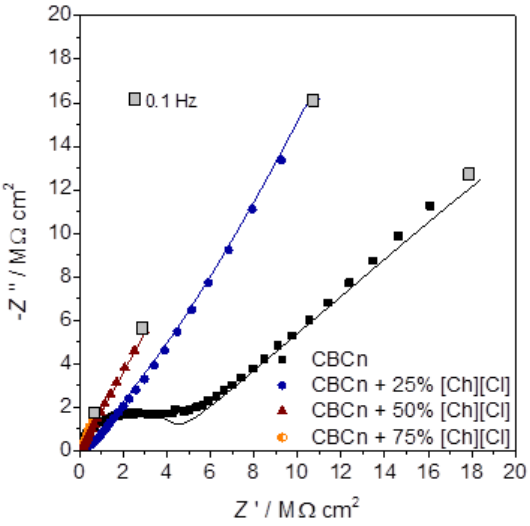

Figure 24. Electrochemical impedance spectra of model cells with CBCn films loaded with (0, 25, 50, 75%) [Ch][Cl] measured by fixing the perturbation amplitude (Rms voltage) at 0.35 V and applied potential at 0.1 V and varying frequencies from 0.1 to 10^6 Hz.

The equivalent circuit used for CBCn systems was the same used before for CS (Figure 22). As can be seen in Table 7, results show that there is a decrease in the charge transfer resistance at the electrode-biopolymer interface, and an increase in both, double layer and polarization capacitance values (CPE_{DL} and CPE_{pol}) when the amount of loaded [Ch][Cl] increases. The decrease in α_1 values suggests a decrease in the homogeneity at the outer parts of the polymer when the IL content increases, while the increase in the α_2 values indicate higher homogeneity in the bulk with an increase in the IL concentration.

Table 7. Components of the equivalent circuit fitted using the Nyquist plots for CBCn films.

Biopolymer	R_{ct} ($M\Omega cm^2$)	CPE_{dl} ($pFcm^{-2}s^{\alpha-1}$)	α_1	Z_W ($M\Omega cm^2 s^{\alpha-1}$)	τ_D (s)	α_2	CPE_{pol} ($nFcm^{-2}s^{\alpha-1}$)	α_3
CBCn	93.75	5.4	0.94	1375	4.4	0.45		
CBCn+[Ch][Cl](25%)	11.06	11.9	0.92	28.6	0.9	0.5	2.5	0.61
CBCn+[Ch][Cl](50%)	1.37	69.0	0.81	-	-	-	6.3	0.68
CBCn+[Ch][Cl](75%)	0.28	72.0	0.82				34.0	0.77
CBCn+[Ch][DHP](75%)				454.4	0.62	0.41	142.0	0.80

Lower R_{CT} and higher CPE_{DL} and CPE_{pol} values are attributed to CBCn films loaded with the higher amount of IL (CBCn+75% [Ch][Cl]), and therefore these are the films that present lower resistance to charge transfer.

Data measured for CBCn films loaded with [Ch][DHP] where fitted without the use of a R_{CT}, considering that the spectra begins directly with a 45º line and follows with a capacitive line for lower frequencies (Figure 25). The polarization capacitance adjusted for the system with [Ch][DHP] was 3 times that for [Ch][Cl] suggesting enhanced charge conductivity within the CBCn+75% [Ch][DHP] system.

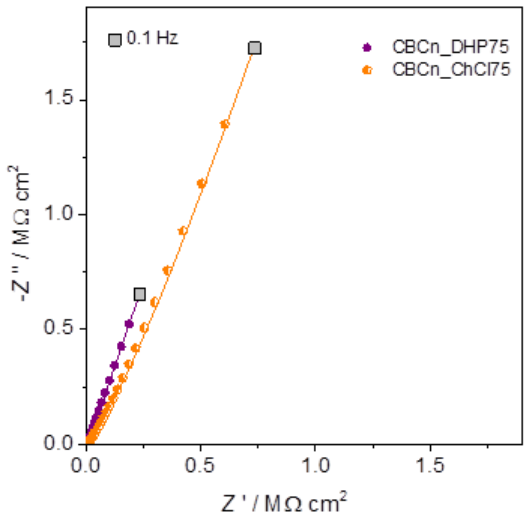

Figure 25. Electrochemical impedance spectra of model cells with CBCn films loaded with 75% of [Ch][Cl] and [Ch][DHP] measured by fixing the perturbation amplitude (Rms voltage) at 0.35 V and applied potential at 0.1 V and varying frequencies from 0.1 to 10^6 Hz.

This study was also performed for CBCa samples in order to check possible differences on the impedance values due to the presence of a higher number of non-substituted protonated amino groups in the polymer chain. The EIS spectra measured

for these systems are presented in Figure 26 and they show that the profiles obtained for CBCa are very similar to the ones obtained for CBCn with the difference that the imaginary impedance values were significantly lower, suggesting an overall better conductivity for CBCa based films. As before, an increase in the [Ch][Cl] loaded amount leads to the decrease of the imaginary impedance values and to higher angle values for the capacitive lines meaning that the presence of the IL favours the capacitive character of the films trough charge distribution homogeneity and mobility. This may be due to the higher ability of IL chloride anions move across polymeric matrix, interacting with charged amino groups.

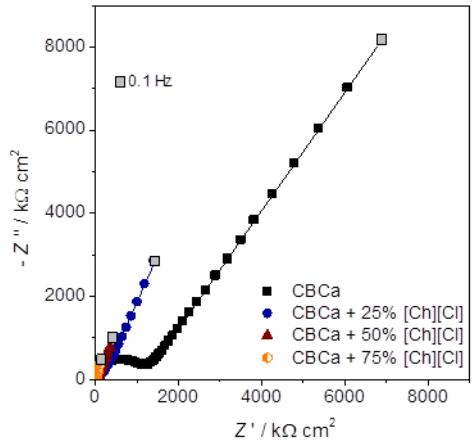

Figure 26. Electrochemical impedance spectra of model cells with CBCa films loaded with (0, 25, 50, 75%) [Ch][Cl] measured by fixing the perturbation amplitude (Rms voltage) at 0.35 V and applied potential at 0.1 V and varying frequencies from 0.1 to 10^6 Hz.

The equivalent circuit used to fit these spectra was the same used before for CS and CBCn films and the results are presented in Table 8. In this case the R_{CT} values decrease significantly with an increase in the IL loaded amount, from 4400 (non-loaded CBCa) to 0.7 kΩcm^2 (CBCa+75% [Ch][Cl]). The diffusional resistance values, Z_w, are much lower than the $R_{CT,}$ which indicate an easier diffusion of charges within the polymer matrix that are loaded with IL.

The different order of magnitudes of CPE_{DL} values (pFcm^{-2}s$^{\alpha-1}$) compared to the ones for CPE_{pol} (μFcm^{-2}s$^{\alpha-1}$) indicate that the intrinsic capacitance of CBCa films loaded with[Ch][Cl] is much higher than the double layer capacitance, which increases when the IL amount increases, while the polarization first decrease for the CBCa+25% [Ch][Cl] film and then increases. This first drop in the CPE_{pol} values may occur due to the fact that the CBCa+25%[Ch][Cl]spectra were fitted with an equivalent circuit which contained a Warburg element, which also includes a

diffusional pseudocapacitance (CD) beside the diffusion resistance ($R_D=\tau_D/C_D$), while the CBCa spectra do not include this element. The need to use different elements to describe the system with 25% IL may indicate that at lower amounts the IL is responsible for a low double layer capacitance, meaning that these films are much more resistive at surface.

As also observed for the CBCn based films, lower R_{CT} and higher $CPE_{DL,}$ and CPE_{pol} are attributed to CBCa films containing the highest IL amount (75% of [Ch][Cl]). The effect of [Ch][DHP] on impedance measurements was not studied for CBCa samples.

Table 8. Components of the equivalent circuit fitted using the Nyquist plots for CBCa films.

Biopolymer	R_{ct} ($k\Omega cm^2$)	CPE_{dl} ($pFcm^{-2}s^{\alpha-1}$)	α_1	Z_W ($\Omega cm^2 s^{\alpha-1}$)	τ_D (s)	α_2	CPE_{pol} ($\mu Fcm^{-2}s^{\alpha-1}$)	α_3
CBCa	4400	84	0.89	-	-	-	0.03	0.61
CBCa+[Ch][Cl](25%)	162.6	32	0.92	1631.7	0.33	0.38	0.16	0.7
CBCa+[Ch][Cl](50%)	7.3	94	0.94	307.3	0.09	0.41	0.53	0.66
CBCa+[Ch][Cl](75%)	0.7	131	0.95	122.0	0.1	0.47	4.39	0.69

To resume the results presented above it can be said that CS based bio-polyelectrolytes were the ones that presented the better capacitive behaviour (lowest values of the impedance imaginary part). This tendency was followed by CBCa based systems and finally by CBCn films due to the absence of acetic acid and due to the number of charged amino groups that are responsible for charge transfer within the films. CS washed films are still less resistive compared to CBCn, according to the Warburg resistance (Z_w), which may be indicative that amino groups play a crucial role on charge mobility and diffusion. The increase in the amount of loaded IL potentiates this effect, promoting the capacitive behavior, due to charge separation between protonated amino groups of the polymer and IL anion. Indeed, CPE_{pol} values are higher for CS films and increase with the amount of IL added. The difference between the values obtained for CS and CBCn systems may be due to fact that CBCn films present a minor number of amino groups compared to CS because of its higher DS. In this way, the amount of IL added to CBCn films, based on molar fraction, was

lower than the amount added to CS, and thus the effect promoted by this additive is not so pronounced.

The results obtained for non washed CS and CBCn films loaded with 75% of [Ch][DHP] showed higher capacitive behavior when compared to films containing the same amount of [Ch][Cl]. However in the case of CS washed films, the IL containing Cl^- have a more capacitive behavior compared to films still containing acetic acid, which is consistent with Xiong and co-authors, as already mentioned, since they showed that small IL anions favor the capacitive effect due to their higher mobility.

Water Swelling

Swelling is one of the most important properties of CS films that strongly influence its use for biomedical applications (Baskar et al, 2009). In fact, for most pharmaceutical applications it is important to know the swelling kinetic of the hydrogels, since it has direct impact on the behaviour of most drug release/delivery systems (Martínez-Ruvalcaba et al, 2009; Yin et al, 2010). The swelling behavior of any polymer network depends on the nature of the polymer, its compatibility with solvents and reticulation degree. In the case of ionic networks, as CS and CBC films, swelling depends also on the matrix hydrophilicity, ionic interactions, degree of crosslinking, ionic strength and nature of counterions of swelling medium (Martínez-Ruvalcaba et al, 2009; Piérog et al, 2009). Moreover, these ionic hydrogels exhibit pH-sensitive swelling behavior because their structures contain acidic or basic (or both) pendant groups which build up a swelling osmotic pressure inside the material that is responsible for swelling (Martínez-Ruvalcaba et al, 2009).

In this work the water swelling capacities of non-loaded and IL-loaded CS and CBC films were studied at different pH conditions in order to understand the effect of these extra ionic species (different amounts and species) on the swelling behavior of these materials. Remarkable swelling changes can be observed due to the presence of different interacting species depending on the pH of the swelling medium (Pourjavadi et al, 2006). The osmostic pressure created due to the difference on charges between the internal and external solution of the polymeric network may also be affected by the addition of other ionic species, working as counter ions. In this work, ILs are the

additives which may cause this effect, and hence produce significantly different swelling behaviors on CS and CBC loaded films.

For this purpose, the equilibrium swelling of CS and CBCn films was studied at various pHs ranging from 4.0 to 10.0. The buffer solution used presented constant ionic strength (0.1M), since this parameter highly affects the equilibrium swelling (Pourjavadi et al, 2006). Besides, there was also an effort to study the swelling behavior of these films in bi-distilled water.

The aim is to evaluate if ILs can change the number of available charged groups that are present in both CS and CBC, depending on the external pH, and also if they can work as cross-linking agents that can be used as alternative biocompatible reticulation agents for CS and CBC. These results will help to understand if the addition of different amounts of ILs to polyelectrolytes may work as an extra parameter to tune the swelling behavior of these biopolymers in order to develop multi-stimuli responsive materials. These results will be also important to explain drug release profiles that will be discussed further.

Influence of pH on the ionizable groups of CS and CBC films

The pH sensitive swelling behavior of ionic hydrogels is unique and it is affected by the ionization of the functional groups along the polymer chains that react differently according to the medium pH depending on the polymer's dissociation rate constant, pKa. According to literature, the pKa of CS is around 6.3 (Spinks et al, 2006; Bhumkar et al, 2006). As previously described, the dissociation rate constant of CBC was determined experimentally in this work and it presents two pKa values around 3.2 and 7.7. A schematic illustration of the pH sensitive behavior of CS and CBC films is shown in Figure 27.

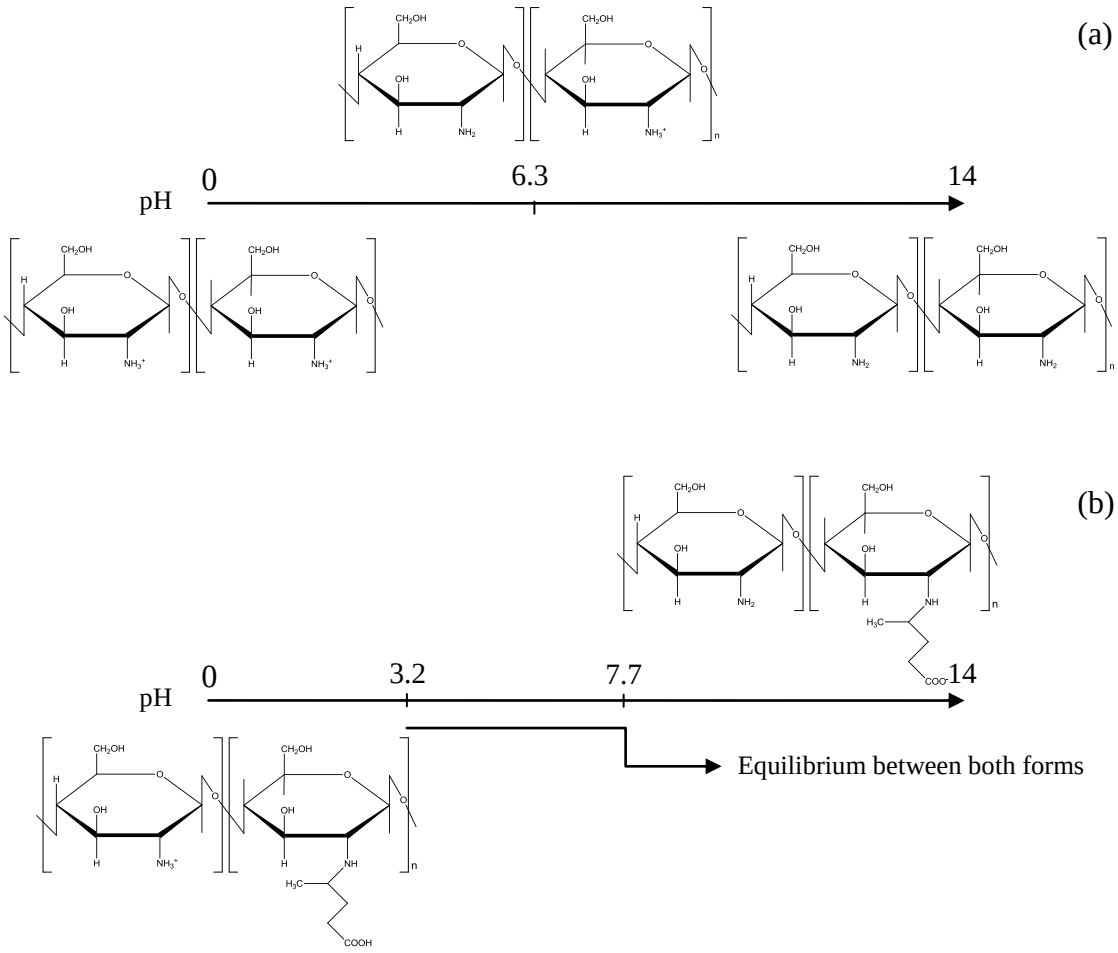

Figure 27. Dissociation rate constants, pKa, of CS (a) and CBC (b). The pKa of CS was taken from the literature (Spinks et al, 2006; Bhumkar et al, 2006). The values presented for CBC were determined experimentally by potentiometric titration.

Based upon the pKa of CS (~6.3), the species involved are NH_3^+ for pH below its pKa and NH_2 for pH values above it. Under acidic medium, the swelling of CS is mainly controlled by the amino group on the C-2 position of the chitosan monomer (Pourjavadi et al, 2006). Indeed, CS is a weak base that may be protonated, leading to an increase on charge density. The resultant osmostic pressure is exacerbated inside the polymer matrix due to NH_3^+-NH_3^+ electrostatic repulsions (Bhumkar et al, 2006; Pourjavadi et al, 2006). This pH dependent behavior justifies the dissolution of this polycation in acidic environments (Pourjavadi et al, 2006).

In case of CBC, the introduction of the also ionisable carboxylic groups (COOH) allowed the coexistence of both cationic and anionic charges at a certain pH range (between 3.2 and 7.7) and therefore it may be considered a polyampholyte. Again, its sensitive behaviour is related to its pKa values as shown in Figure 27: at pH below 3.2, amino and carboxylic groups are both protonated (NH_3^+ and COOH,

respectively) while the species involved at pH values above 7.7 are NH_2 and COO^-. At intermediate pH (3.2 < pH < 7.7), which includes to the resultant pH of synthesis for CBC (pH~4.6), there is an equilibrium between all the species.

Swelling of non-loaded and IL-loaded CS and CBCn films swelling at pH 10

At pH 10, CS and CBCn loaded and non-loaded films do not experiment dissolution and its swelling behavior corresponds to a stable process. The swelling capacity of CS at pH 10 is presented in Figure 28. At this conditions, and according to its pKa, the species involved are exclusively unionized amino groups (NH_2) which means that ionic repulsions between charged groups are minimized and the amount of water that enters into the polymeric matrix is low (when compared with lower pHs) (Martínez-Ruvalcaba et al, 2009; Pourjavadi et al, 2006). As a consequence hydrogen bonding between functional groups, NH_2-NH_2 and NH_2-OH, is favored leading to a more compact structure characterized by a lower equilibrium water swelling capacity.

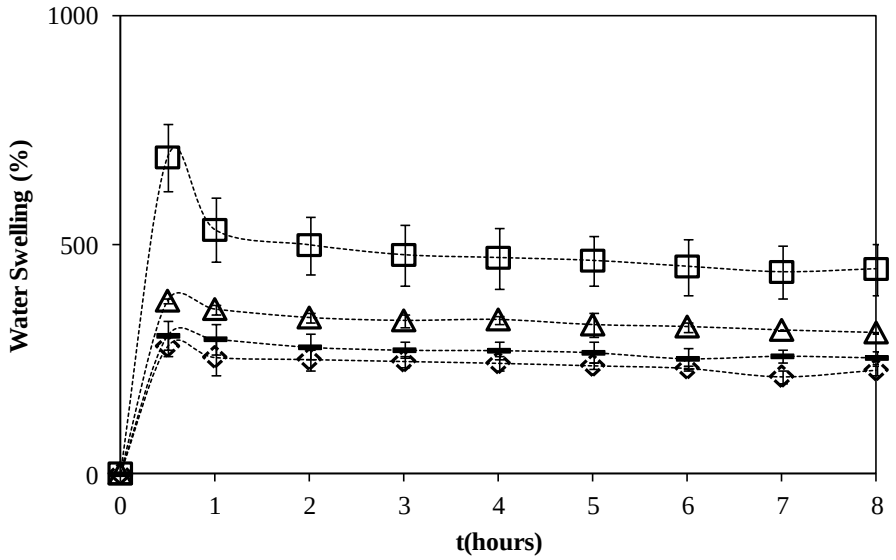

Figure 28. Water swelling kinetics for non-loaded and loaded CS films with different molar ratios of [Ch][Cl]: non loaded CS (□) and 25% (△), 50% (◊) and 75% [Ch][Cl] loaded CS films (—), at pH 10 and constant ionic strength (0.1M).

The swelling profile of non-loaded CS shows the existence of an overshooting effect during swelling: the swelling curve attain a maximum and then decrease until the swelling equilibrium. According to Yin and co-authors, this effect is explained taking into account the dynamic interactions that are established within the polymer matrix and external medium. At the initial state (t=0h) films present dry and collapsed

network with some retained acetic acid molecules. Acetic acid itself may induce some osmotic gradient that enhance water swelling. However, as soon as the network gets hydrated, osmotic pressure starts to be the ruling factor as water is spelled out from the matrix to compensate/dilute the larger charges gradient promoted by the Na^+ and CO_3^{2-} from the buffer. Since the water content of the structure is higher than the equilibrium value, the water is released (Yin et al, 2010) and it can be said that the equilibrium swelling behavior of non-loaded CS at pH is around 450 %.

The influence of different amounts of [Ch][Cl] on the swelling kinetics is also presented in Figure 28 where it is clear that the presence of the IL into the CS films induces a decrease in its swelling capacity. Theoretically at basic conditions, the number and type of possible interactions that may exist between CS and [Ch][Cl] are schematized in Figure 29**Erro! A origem da referência não foi encontrada.**.

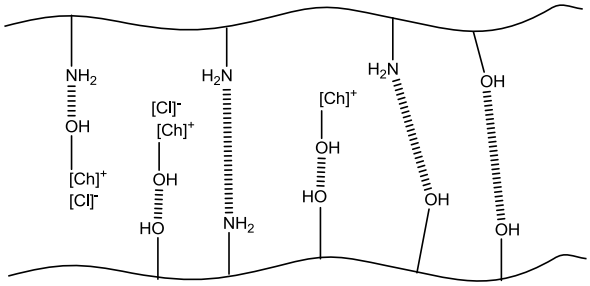

Figure 29. Esquematic representation of the possible interactions that may exist between CS chains and [Ch][Cl], at pH 10**.**

According to this scheme it may be assumed that in this case the IL is not working as a cross-linking agent since the main possible polymer-IL interactions are due to hydrogen bonding between the cation and the hydrophilic OH and NH_2 from the polymer. Therefore, the effect of the IL is to decrease the osmotic pressure between the polymer network and the buffer solution (when comparing to non-loaded CS films) with a consequent decrease (almost 50%) in the swelling capacity of the IL loaded film. The effect of [Ch][DHP] on the swelling capacity of CS at pH 10 is shown in Figure 30.

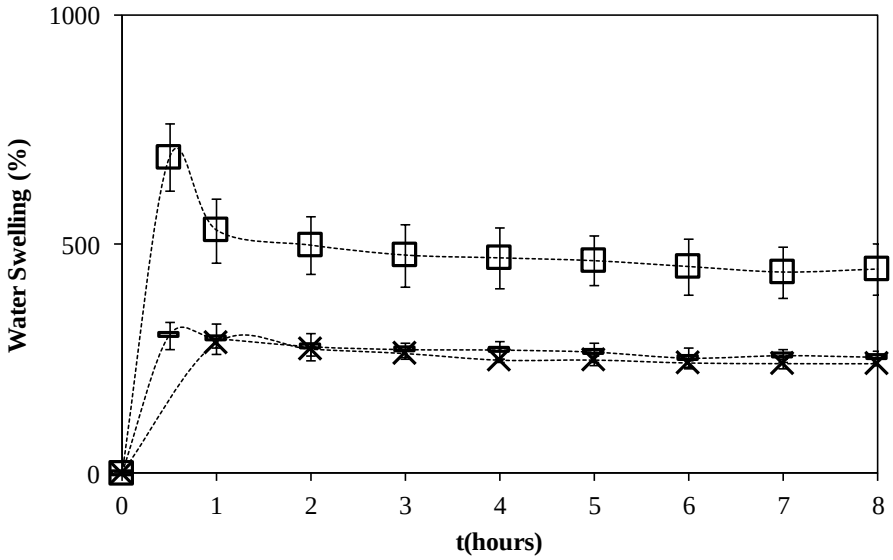

Figure 30. Water swelling kinetics for non-loaded CS (□) and CS films loaded with 75% (molar fraction) of [Ch][Cl] (—) and [Ch][DHP] (X), at pH 10.

The results show that there is no significant differences between the swelling behavior of CS films loaded with [Ch][Cl] and [Ch][DHP]. Moreover in both cases the overshooting effect is almost null comparing to non-loaded films. This is because both ILs induce a similar osmostic pressure difference between the polymer network (containing IL) and the buffer solution and that both ILs interact similarly with CS. It could be possible that the anion $[DHP]^-$ could also interact through hydrogen bonding with the OH and NH_2 from the polymer chain. However this would lead to different interactions, including higher reticulation degree that would affect the swelling capacity of the film which was not observed. This may occur because the IL cation-anion electrostatic interaction is stronger than hydrogen bonding between anion/cation and OH/NH_2 groups.

FTIR-ATR analysis was performed to identify the referred hydrogen bonding interactions and to verify if the IL is leached from the polymer matrix during swelling (Appendix C). The analysis showed that there were modifications in peaks in the range between 1600 and 1300 cm^{-1} for both non loaded and loaded CS films which may confirm that new interactions are established within the structures due to the influence of the medium pH and as discussed before. However the spectra also show that some IL is leached during swelling, since its characteristic peak (at 952 cm^{-1} for the IL's cation) is not present for the samples analyzed after swelling. Future work

should consider the grafting of the IL to the polymer to avoid leaching depending on the envisaged applications.

The swelling capacity of loaded and non-loaded CBCn films is presented in Figure 31. As discussed before, at pH 10, the amino groups are deprotonated (NH_2) and the carboxylic acid groups ionized (COO^-) and therefore CBCn behaves as an anionic hydrogel.

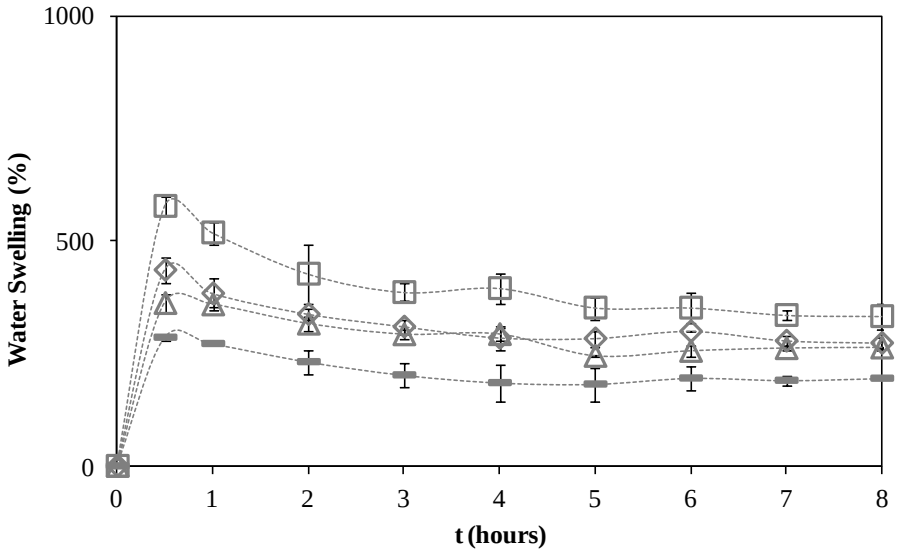

Figure 31. Water swelling kinetics for non-loaded and loaded CBCn films with different molar ratios of [Ch][Cl]: non loaded CBCn (□) and 25% (△), 50% (◊) and 75% [Ch][Cl] loaded CS films (—), at pH 10 and constant ionic strength (0.1M).

At basic pH CBCn presents a swelling capacity that is lower (about 30%) than that of CS films. Despite that, the same tendency is found for films loaded with increasing amounts of [Ch][Cl] and the overshooting effect on the first hour is also observed. When the carboxylic acid groups become ionized, an electrostatic repulsive force is generated between the negatively charged sites, increasing the swelling capacity. However, the presence of ions into the buffer solution induces a decrease in the osmotic pressure between the hydrogel and the medium, which limits the swelling capacity of CBCn. Moreover Na^+ from the buffer solution may also shield some of the COO^- groups from CBCn leading to a decrease in the water swelling capacity of the hydrogel since electrostatic COO^- - COO^- repulsions are minimized. These results are in good agreement with the ones obtained by Pourjavadi and co-authors that studied the super-absorbency and pH-sensitivity of partially hydrolyzed Chitosan-g-poly(Acrylamide) hydrogels (Pourjavadi et al, 2006).

As can be also seen in Figure 31, the presence of [Ch][Cl] decreases the swelling capacity of CBCn (in a IL concentration dependent manner) by two possible mechanisms: *i)* it induces cross-linking in polymeric matrix, due to hydrogen bonding and electrostatic interactions between the polymer and the IL, as shown in Figure 32 and *ii)* it increases the ionic strength inside the polymer network with a consequent decrease in the osmotic pressure between polymer bulk and external medium. On the other hand, electrostatic interactions between ionized carboxylic groups and choline cation may also decrease the electrostatic repulsions between COO^- groups.

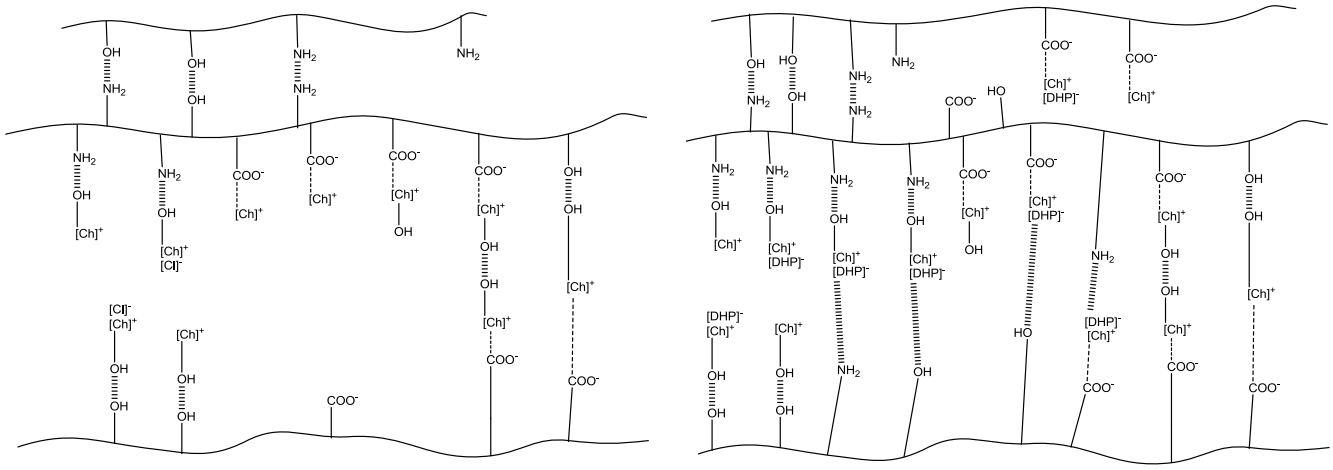

Figure 32. Esquematic representation of the possible interactions that may exist between CBCn chains and [Ch][Cl] (left) and [Ch][DHP] (right) at pH 10.

Unlike CS loaded films, the addition of [Ch][DHP] to CBCn lead to higher water sorption capacity than [Ch][Cl] (Figure 33). This may be due to an increase in the cross linking density promoted by [Ch][DHP] that decrease the ionic strength promoted by the IL within the network. Therefore the osmostic pressure between the polymer bulk and buffer solution is higher for these films and consequently their water swelling capacity.

FTIR analysis permit to identify similar modifications into peaks between 1600-1350 cm^{-1} as the ones observed for CS films, meaning that the same kind of interactions are present for CBCn. Moreover, the modifications seems to have a bigger effect on films loaded with [Ch][DHP] than [Ch][Cl] which is in accordance to the previous discussion. Leaching of some IL amount was also detected when comparing FTIR spectra measured before and after swelling.

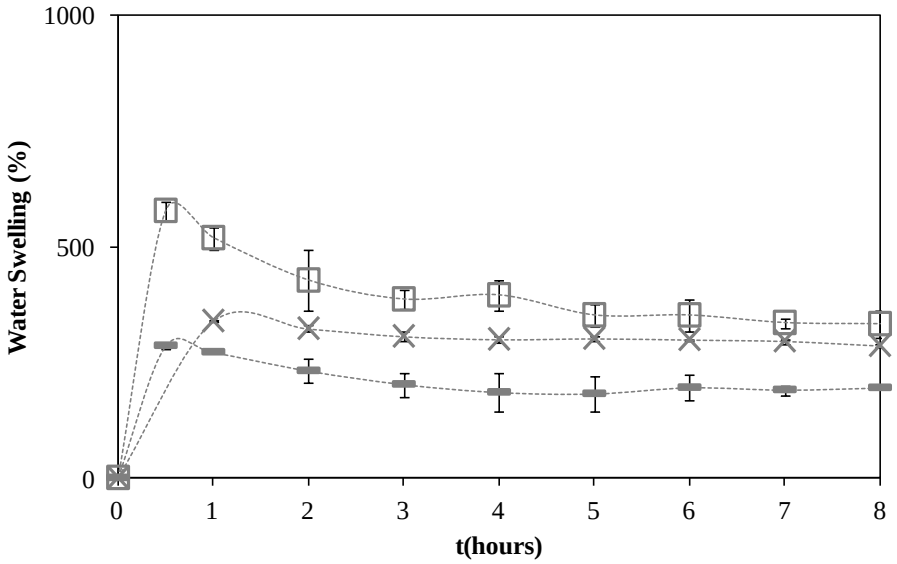

Figure 33. Water swelling kinetics for non-loaded CBCn (□) and CBCn films loaded with 75% (molar fraction) of [Ch][Cl] (—) and [Ch][DHP] (X), at pH 10.

Swelling of non-loaded and IL-loaded CS and CBC films swelling at pH 7

According to the pKa value reported in the literature for CS (6.3-6.5) at pH 7 it will have both NH_3^+ and NH_2 species. In this case, the electrostatic repulsions between the positively charged amino groups will be responsible for the higher swelling capacity of these films (Martínez-Ruvalcaba et al, 2009) which is in fact 5.5 times higher than that at basic conditions as shown in Figure 28. Moreover, these films were not neutralized and thus, the presence of acetic acid from CS dissolution may also contribute to this effect. The overshooting effect is longer at this pH condition (almost 3h) as a result of the balance between ionic repulsion that enhance water swelling and osmotic pressure between bulk and buffer. Moreover, a shield effect may also occur between CO_3^{2-} anions from the buffer and protonated amino groups leading to a decrease in the number of electrostatic repulsions. Both factors lead to an equilibrium value that is lower than 3.3 times lower than the initial swelling burst. The larger errors obtained after 6h of immersion and the slight decrease in the water swelling capacity may indicate that the film is dissolving (Baskar et al, 2009).

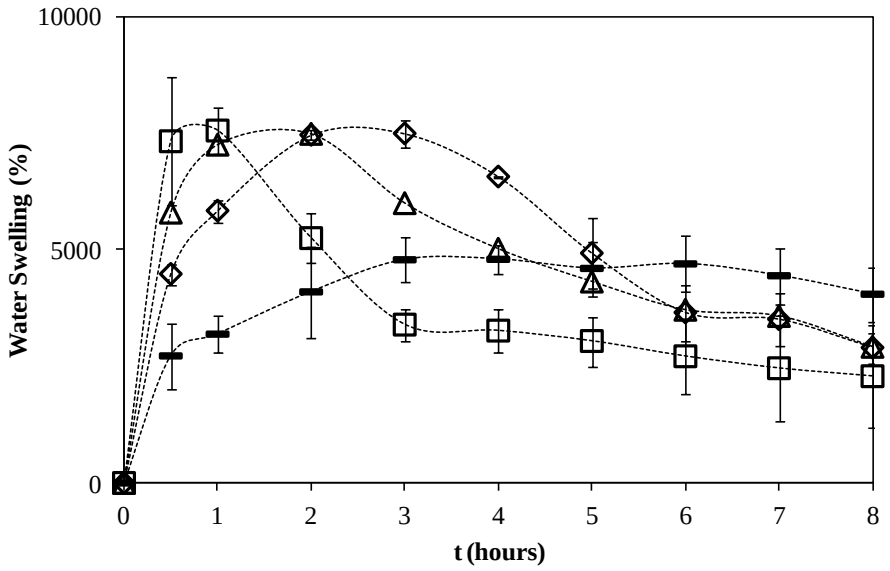

Figure 34. Water swelling kinetics for non-loaded and loaded CS films with different molar ratios of [Ch][Cl]: non loaded CS (□) and 25% (△), 50% (◊) and 75% [Ch][Cl] loaded CS films (—), at pH 7 and constant ionic strength (0.1M).

Films loaded with 25 and 50% of [Ch][Cl] exhibit a prolonged overshooting effect because the effect of the osmotic pressure is delayed as more charges are added to the polymer network (since the osmotic pressure decreases). At 75% of IL loaded amount the overshooting effect disappears due to the following combination of factors: *i)* the reticulation degree promoted by the IL increases as shown in Figure 36 and which is in good agreement with the results reported by Bhumkar et al which studied the effect of cross-linking density on the swelling behavior of CS films using sodium tripolyphosphate as crooslinker (Bhumkar et al, 2006); *ii)* there is a shielding effect on the NH_3^+ groups due to the increased number of chlorine anions; *iii)* the osmotic pressure between the polymer network and the buffer is decreased meaning that the number of charges inside and outside the polymer is equilibrated.

The effect of the [DHP] anion on the swelling behavior of CS films at neutral pH is shown in Figure 35.

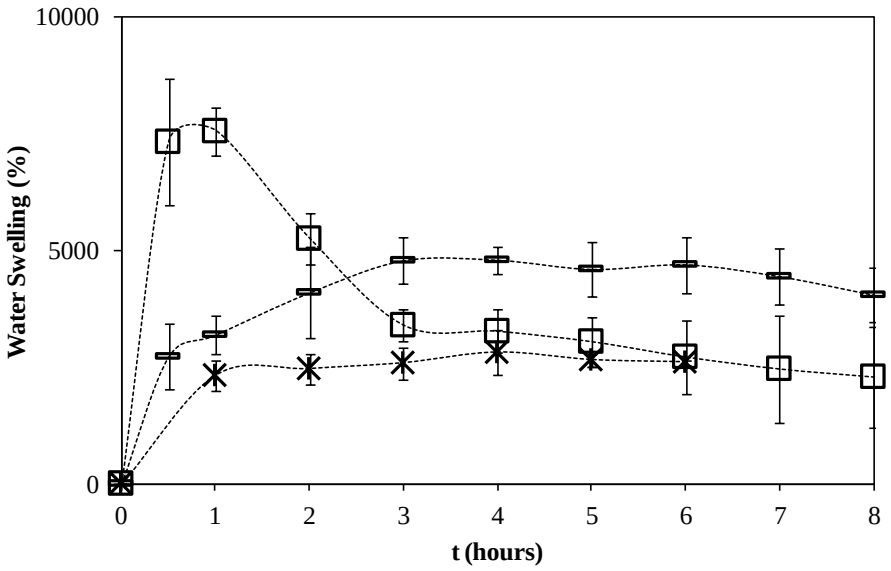

Figure 35. Water swelling kinetics for non-loaded CS (□) and CS films loaded with 75% (molar fraction) of [Ch][Cl] (—) and [Ch][DHP] (X), at pH 7.

This comparison shows that both ILs avoid the appearance of the overshooting effect and that [Ch][DHP] decreases the swelling capacity of CS at pH 7. This is most probably because this IL induces higher polymer reticulation as shown in Figure 36 which decreases the swelling capacity of the material (and considering that both ILs originate the same ionic strength into the polymer network).

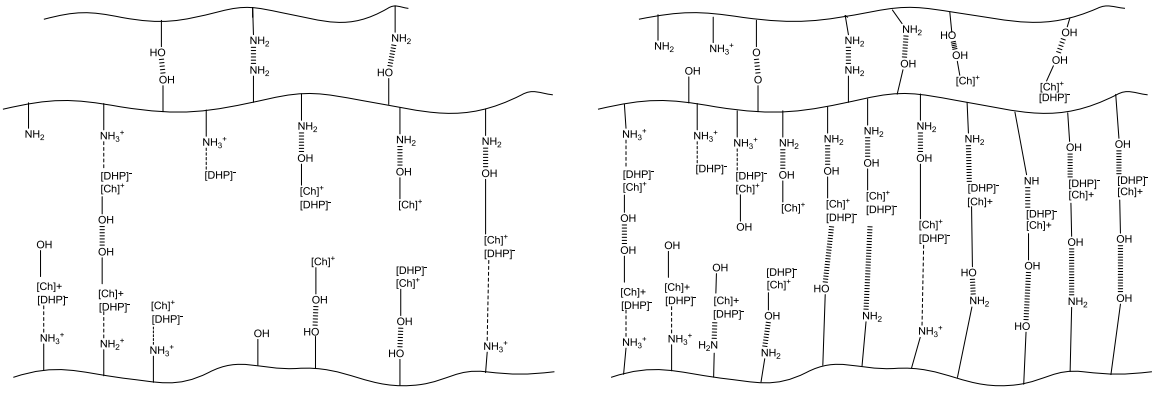

Figure 36. Esquematic representation of the possible interactions that may exist between CS chains and [Ch][Cl] (left) and [Ch][DHP] (right) at pH 7.

Owing to the higher swelling capacity of these films at this pH that was followed by jellification and dissolution it was not possible to completely recover the films after 8 hours of immersion. Thus, FTIR analysis was not performed in order to verify the assumed possible interactions.

As discussed before, at neutral pH CBCn behaves as a polyampholyte (due to the coexistence of charged and non-charged amino and carboxylic groups) as previously discussed. The higher number of electrostatic repulsions promoted by the charged groups associated with the larger void volumes between polymer chains (due to alkylation) lead to complete dissolution of the films at pH 7. When Ils are loaded to the matrix a higher reticulation was expected according to the scheme presented in Figure 37.

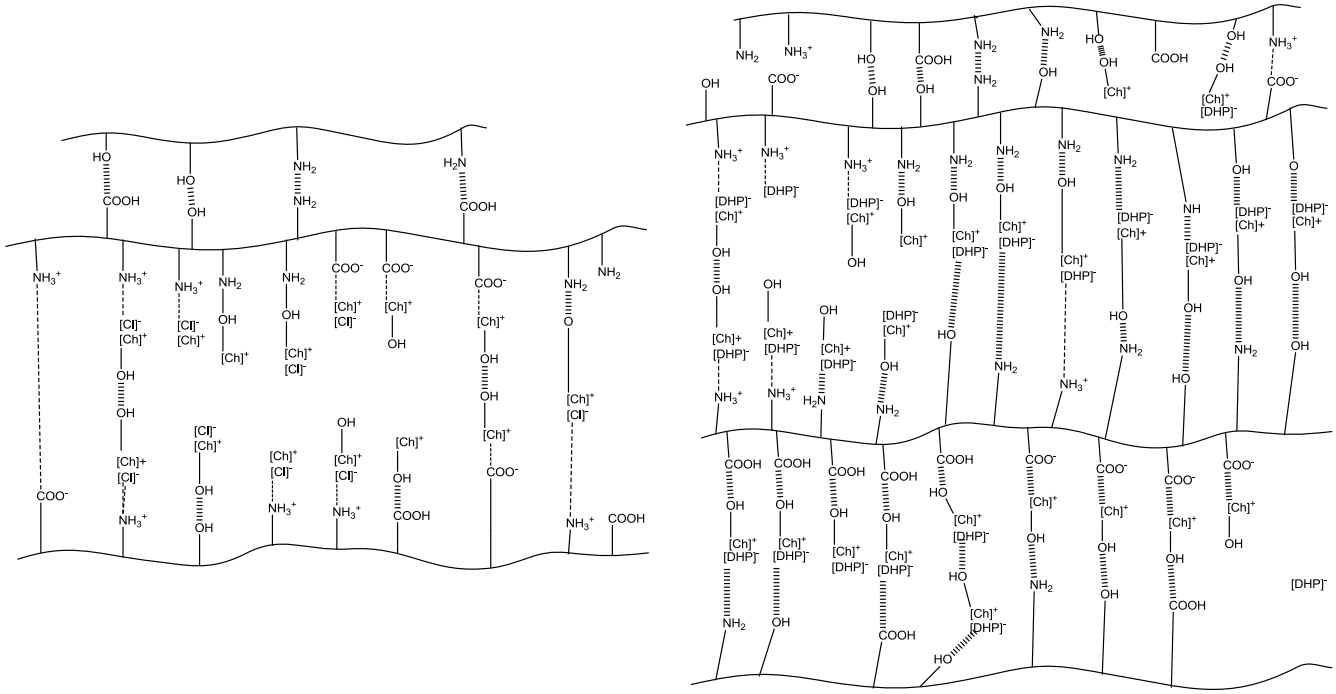

Figure 37. Esquematic representation of the possible interactions that may exist between CBCn chains [Ch][Cl] (left) and [Ch][DHP] (right) at pH 7.

However even in this case dissolution was almost instantaneously and complete. The only exception was at higher IL loaded amount for which CBCn films maintain a defined and organized structure after 8h immersion as shown in Figure 38. Even if some dissolution occurred (which limited swelling measurements) it may be concluded that at higher [Ch][Cl] loaded amount reticulation starts to compete for ionic repulsions delaying the dissolution of the film.

Figure 38. Visual aspect of a CBCn film loaded with 75% of [Ch][Cl] after 8 hours immersion at pH 7.

The dominant factor that ruled the dissolution behavior of CBCn was the repulsion between COO- groups and this was confirmed by analysis of the swelling capacity of CBCa at the same pH presented in (Figure 39).

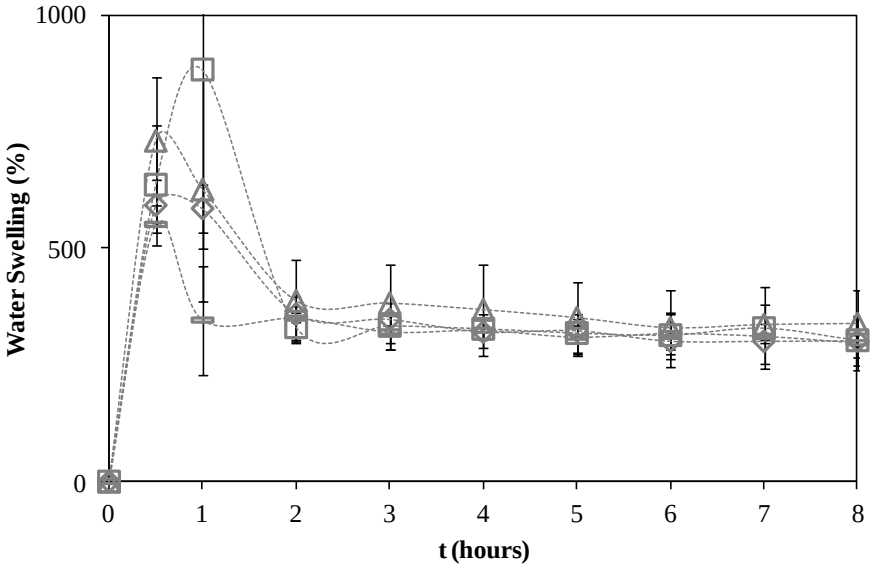

Figure 39. Water swelling kinetics for non-loaded and loaded CBCa films with different molar ratios of [Ch][Cl]: non loaded CBCa (□) and 25% (△), 50% (◊) and 75% [Ch][Cl] loaded CBCa films (—), at pH 7 and constant ionic strength (0.1M).

It can be seen that when the predominant COO^- groups are protonated the number of electrostatic repulsions is lower and hydrogen bonding may be promoted which decreases the water swelling capacity of CBCa films. The effect of [Ch][Cl] seems to be mainly a decrease in the overshooting behavior because of the differences in the ionic strength inside and outside the network, as already discussed. The effect of [Ch][DHP] in CBCa water swelling capacity was not studied.

Swelling behaviour at pH 4 and bi-distilled water

CS and CBCn loaded films experienced dissolution at acidic conditions. When the films were introduced in pH 4 buffer solution, a fast and pronounced swelling was observed with the formation of a gel that maintained its structure only for a short period of time and immediately started to dissolve. At low pH amino groups get protonated and become positively charged making transforming CS into a water soluble cationic polyelectrolyte (Dash et al, 2011; Mourya et al, 2008). In the case of CBC and according to its pKa values, at low pH NH_3^+ and COOH are the predominant species in the polymeric matrix, potentiating the solubility of these films. At this condition the reticulation induced by the presence of the ILs was not enough to avoid the matrices to dissolve.

The fast dissolution of these materials was also observed in bi-distilled water. However in this case that effect was more pronounced for non-loaded CS and CBCn films than for those containing higher amounts of [Ch][Cl] indicating that the IL is indeed reticulating the polymer chains although to a low extent that was not enough to avoid the dissolution of the films. Finally it was observed that the swelling of the films when immersed in saline (buffer) solutions was generally lower when compared to swelling measured in bi-distilled water. According to the literature, this well-known phenomenon is commonly observed in the swelling behavior of ionic hydrogels and often attributed to the effect of the additional ions that cause non-perfect electrostatic repulsions, leading to a decreased in the osmostic pressure difference between the film and the swelling medium. When the ionic strength of the external solution increases, the difference in the osmostic pressure decreases, with consequent decrease of the film's swelling capacity (Pourjavadi et al, 2006).

DXMTNa release studies

Dexamethasone (DXMT) is a drug from the glucocorticoids family with gluconeogenic, immunosuppressive and anti-inflamatory properties (Maheshi et al, 2005). It is prescribed for treatment of various inflammatory conditions, lymphomas and used in combination therapy to treat acute and delayed emesis in patients receiving chemotherapy (Maheshi et al, 2005; Cázares-Delgadillo et al, 2010). Recent literature also refers DXMT as able to induce the differentiation of masenchymal stem

cells into osteoblast lineage in vitro (Chiang et al, 2012). The poor solubility of dexamethasone is overcome by the formulation of a derivative ionic produg, sodium phosphate dexamethasone (DXMTNa) which allows rapid input after parenteral administration (Maheshi et al, 2005). This synthetic adrenocortical steroid is a white, or slightly yellow, crystalline powder, chemically named 9-fluoro-11β,17-dihydroxy-16α-methyl-21-(phosphonooxy) pregna-1, 4-diene-3,20-dione disodium salt (FDA). DXMTNa presents a phosphate ester and as a consequence two ionizable groups with pKa_1 and pKa_2 at pH 2.04 and 6.0, respectively (Cázares-Delgadillo et al, 2010). Under physiological conditions, DXMTNa exists principally as a di-anion (Cázares-Delgadillo et al, 2010) as shown in Figure 40. The knowledge of the pH sensitive behavior of DXMTNa is crucial to predict and understand its kinetic release at different pH media, since sodium phosphate groups may also interact with the polymer chains in different ways.

DXMTNa was chosen in this work as a model drug to study the potentiality of CS and CBCn films doped with biocompatible ionic liquids to originate tunable sustained release systems for charged drugs. The aim is to use ILs as compounds that can change the electrostatic repulsion/attraction between the drug and the polymer network with a direct influence on the release profile of the drug. As expected these systems will be significantly dependent on the pH of the release medium. It is well known that release from polymers is largely dependent on the materials water swelling capacities. In this work it is also aimed to see if the presence of the ILs can change the swelling dependent release profiles.

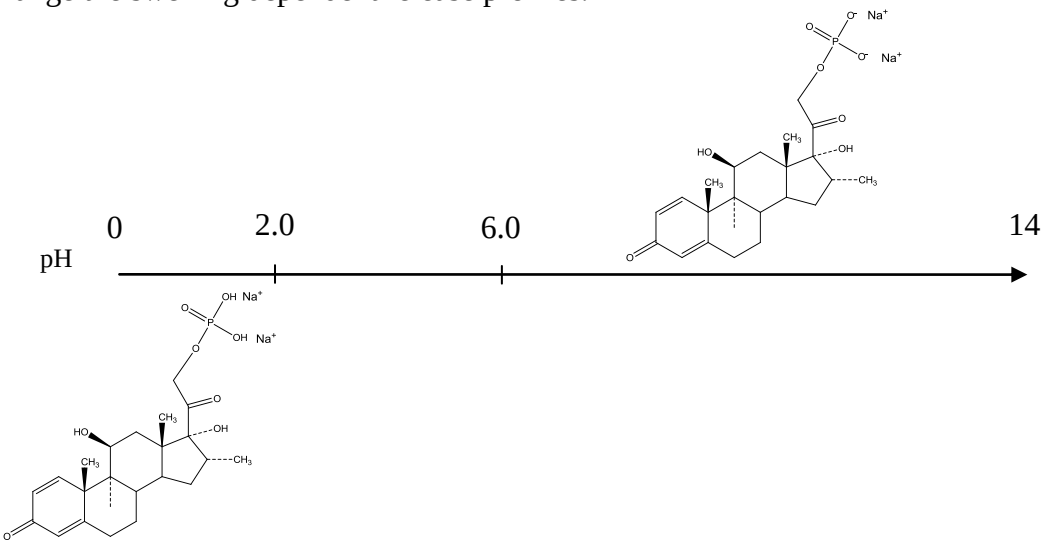

Figure 40. pH sensitive behaviour of DXMTNa according to its pKa values taken from the literature (Cázares-Delgadillo et al, 2010).

DXMTNa release kinetics at pH 10 and pH 7

The most attractive route for sustained drug release is by pH triggering. The pH gradient in the human body ranges from acidic to alkaline values. For example certain regions of human body, like stomach, present pH ranges from 1 to 3, while small intestine presents alkaline pH, between (6.6-7.5) (Bhattarai et al, 2010). In this work DXMTNa release was studied at pH 7 and 10 because the films dissolve at lower pH. At these pH conditions it was mentioned that CS and CBCn films present different swelling capacities or degradation/dissolution depending on the medium pH and amount of loaded IL and therefore different release profiles are expected for these systems. The release profiles obtained for non-loaded and loaded CS and CBCn films at pH 7 and 10 are compared in Figure 41. This study only considered the films that were loaded with the maximum IL amount (75%). The drug DXMTNa and each IL were added to the polymer solution under stirring at the same time to guarantee the effective addition of the drug and promote "competition" between both charged species (IL and drug).

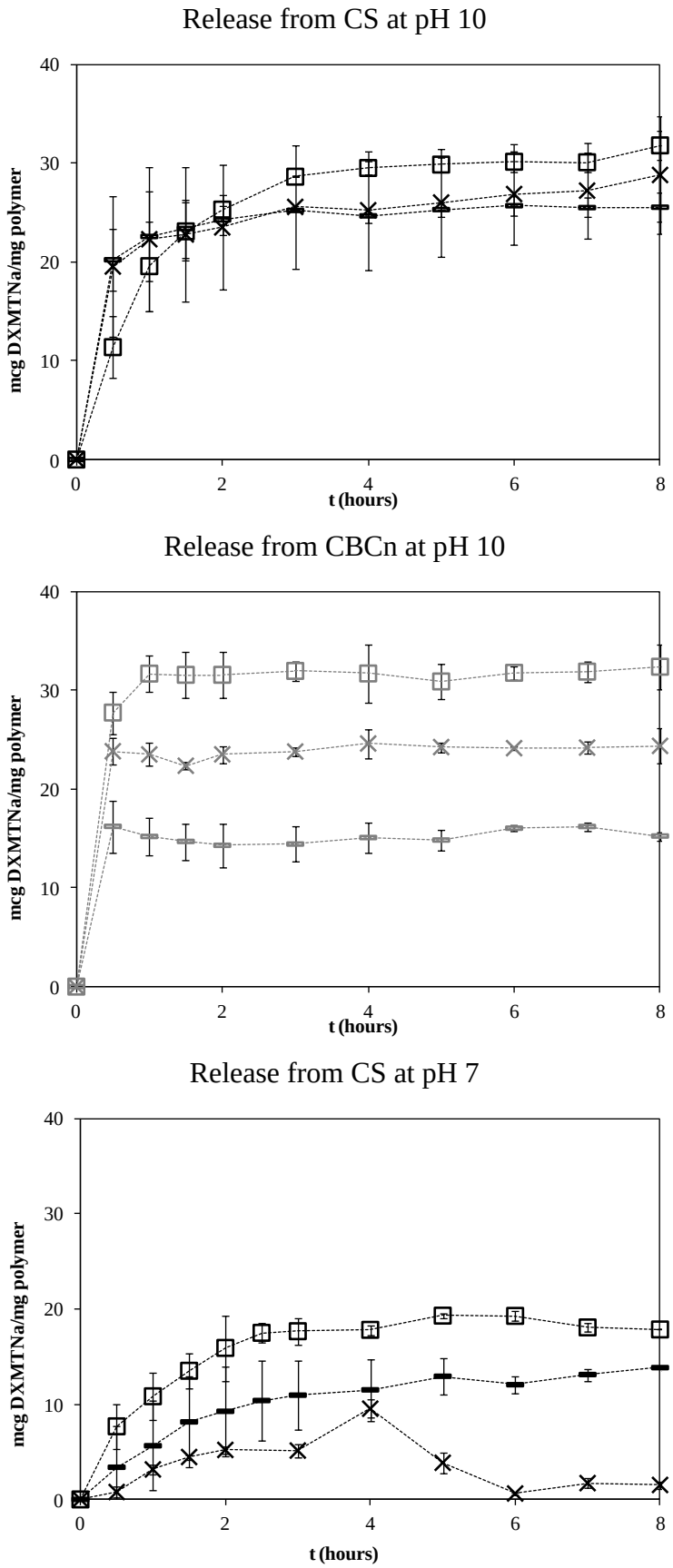

Figure 41. Release profiles for DXMTNa from CS (on top) and CBCn (middle) non-loaded films (□), loaded with 75% [Ch][Cl] (—) and loaded with 75% [Ch][DHP] (X) at pH 10 and pH 7 (bottom).

The presented release profiles are corrected values meaning that the effect of polymer dissolution into the medium was removed. This was done by subtracting the absorbance measured for drug loaded samples by the absorbance of samples without the drug and that worked as a blank.

The obtained results will be discussed in terms of drug-polymer, IL-polymer and IL-drug-polymer interactions as well as on the swelling profiles of the films. At pH 10, non-loaded CS films present a more sustained release of DXMTNa than CBCn, despite their slightly higher water swelling capacity (Figure 41). The faster release observed for CBCn may be justified by electrostatic repulsions between negative charges of non-linked sodium phosphate group of DXMTNa (PO_4^{2-}) and the acid carboxylic group of CBCn, (COO^-).

At basic pH, the effect of both ILs on the release profiles follow the tendency previously observed for the swelling results: in the case of CS both ILs decrease the swelling capacity in a similar extent (Figure 30, pp 70) while in the case of CBCn, [Ch][Cl] induced lower swelling capacity. In all cases, lower swelling lead to lower amount of released DXMTNa and this effect is particularly evident for CBCn loaded films (until 8h). Although both ILs promote a burst release it is clear that different amounts of drug are released from each film. The amount of drug released from non-loaded and loaded films after 8h is given in Table 9.

Table 9. Total amount of DXMTNa released (%) after 8h from loaded and non-loaded CS and CBCn films, at pH 10.

	CS			**CBCn**		
t (hours)	**0% IL**	**75% [Ch][Cl]**	**75% [Ch][DHP]**	**0% IL**	**75% [Ch][Cl]**	**75% [Ch][DHP]**
8	46.92	38.15	31.14	35.70	22.59	28.62

The results show that [Ch][DHP] have a higher effect on the amount of drug delivered from CS films while [Ch][Cl] has a higher effect in CBCn films. Moreover the drug is not completely released from any of the studied systems which mean that it is entrapped in the polymer network, due to its large volume, and/or interacting with the polymer chains and the IL through hydrogen bonding and electrostatic interactions. The drug that is still entrapped into the networks will be slowly released at a rate that depends on the dissolution of the film.

The observed release profiles are therefore driven by different factors/interactions that include: film's water swelling capacity, film's reticulation degree (polymer-polymer and IL-polymer) and electrostatic interactions between polymer charged groups, ILs and the ionic drug, as already mentioned. Figure 42 presents the possible interactions between polymer, [Ch][Cl] and DXMTNa at pH 10, as an example. The systems containing [Ch][DHP] instead of [Ch][Cl] may present a similar structure but the nature of sodium phosphate anion seems to induce repulsion between the IL and the drug and, thus, DXMTNa is faster released.

At neutral pH, the release profiles obtained for CS are more sustained when compared no basic pH and despite the higher swelling capacity observed at this pH. The total amount of drug delivered is even lower than at pH 10 and the lowest amount is observed for CS films loaded with [Ch][Cl] (20.48 ± 0.99 for CS and 16.31 ± 1.00 for CS loaded with [Ch][Cl]). In the case of [Ch][DHP] the films experienced dissolution after 3h analysis but they also presented an initial more sustained release. These results show that at neutral pH electrostatic interactions between the drug and the protonated amino groups from CS are also significantly affecting its release profile since results are not directly related with the swelling behavior observed for the films.

The release profiles for CBCn loaded and non-loaded films were also studied for this pH. However, due to the high dissolution/degradation, as already mentioned and according to their chaotic swelling behavior, this data present large deviation and it is impossible to make accurate conclusions from it.

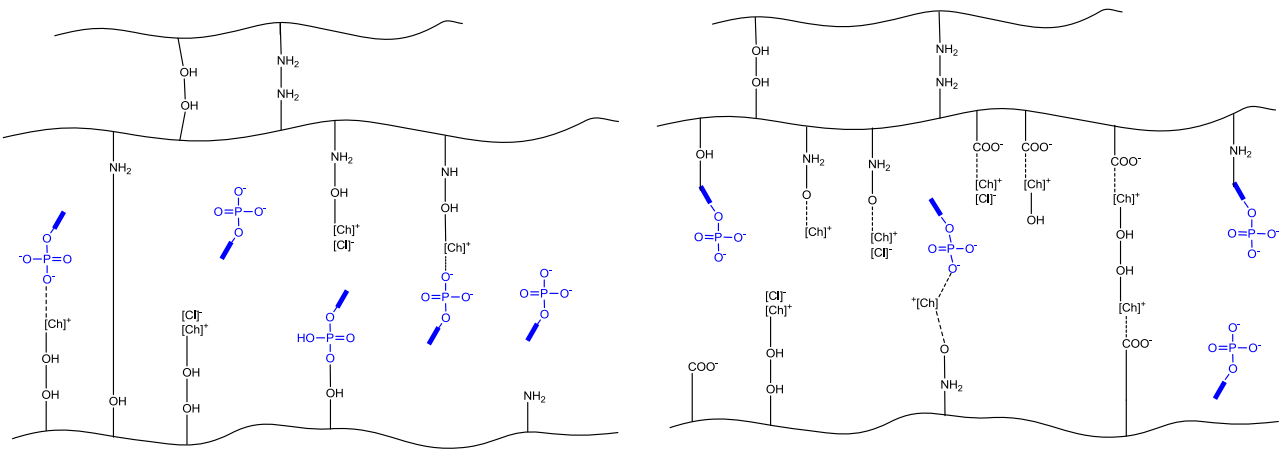

Figure 42. Possible interactions between CS (on the left) and CBCn (on the right) polymeric chains, [Ch][Cl] and DXMTNa, at pH 10.

Diffusion coefficients

The Korsmeyer-Peppas model is a simple mathematical relationship which describes the drug release profile from a polymeric system. Usually, these systems are cylindrical shaped matrices (Suvakanta et al, 2010). Since diffusion from the gel phase to the surroundings can be considered a one-dimentional isothermic process for hydrogel samples with a small thickness respect to its diameter (Martínez-Ruvalcaba et al, 2009), this kinetic model was applied to loaded and non-loaded CS and CBCn square disk samples, where the relationship between diameter and thickness allows this approximation. From Figure 41, it may be assumed that generally the release of DXMTNa from the films may be divided into two stages: an initial faster release period followed by a much slower and constant release period. The individual DXMTNa release profiles were fitted to Eqs. 8 and 9 and the correlation results are presented in Table 10.

Table 10. Correlated release kinetic parameter (n and k) and diffusion coefficients (D_1) from Eqs. (8) and (9) for DXMTNa release from loaded and non-loaded CS films at pH 10 and pH 7 and 37ºC.

	Kinetic parameters			**Diffusion coefficients (cm^{-2} h^{-1})**	
	n	k/h^{-n}	R^2	D_1 ($x10^{-7}$)	R^2
pH 10					
CS	0.646	0.576	0.970	44.46	0.968
CS+[Ch][Cl]	0.141	0.888	0.948	5.37	0.917
CS+[Ch][DHP]	0.151	0.746	0.979	4.80	0.947
pH 7					
CS	0.511	0.607	0.997	16.06	0.968
CS+[Ch][Cl]	0.526	0.661	0.995	32.22	0.992

Fickian-controlled release ($n \leq 0.5$) suggests that the release process is controlled by diffusion only, promoted by swelling for example (Dias et al, 2011), while non-Fickian diffusion ($0.5 \leq n \leq 0.89$) refers to the combination of both diffusion and polymer's relaxation or erosion controlled rate release (Martínez-Ruvalcaba et al, 2009; Suvakanta et al, 2010; Dias et al, 2011). According to the obtained n values, DXMTNa release occurred by non-Fickian-controlled release (Kuksal et al, 2006; Suvakanta et al, 2010) for CS non-loaded films, while loaded CS films are said to follow a Fickian diffusion transport mechanism, at both pH 10 and 7. These results are consistent with the water absorption capacity of these films. The

release rate constant (*k*) is normally related to profile in the first release period and it was expected to be lower for more sustained release profiles. This tendency is verified for non loaded CS films that present always the more sustained behavior (Figure 41) and lower *k* values compared to loaded films, at both pH conditions.

It was expected to obtain similar trends for the DXMTNa short-time approximation diffusion coefficients (D_1 from Eq. (9)), also presented in Table 10. However D_1 values are not consistent with *k* values and that may be indicative that the fitting done according to Eq. (9) is not appropriate for the release kinetic profiles obtained at pH 10. This may be due to the large amount of drug released on the first period of time that do not allow to obtain a proper a linear relationship that permitted to correctly calculate the diffusion coefficient (Martínez-Ruvalcaba et al, 2009). At pH 7, D_1 values are consistent with *k* in all cases and the values confirm that the addition of IL lead to higher values and therefore IL promoted a faster release of the drug from the film. The long-time approximation diffusion coefficients (D_2 from Eq. (10)) which corresponds to the fractional uptake between 60 and 100% were not calculated due to the constant release profile observed in this period.

CS/CBC composites as an alternative to improve DXMTNa sustained release

Due to the dissolution problems observed for both CS and especially for CBCn, complexes formed between CS and CBCn were prepared in order to obtain materials that are more stable at neutral conditions. It was expected that the direct interactions between the polymer chains lead to the formation of a polyelectrolyte complex (PEC) network with non-permanent structures, avoiding the use of covalent cross-linkers (Hamman, 2010) and decreasing the concern about safety in the body or cross-reactions with the drug (Bhattarai et al, 2010). A schematic representation of the possible interactions is given in Figure 43.

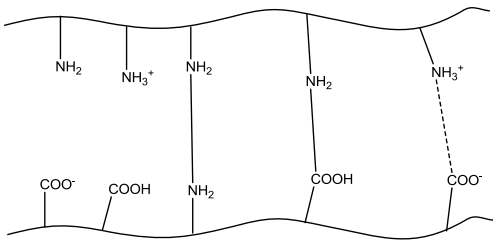

Figure 43. Possible interactions between CS and CBC characteristic groups in CS/CBC composite films.

To guarantee the maximum complexation between charged amino groups (NH_3^+) of CS and ionized carboxylic groups (COO^-) of CBCn, the pH of each solution was adjusted according to its pKa values: pH(CS) = 3.5 and pH(CBCn) = 7.7. After the addition of CBCn to the CS solution, it was observed the formation of small precipitates that disappeared after several hours of agitation. Initially this precipitates were thought to be small aggregates of complexes, however according to literature when polyelectrolytes are mixed in such a ratio that there is an excess of one charge (positive in this case), a non-stoichiometric complex is formed that is usually soluble (Hamman, 2010). Indeed, the final solution of CS/CBC was homogeneous, slightly viscous and presented an acidic pH similar to the CS (pH = 3.80), which may be due to the excess of amino groups from both polyelectrolytes. Like for CS and CBC, the composites were also loaded with 75% [Ch][Cl] and [Ch][DHP]. Same mass quantities of IL were added as for CS loaded films.

However, by FTIR-ATR analysis it was not possible to identify the characteristic electrostatic interactions or other new interactions between hydroxyl and/or amino groups from CS and carboxylic groups from CBCn. Perhaps, this could be due to the charge distribution over CBCn polymeric chains and its molecular weight, as well as to the CS/CBC mixing ratio used. According to Berger et al, PEC are formed by ionic interactions or ionically crosslinked networks that require molecules with different MW distribution (Berger et al, 2004). Therefore, it was considered that the prepared mixture corresponds to a CS/CBC physical mixture. The swelling behavior and DXMTNa release profiles for non-loaded and 75% [Ch][Cl] and [Ch][DHP] loaded composite were measured at pH7 and pH 10 and compared to the ones obtained when each polyelectrolyte is used alone.

Swelling behavior at different pH of non-loaded and loaded CS/CBC composites

The water swelling profiles for CS/CBC composite films measured at pH 10 and pH 7 are represented in Figures 44 and 45, respectively. The profiles at pH 10 are similar to the ones observed for CS and CBCn and the composite swelling capacity is similar to that of pure CBCn (approximately 330%). The addition of IL decreases the water swelling capacity of the material (as before) and the profiles are again more alike to those of CBCn.

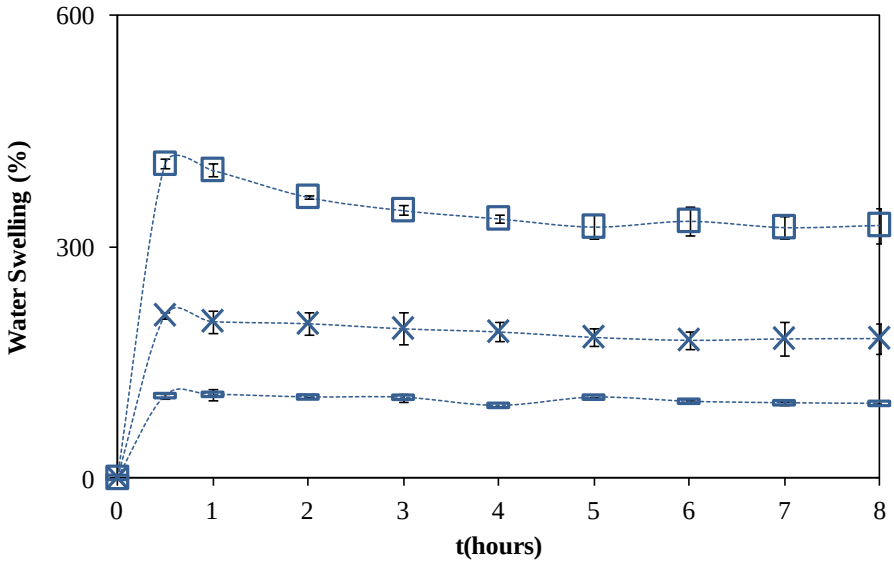

Figure 44. Water sorption kinetics for non-loaded (□) and loaded CS/CBC composite films with 75% (molar fraction) of [Ch][Cl] (—) and [Ch][DHP] (X), at pH 10.

At neutral pH, non-loaded and [Ch][DHP] loaded CS/CBC composite films experienced high degree of swelling followed by fast dissolution (Figure 45). This behavior is again similar to the one previously reported for CBCn and this may indicate that this is the predominant polymer in the composite and that probably the CS/CBCn ratio used in this work has to be optimized in order to form a more stable complex. The composite loaded with [Ch][Cl] is the most stable and do not dissolve. As before, this was the IL that permitted CBCn to resist to complete dissolution over a large time period at neutral pH (Figure 37, pp 76).

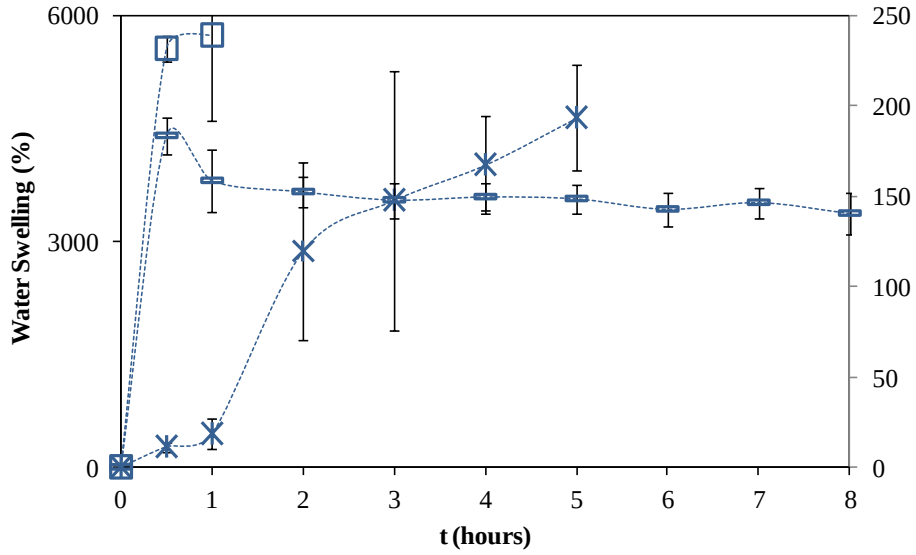

Figure 45. Water swelling kinetics for non-loaded (□) and loaded CS/CBC composite films with 75% (molar fraction) of [Ch][Cl] (—) and [Ch][DHP] (X), at pH 7. The right axis is referent to the water swelling capacity of loaded films with [Ch][Cl].

DXMTNa kinetic release at different pH

The release kinetic profile of DXMTNa from CS/CBC composite films at pH 10 do not show significant differences compared to CS non loaded films (Figure 46). However, compared to CBCn films, the composites present a more sustained release profile. Composite films loaded with IL present the same profile but a lower amount of DXMTNa is released when compared to CS loaded films, which may indicate that the drug is interacting more with the new polymeric-IL structure or that is entrapped due to the larger number of CS-CBCn interactions. The kinetic diffusion coefficients were also calculated for these systems at both pH and the results are given in Table 11.

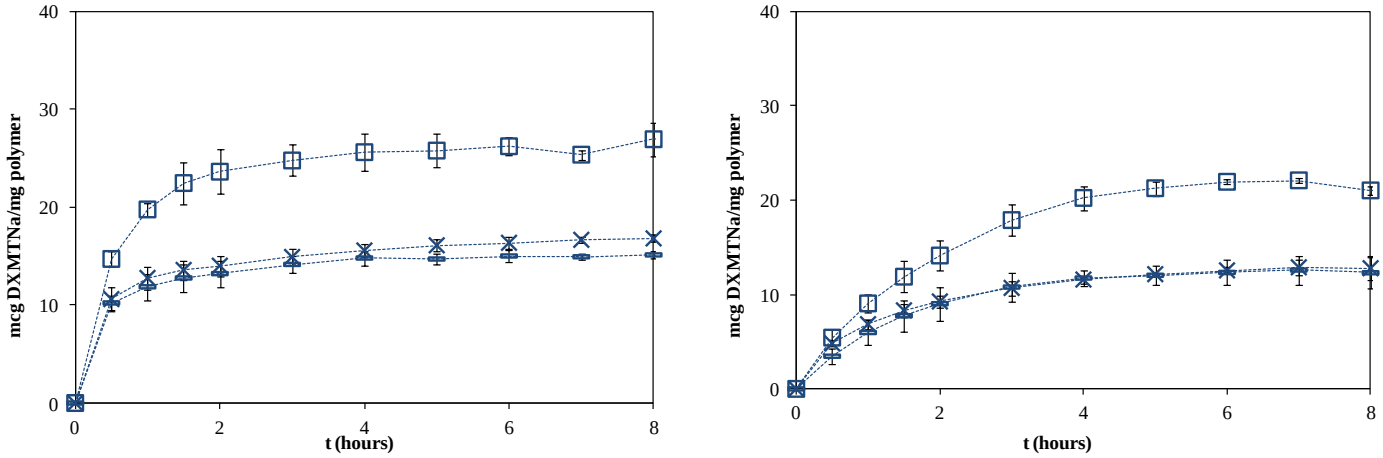

Figure 46. Release profiles of DXMTNa from CS/CBC composite films (□), CS/CBC composite films loaded with 75% [Ch][Cl] (—) and CS/CBC composite films loaded with 75% [Ch][DHP] (X), at pH 10 (on the left) and at pH 7 (on the right).

In general terms it can be said that the behavior observed at pH 10 is similar to that of CS however a slower release is observed at pH 7 and therefore CS/CBC films seem to be a good alternative to prevent an initial burst/overshooting of DXMTNa release at this conditions. That effect is more pronounced for non-loaded films since after 4 hours CS/CBC films doped with [Ch][Cl] or [Ch][DHP] the amount of DXMTNa released is constant. These systems also showed that a smaller amount of DXMTNa is released in relation to the total amount available for all the reasons previously discussed. Moreover in this case the interactions between DXMTNa and the polymer are again evident. In fact, non-loaded and [Ch][DHP] loaded composite films without drug experienced dissolution at pH 7. However when the drug is present, films maintain their physical structure for a longer period (at least 8h). This is confirmed also by the kinetic parameter *n* which corresponds to non-Fickian behavior meaning that swelling is not the only factor ruling drug release at these conditions (Table 11). A similar result was obtained by Labuschagne and co-authors that referred specific drug-polymer interactions between ibuprofen and PEG-PVP complexes (Labuschagne et al, 2011).

Finally and once again, the kinetic parameters may not be consistent with the diffusion coefficient (D_1). In fact the Eq. (9) and (10) may not be the ideal model to describe the short and long-time approximations for the diffusion-controlled release periods.

Table 11. Correlated release kinetic parameter (*n* and *k*) and diffusion coefficients (D_1) from Eqs. (8) and (9) for DXMTNa release from CS/CBC composite loaded and non-loaded films at pH 10 and pH 7 and 37ºC.

	Kinetic parameters			**Diffusion coefficients (cm^{-2} h^{-1})**	
	n	k/h^{-n}	R^2	D_1 ($x10^{-7}$)	R^2
pH 10					
CS/CBC	0.438	0.720	0.992	50.16	0.971
CS/CBC+[Ch][Cl]	0.217	0.780	0.972	6.52	0.965
CS/CBC+[Ch][DHP	0.207	0.767	0.967	5.96	0.946
pH 7					
CS/CBC	0.718	0.427	0.998	69.80	0.998
CS/CBC+[Ch][Cl]	0.742	0.471	0.997	35.23	0.999
CS/CBC+[Ch][DHP]	0.497	0.538	0.999	22.95	0.999

Conclusion

These work proved the potential of natural based polyelectrolyte films for biomedical purposes. Furthermore, the addition of biocompatible ionic liquids to those polyelectrolytes (CS and CBC polyzwitterions) showed to improve several properties of the films without resorting other non-environmentally or less biocompatible additives that would confer toxicity in physiological conditions.

Chitosan has been widely studied for several biomedical applications as films, foams or hydrogels and *N*-carboxybutylchitosan as already been mentioned in literature as a chitosan derivative with improved hydrophilicity and film forming ability, conferred by the alkyl chain and carboxylic groups. However, its thermal and mechanical properties, hydrophylicity, WVS, WVP, pH-dependant swelling behavior and capacitive behavior have never been studied. Furthermore, the effect of the addition of ILs to these biopolymers have been only reported for CS, although for different ILs, but not for its derivative, CBC. The ILs used in this work are different from the others already reported due to their enhanced hydrophilicity, biocompatibility and non-toxicity in biological systems. However further characterization is necessary to conclude about the overall biocompatibility of CS and CBC doped with [Ch][Cl] or [Ch][DHP].

Several conclusions were taken from the obtained results, and some of the most important include:

- The synthesis of CBC involves specific ratios of acid/CS/reducing agent that maximizes the substitution degree of CS to originate CBC and minimizes that for MPC (other possible CS derivative). FTIR and H-NMR are appropriate techniques to qualitative and quantitative monitor and confirm CS modification;

- It was confirmed by SEM that both non-loaded CS and CBC films present very similar and homogeneous morphological surfaces and cross sections. The addition of the IL seemed to induce some structural modifications only in the internal structure of films loaded with [Ch][DHP], maybe due to the higher number of interactions between this IL and the polymeric matrix. Further studies should be performed, including SEM-EDX analysis in order to conclude about the homogeneous distribution of the IL through the matrices;

- TGA curves showed that CBCn films have higher thermal stability than CS films. IL addition decreases the T_{deg} and that effect is more pronounced for CBCn loaded films with [Ch][Cl] when compared to [Ch][DHP]. DSC results confirmed that both ILs are highly hydrophilic and hygroscopic and, in general, the results indicate that their presence induces different water absorbing capacity and also different water-polymer interaction strengths. Some considerations were taken about the Tg values on these films and it was concluded that further studies should include dynamic mechanical analysis in order to confirm if the observed endothermic event is indeed related with a plasticization effect;

- Mechanical properties showed that the introduction of the alkyl chain with the COOH termination into the CS polymer matrix decreases the polymer chains stiffness. Moreover the presence of ILs leads to a significant decrease in the elastic modulus (*E*) of the IL loaded films. The lowest *E* values were registered for CS films loaded with [Ch][Cl], while in the case of CBCn films, [Ch][DHP] originate films that are more elastic and that do not experience rupture under the tested conditions;

- CBC films present higher water sorption capacity than CS films despite its relatively lower surface hydrophilicity. Both ILs increase the intrinsic hydrophilicity of both CS and CBC films, and that effect is more pronounced for CS films, while [Ch][DHP] decreases the ability of CBCn films to absorb water vapor molecules;

- The WVP of non-loaded films is higher for CBCn compared to CS. The IL anion seems to have different effects on this property and in the case of CBCn films, [Ch][DHP] induces a reticulation degree that enhances the WVP. It was also concluded that WVP is highly dependent on hydrophilicity and film's thickness.

- Impedance measurements showed that CS, CBCa and CBCn films naturally promote charge diffusion, since they are polyelectrolytes, and their capacitive character follow the sequence: CS > CBCa > CBCn. The addition of IL decreases the resistive behavior of these films, especially in case of [Ch][DHP];

- The water swelling behavior of the films is highly dependent on the pH value and composition of the external medium and swelling is a direct consequence of the osmotic pressure between the film network and the surrounding medium. At neutral pH films have a higher water swelling capacity than at basic pH as expected due to the higher number of electrostatic repulsions that exist at pH originated by the ionized amino and carboxylic groups of CS and CBC. The presence of the ILs leads to a decrease in the films swelling capacity because their presence increase the ionic strength inside the network. CBC films experience dissolution at neutral pH even when loaded with IL, but CBCn films loaded with 75% [Ch][Cl] still present a physical structure after 8 hours of immersion which may confirm reticulation of the structure due to the presence of the IL.

- DXMTNa release kinetics is highly affected by the swelling behavior according to the pH of the surrounding medium. The presence of the ILs lead to a lower drug released amount meaning that the studied ILs can work as biocompatible agents to tune the delivery of charged drugs. Sustained release profiles were obtained when using the CS/CBC composite (physical mixture) and they shoed to be more stable at neutral pH however further optimization of the CS/CBC ratio is needed to obtain more stable complexes;

During the development of this work, there were some difficulties that started with the synthesis of *N*-carboxybutylchitosan from CS since the relative amounts of levulinic acid and reducing agent had to be optimized in order to have the maximum and minimum substitution degree for *N*-carboxybutylchitosan and 5-methylpyrrolidione (cyclic derivate), respectively. It was also planned to study the effect of the ILs on the bending angle of the films promoted by an electrical field in order to see if they could be applied as electrochemical actuators for artificial muscles. This was not possible during this theses but it will be done in a near future, since the films were already sputter-coated with gold (in order to work as an electrode) and favor the ion diffusion, as shown in Figure 47.

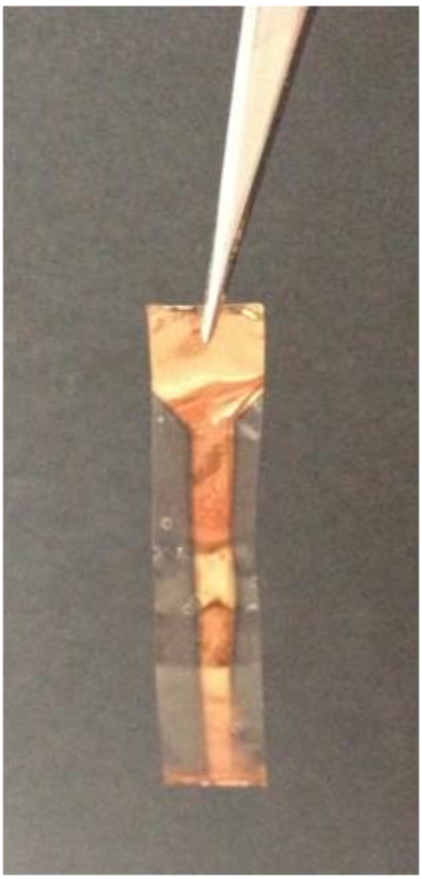

Figure 47. CS film sputter-coated with gold to study the bending angle of the films promoted by an electrical field.

References

Abbott A. P., Bell T. J., Handa S., Stoddart B. Cationic functionalisation of cellulose using a choline based ionic liquid Analogue. Green Chemistry 2006; 8: 784-786.

Alarcón C.H.A., Pennadam S., Alexander C. Chemical Society Reviews 2005; 34: 276-285.

Armand M., Endres F., MacFarlane D. R., Ohno H., Scrosati B. Ionic-liquid materials for the electrochemical challenges of the future. Nature Materials 2009; 8: 621-629.

Arora S., Lal S., Kumar S., Kumar M., Kumar M. Comparative degradation kinetic studies of three biopolymers: Chitin, chitosan and cellulose. Archives of Applied Science Research 2011; 3: 188-201.

Baskar D., Kumar T.S.S. Effect of deacetylation time on the preparation, properties and swelling behavior of chitosan films. Carbohydrate Polymers 2009; 78: 767-772.

Berger J., Reist M., Mayer J.M., Felt O., Gurny R. Structure and interactions in chitosan hydrogels formed by complexation or aggregation for biomedical applications. European Journal of Pharmaceutics and Biopharmaceutics 2004; 57: 35-52.

Bhattarai N., Gunn J., Zhang M. Chitosan-based hydrogels for controlled, localized drug delivery. Advanced Drug Delivery Reviews 2010; 62: 83-99.

Bhumkar D.R., Pokharkar V.B. Studies of Effect on pH on Cross-linking of Chitosan With Sodium Tripolyphosphate: A Technical Note. AAPS PharmSciTech 2006; 7: E1-E6.

Biagini G., Bertani A., Muzzarelli R., Damadei A., DiBenedetto G., Belligolli A., Riccotti G.. Wound management with *N*-carboxybutyl chitosan. Biomaterials 1991; 12: 281-286.

Cai K., Liu W., Li F., Yao K., Yang Z., Li X., Xie H. Modulation of osteoblast function using poly(D,L-lactic acid) surfaces modified with alkylation derivative of chitosan. of Biomaterials Science, Polymer Edition 2002; 13: 56-66.

Carreira A.S., Gonçalves F.A.M.M., Mendonça P.V., Gil M.H., Coelho J.F.J. Temperature and pH responsive polymers based on chitosan: Applications and new graft copolymerization strategies based on living radical polymerization. Carbohydrate Polymers 2010; 80: 618-630.

Caykara T., Alaslan A., Eroglu M.S., Güven O. Surface energetics of poly(*N*.vinyl-2-pyrrolidone)/chitosan blend films. Applied Surface Science 2006; 252: 7330-7435.

Cázares-Delgadillo J., Balaguer-Fernández C., Calatayud-Pascual A., Ganem-Rondero A., Quintanar-Guerrero D., López-Castellano A.C., Merino V., Kalia Y.N. Transdermal iontophoresis of dexamethasone sodium phosphate *in vitro* and *in vivo*: Effect of experimental parameters and skin type on drug stability and transport kinetics. European Journal of Pharmaceutics and Biopharmaceutics 2010; 75: 173-178.

Chang B. Y., Park S. M. Electrochemical Impedance Spectroschopiy. Annual Review of Analytical Chemistry 2010; 3: 207-229.

Chiang Z.C., Yu S.H., Chao A.C., Dong G.C. Preparation and characterization of dexamethasone-immobilized chitosan scaffolds. Journal of Bioscience and Bioengineering 2012; Article in Press.

Crespy D., Rossi R.M. Mini review: Temperature-responsive polymers with LCST in the physiological range and their applications in textiles. Polymer International 2007; 56: 1461-1468.

Dash M., Chiellini F., Ottenbrite R.M., Chiellini E.. Chitosan – a versatile semi-synthetic Mpolymer in biomedical applications. Progress in Polymer Science 2011; 36: 981-1014.

Dautzenberg H., Gao Y., Hahn M. Formation, structure, and temperature behavior of polyelectrolyte complexes between ionically modified thermosensitive polymers. Langmuir 2000; 16: 9070-81.

De Britto D., Assis O.B.G. A novel method for obtaining a quaternary salt of chitosan. Carbohydrate Polyemrs 2007; 69: 305-310.

Dias A. M. A., Braga M. E. M., Seabra I. J., Ferreira P., Gil M. H: de Sousa H. C. Development of natural-based wound dressings impregnated with bioactive compounds and using supercritical carbo dioxide. International Journal of Pharmaceutics 2011; 408: 9-19.

Dias A.M.A., Braga M.E.M., Seabra I.J., Ferreira P., Gil M.H., de Sousa H.C. Development of natural-based wound dressings impregnated with bioactive compounds and using supercritical carbon dioxide. International Journal of Pharmaceutics 2011; 408: 9-19.(2)

Dias A.M.A., Marceneiro S., Braga M.E.M. Coelho J.F.J., Ferreira A.G.M., Simões P.N., Veiga H.I.M., Tomé L. C., Marrucho I.M., Esperança J.M.S.S., Matias A. A., Duarte C.M.M., Rebelo L.P.N., de Sousa H. C. Acta Biomaterialia 2011; 8: 1366-1379.

Dias A.M.A., Seabra I.J., Braga M.M.E., Gil M.H., de Sousa H.C.. Supercritical solvent impregnation of natural bioactive compounds in *N*-carboxybutyl chitosan

membranes for the development of topical wound healing applications. Journal of Controlled Release 2010; 148: e21-e56.

Dobryinin A.V., Rubinstein M. Theory of Polyelectrolytes in solutions and at surfaces. Progress in Polymer Science 2005;30: 1049-1118.

Dong Y., Ruan Y., Wang H., Zhao H., Bi D. Studies on Glass Transition Temperature of Chitosan with Four Techniques. Journal of Applied Polymer Science 2004; 93: 1553-1558.

Dormidontova E.E. Role of Competitive PEO-Water and Water-Water Hydrogen Bonding in Aqueous Solution PEO Behavior. Macromolecules, 2002, 35, 987-1001.

dos Santos K.S.C.R., Silva H.S.R.C., Ferreira E.I., Bruns R.E.. 3^2 Factorial design and response surface analysis optimization of *N*-carboxybutylchitosan synthesis. Carbohydrate Polymers 2005; 59: 37-42.

Duttar P.K., Dutta J., Tripathi V.S. Chitin and chitosan: Chemistry, properties and applications. Journal of Scientific & Industrial Research 2004; 63: 20-31.

Egashira M., Okada S., Yamaki J., Yoshimoto N., Morita M. Effect of small cation addition on the conductivity of quaternary ammonium ionic liquids. Electrochimica Acta 2005; 50: 3708-3712.

Felber A.E., Dufrene M.H., Leroux J.C. pH-sensitive vesivles, polymeric micelles, and nanosphere prepared with polycarboxylates. Advanced Drug Delivery Reviews 2011; Article in Press.

Garneiro-da-Cunha M.G. Cerqueira M.A. Souza B.W.S. Carvalho S. Quintas M.A.C. Teixeira J.A. Vicente A.A. Physical and termal properties of a chitosan/alginate nanolayered PET films. Carbohydrate Polymers 2010; 82: 153-159.

Gil E.S., Hudson S.M. Stilumi-responsive polymers and their bioconjugates. Progress in Polymer Science 2004; 29: 1173-1222.

Guimard N.K., Gomez N., Schmidt C. E. Conducting polymers in biomedical engineering. Progress in Polymer Science 2007; 32: 876-921.

Haerens K., Matthijs E., Chmielarz A., Bruggen B.V. The use of ionic liquids based on choline chloride for metal deposition: A green alternative? Journal of Environmental Management 2009; 90: 3245-3252.

Hamman J.H. Chitosan Based Polyelectrolyte Complexes as Potential Carrier Materials in Drug Delivery Systems. Marine Drugs 2010; 8: 1305-1322.

Heras A.C., Pennadam S., Alexandre C. Stimuli responsive polymers for biomedical applications. Chemical Society review 2005; 34: 276-285.

Holzapfel B.M., Reichert J.C., Schantz J.T., Gbureck U., Rackwitz L., Nöth U., Jakob F., Rudert M., Groll J., Hutmacher D.W. How smart do biomaterials need to be? A translational science and clinical point of view. Drug Delivery Reviews 2012: Article in press.

Honarkar H., Barikani M. Applications of biopolymers I: chitosan. Monatsh Chem 2009; 140: 1403-1420.

Hossain M. A., Isıklan M., Pramanik A.,. Saeed M. A., Fronczek F. R. Anion Cluster: Assembly of Dihydrogen Phosphates for the Formation of a Cyclic Anion Octamer. Crystal Growth & Design 2012; 12: 567−571.

Izawa H., Kadokawa J. Preparation and characterizations of functional ionic liquid-gel and hydrogel materials of xanthan gum. Journal of Materials Chemistry 2010; 20: 5235-5241.

Izawa H., Kaneko Y., Kadokawa J. Unique gel of xanthan gum with ionic liquid and its conversion into high performance hydrogel. Journal of Materials Chemistry 2009; 19: 6969-6972.

Jayakumar R., Menon D., K Manzoor., Nair S.V., Tamura H.. Biomedical applications of chitin and chitosan based nanomaterials – A short review. Carbohydrate Polymers 2010; 82: 227-232.

Jia Y., Yue D., Jing Y., Yao Y., Sun J.. Structure and electrochemical behavior of ionic liquid analogue based on choline chloride and urea. Electrochimica Acta 2012: 65; 30-36.

Kean T., Thanou M.. Chitin and chitosan – sources, production and medical applications. Williams PA, Arshady R, editors. Desk reference of natural polymers,their sources, chemistry and applications. London: Kentus Books; 2009. pp. 327-361.

Kirchner B. Ionic Liquids. Clare B., Sirwardana A., MacFarlane D.R. Synthesis, Purification and Characterization of Ionic Liquids. Springer. Verlag Berlin Heidelberg. 2009. pp 1-40.

Kittur F.S., Kumar K.R., Tharanathan R.N. Functional packaging properties of chitosan films. Z Lebensm Unters Forsch A 1998; 206: 44-47.

Kittur F.S., Prashanth K.V., Sankar K.U., Tharanathan R.N. Characterization of chitin, chitosan and their carboxymethyl derivatives by differential scanning calorimetry. Carbohydrate Polymers 2002; 49: 185-193.

Koetz J., Kosmella S. Polyelectrolytes and Nanoparticles. Springer. Verlag Berlin Heidelberg.2007. pp 5.

Kost J., Langer R. Responsive polymeric delivery systems. Advanced Drug Delivery Reviews 2001; 46: 125-148.

Kubisa P. Ionic Liquids in the Synthesis and Modification of Polymers. Journal of Polymer Science Part A: Polymer Chemistry 2005; 43: 4676-4683.

Kuksal A., Tiwary A. K., Jain A. K., Jain S. Formulation and in vitro, in vivo evaluation of esxtended-release matrix tablet of zidovudine: influence of combination of hydrophilic and hydrophobic matrix formers. AAPS PharmSciTech 2006; 7: 1-9.

Kumar M.N.V.R. A review of chitin and chitosan applications. Reactive & Functional Polymers 2000; 46: 1-27.

Labuschagne P. W., Kazarian S. G., Sadiku R. E. Supercritical CO_2-assisted preparataion of ibuprofen-loaded PEG-PVP complexes. The Journal of Supercritical Fluids 2011; 57: 190-197.

Lazaridou A., Biliaderis C. G. Thermophysiacal properties of chitosan, chitosan-starch and chitosan-pullalan films near the glass transition. Carbohydrate Polymers 2002; 48: 179-190.

Lazaridou A., Biliaderis C. G. Thermophysiacal properties of chitosan, chitosan-starch and chitosan-pullalan films near the glass transition. Carbohydrate Polymers 2002; 48: 179-190.

Leceta I., Guerrero P., de la Caba K. Functional properties of chitosan-based films. Carbohydrate Polymers 2012; Article in Press.

Li J., Gong Y., Zhao N., Zhang X. Preparation of *N*-Butyl Chitosan and Study of Its Physicl and Biological properties. Journal of Applied Polymer Science 2005; 98: 1016-1024.

Li J., Ma W., Song L., Niu Z., Cai L., Zeng Q., Zhang X., Dong H., Zhao D., Zhou W., Xie S. Superfast-Response and Ultrahigh-Power-Density Electromechanical Actuators Based on Hierarchal Carbon Nanotube Electrodes and Chitosan. Nano Letters – American Chemical Society 2011; 11: 4636-4641.

Lin J., Liu Y., Zhang Q. M. Charge dynamics and bending actuation in Aquivion membrane swelled with ionic liquids. Polymer 2011; 52: 540-546.

Liu W., Sun S.J., Zhang X., De Yao K. Self-aggregation behavior of alkylated chitosan and its effect on the release of a hydrophobic drug. Journal of Biomaterials Science, Polymer Edition 2003; 14: 851-859

Liying G. Synthesis of Ionic Liquids, Solubility for Wood and Its Application for Graft Copolymer with Acrylamide. Ionic Liquids: Applications and Prespectives. InTech 2011 (livro).

Lu W., Fadeev A. G., Qi B., Smela E., Mattes B. R., Ding J., Spinks G. M., Mazurkiewicz J., Zhou D., Wallace G. G., MacFarlane D. R., Forsyth S. A., Forsyth M.Use of ionic liquids for pi-conjugated polymer electrochemical devices. Science 2002; 297: 983-987.

Lu X., Hu J., Yao X., Wang Z., Li J. Composite System Based on Chitosan and Room-Temperature Ionic Liquid: Direct Electrchemistry and Electrocatalysis of Hemoglobin. Biomacromolecules 2006; 7: 975-980.

Maheshi N.S., Jusko W.J. Stability of sodium phosphate dexamethasone in rat plasma. International Journal of Pharmaceuticals 2005; 301: 262-266.

Marsh K.N., Boxall J.A., Lichtenthaler R. Room temperature ionic liquids and their mixtures –a review. Fluid Phase Equilibria 2004; 219: 93-98.

Martínez J.M.L., Chattah A.K., Sánchez R.M.T., Buldain G.Y., Campo Dall'Orto V. Synthesis and characterization of novel polyampholyte and polyelectrolyte polymers containing imidazole, triazole or pyrazole. Polymer 2012; 53: 1288-1297.

Martínez-Camacho A.P., Cortez-Rocha M.O., Ezquerra-Brauer J.M., Graciano-Verdugo A.Z., Rodriguez-Félix F., Castilho-Ortega M.M., Yépiz-Gómez M.S., Plascencia-Jatomea M. Chitosan composite films: Thermal, structural, mechanical and antifungal properties. Carbohydrate Polymers 2010; 82: 305-315.

Martínez-Ruvalcaba A., Sánchez-Díaz J.C., Becerra F., Cruz-Barba L.E., González-Álvarez A. Swelling characaterization and drug delivery kinetics of polyacrylamide-co-itaconic acid/chitosan hydogels. eXPRESS Polymer Letters 2009; 3: 25-32.

Maugeri Z., de María P. D. Novel choline-chloride-based deep-eutectic-solvents with renewable hydrogen bond donors: levulinic acid and sugar-based polyols. RSC Advances 2012; 2: 421–425.

Mecerreyes D. Polymeric ionic liquids: Broadening the properties and applications of polyelectrolytes. Progress in Polymer science 2011: 36; 1629-1648.

Mourya V.K., Inamdar N.N. Chitosan-modifications and applications: Opportunities galore. Reactive & Functional Polymers 2008; 68: 1013-1051.

Murdan S. Electro-responsive drug-delivery from hydrogels. Journal of Controlled Release 2003; 92: 1-17.

Muzzarelli R., Weckx M., Filipini O., Lough C.. Characteristic Properties of *N*-Carboxybutyl Chitosan. Carbohydrate Polymers. 1989; 11: 307-320.

Narambuena C.F., Leiva E.P.M., Chávez-Páez M., Pérez E. Effect of chain stiffness on the morphology of polyelectrolyte complexes. A Monte Carlo simulation study. Polymer 2010; 51: 3293-3302.

Noble R.D., Gin D.L. Perspectives on ionic liquids on ionic liquids membranes. Journal of Membrane Science 2011; 369: 1-4.

Nockemann P., Thijs B., Driesen K., Janssen C. R., Hecke K. V., Meervelt L. V., Kossmann S., Kirchner B., Binnemans K. Choline Saccharinate and Choline Acesulfamate: Ionic Liquids with Low Toxicities. Journal of Physical Chemistry B 2007; 11: 5254-5263.

OECD SIDS- Screening information Data Set (SIDS) for High Production Volume Chemicals. IPCSIN CHEM. Germany 2004 in http://www.inchem.org/documents/sids/sids/67481.pdf on 27th of February 2012.

Oliver L., Meinders M. B. J. Dynamic water vapour sorption in gluten and starch films. Journal of Cereal Science 2011; 54: 409-412.

Orto V.C.D., Martínez J.M.L.,Chattah A.K., Sánchez R.M.T., Buldain G.Y. Synthesis and characterization of novel polyampholyte and polyelectrolyte polymers containing imidazole, triazole or pyrazole. Polymer 2012; 53: 1288-1297.

Park J. B., Bronzino J. D. Biomaterials: Principles and Applications. CRC PRESS. Boca Raton. 2003. pp: preface.

Pereda M., Aranguren M. I., Marcovich N. E., Water vapor absorption and permeability of films based on chitosan and sodium caseinate. Journal of Applied Polymer Science 2009; 111: 2777-2784.

Pereda M., Ponce A. G., Marcovich N. E., Ruseckaite R. A., Martucci J. F., Chitosan-gelatin composites and bi-layer films with potential antimicrobial activity. Food Hydrocolloids 2011; 25: 1372-1381.

Perez R.A., Won J.E., Knowles J.C., Kim H.W. Naturally and synthetic smart composite biomaterials for tissue regeneration. Advanced Drug Delivery Reviews 2012; In press.

Pernak J., Chwala P. Synthesis and ani-microbial activities of choline-like quaternary ammonium chlorides. European Journal of Medicinal Chemistry 2003; 38: 1035-1042.

Pernak J., Syguda A., Mirska I., Pernak A., Nawrot J., Pradzynska A., Griffin S. T., Rogers R. D. Choline-Derivative-Based Ionic Liquids. Chesmistry – A European Journal 2007; 13: 6817-6827.

Petkovic M., Ferguson J.L., Gunaratne H.Q.N., Ferreira R., Leitão M.C., Seddon K.R., Rebelo L.P.N. Pereira C.S. Novel biocompatible cholinium-bsed ionic liquids – toxicity and biodegradability. Green Chemistry 2010; 10: 643-649.

Philippova O.E., Khokhlov A.R. In: Osada Y., Khokhlov A.R., eds: Polymer Gels and Networks. Marcel Dekker Inc. New York 2002. pp 161-173. ISBN 0-203-90839-2.

Piérog M., Gierszewska-Drużyńska M., Ostrowska-Czubenko J. Effect of ionic crosslinking agents on swelling behavior of chitosan hydrogel membranes. Progress on Chemistry and Application of Chitin and Its derivatives 2009; 14: 75-82.

Pocius A. V. Adhesionand Adhesives Technoloy: An Introduction. Hanser 2nd edition. Munich 2002. Pp 17-19. ISBN 1-446-21731-2.

Pourjavadi A., Mahdavinia G.R. Superabsorbency, pH-Sensitivity and Swelling Kinetics of Partially Hydrolyzed Chitosan-g-poly(Acrylamide) Hydrogels. Turkish Journal of Chemistry 2006; 30: 595-608.

Prasad K., Kaneko Y., Kadokawa J. Novel Gelling of κ-,ι- and λ- Carregeenans and their composite gels with cellulose using Ionic Liquid. Macromolecular Biosceince 2009; 9: 376-382.

Prasad K., Mine S., Kaneko Y., Kadokawa J. Preparation of cellulose-based ionic porous material compatibilized with polymeric ionic liquid. Polymer Bulletin 2010; 64: 341-349.

Radeva T. Physical Chemistry of Polyelectrolytes. Vol.99. Dautzenberg H. Polyelectrolyte Complexa Formation in Highly Aggregating Systems: Methodical Aspects and General Tendencies. Marcel Dekker. New York. 2001. pp 743.

Rana U. A., Bayley P. M., Vijayaraghavan R., Howlett P., MacFarlane D. R., Forsyth M. Proton transport in choline dihydrogen phosphate/H3PO4 mixtures. Chemical Physics 2010; 12: 11291-11298.

Reis R.L., Mano J.F., Silva G.A., Azevedo H.S., Malafaya P.B., Sousa R.A., Silva S.S., Boesel L.F., Oliveira J.M., Santos T.C., Marques A.P., Neves N.M. Natural origin biodegradable systems in tissue engineering and regenerative medicine: present status and some moving trends. J.R.Soc.Interface 2007; 4: 999-1030.

Rinaudo M., Desbrières J., Dung P.L., Binh P.T., Dong N.T. NMR investigation of chitosan derivatives formed by the reaction of chitosan with levulinic acid. Carbohydrate Polymers 2001; 46: 339-348.

Rinaudo M. Chitin and chitosan: Properties and applications. Progress in Polymer Science 2006; 31: 603-632.

Rooney D., Jacquemin J., Gardas R. Thermophysical Properties of Ionic Liquids. Top Curr. Chem. 2009; 290: 185-212. Springer-Verlag Berlin Heidelberg 2009.

Roy D., Cambre J.N., Sumerlin B.S. Future perspectives and recent advances in stimuli-responsive materials. Progress in Polymer Science 2010; 35: 278-301.

Rueda D.R., Secall T., Bayer R. K. Differences in the interaction of water with starch and chitosan films as revealed by infrared spectroscopy and differential scanning calorimetry. Carbohydrate Polymer 1999; 40: 49-56.

Sahu A.K., Pitchumani S., Srighar P., Shukla A.K. Nafion and modified-Nafion membranes for polymer electrolyte fuel cells: An overview. Bulletin of Material Science 2009; 21: 285-294.

Saville P. Polypyrrole: formation and use. Defense Research and Development Canada – Atlantic 2005.

Schwartz M. Smart Materials.1st edition. USA. CRC Press Boca Raton, 2008. pp 222-226. ISBN 978-1-4200-4372-3.

Schwenzer B., Kim S., Vijayakumar M., Yang Z., Liu J. Correlation of structural differences between Nafion/polyaniline and Nafion/polypyrrole composite membranes and observed transport properties. Journal of Membrande Science 2011; 372: 11-19.

Scrantom A. B., Rangarajan B., Klier J. Biomedical applications of Polyelectrolytes. Advances in Polymer Science 1995; 122: 1-54.

Sebastião V., Canevarolo J. Técnicas de Caracterização de Polímeros. ArtLiber Editora 2004. pp 209-360. ISBN 85-88098-19-9.

Shakya A.K., Sami H., Srivastava A., Kumar A. Stability of responsive polymer-protein bioconjugates. Progress in Polymer Science 2010; 35: 459-486.

Shanta K.L., Harding D.R.K. Synthesis and characterization of chemically modified chitosan microspheres. Carbohydrate Polymers 2002; 48: 247-253.

Shen Y., Zhang Y., Zhang Q., Niu L., You T., Ivaska A. Immobilization of ionic liquid with polyelectrolyte as carrier. Chemistry Communications 2005; 4193-4195.

Siepmann J., Peppas N. A. Modeling of drug release from delivery systems based on hydroxypropyl methylcellulose (HPMC). Advanced Drug Delivery Reviews 2001; 48: 139-157.

Sigma-Aldrich. AldrichimicaActa 2004; 37.

Silva C.L., Pereira J.C. Ramalho A., Pais A.A.C.C., Sousa J.J.S. Films based on chitosan polyelectrolyte complexes for skin drug delivery: Development and characterization. Journal of Membrane Science 2008; 320: 268-279.

Silva S.S., Duarte A.R.C., Carvalho A.P., Mano J.F., Reis R.L.. Green processing of porous chitin structures for biomedical applications combining ionic liquids and supercritical fluid technology. Acta Biomaterialia 2011; 7: 1166-1172.

Singh P. K., Bhattacharya B., Nagarale R.K., Kim K., Rhee H. Synthesis, characterization and application of biopolymer-ionic liquid composite membranes. Synthetic Metals 2010; 160: 139-142.

Sionkowska A. Current research on the blends of natural and synthetic polymers as new biomaterials: Review. Progress in Polymer Science 2011; 36: 1254-1276.

Slade S., Campbell S. A., Ralph T. R., Walsh F. C. Ionic Conductivity of an Extruded Nafion 1100 EW Series of Membranes. Journal of The Electrochemical Society 2001; 149: A1556-A1564 .

Spinks G.M., Lee C.H., Wallace G.G., Kim S.I., Kim S.J. Swelling behavior of Chitosan Hydrogels in Ionic Liquid-Water Binary Systems. Langmuir 2006; 22: 9375-9379.

Stuart M.A., Huck W.T.S., Genzer J., Müller M., Ober C., Stamm M., Sukhorukov G.B., Szleifer I., Tsukruk V.V., Urban M., Winnik F., Zauscher S., Luzinov I., Minko S. Emerging applications of stimuli-responsive polymer materials. Nature Materials 2010; 9: 101-113.

Suvakanta D., Murthy P. N., Nath L., Chowdhury P. Kinetic modelling on drug release from controlled drug delivery systems. Acta Poloniae Pharmaceutica – Drug Research 2010; 67: 217-223.

Suyatma N.E., Tighzert L., Copinet A. Effects of Hydrophilic Plasticizers on Mechanical, Thermal and Surface Properties of Chitosan films. Journal of Agricultural and Food Chemistry 2005; 53: 3950-3957.

Tiwary A.K., Rana V. Cross-linked chitosan films: effect on cross-linking density and swelling parameters. Journal of Pharmaceutical Sciences 2010; 23: 443-448.

Tokarev I., Motornov M., Minko S. Molecular-engineered stimuli-responsive thin polymer film: a platform for the development of integrated multifunctional intelligent materials. Journal of Materials Chemistry 2009; 19: 6932-6948.

Vijayaraghavan R., Thompson B. C., MacFarlane D. R., Kumar R., Surianarayanan M., Aishwarya S., Sehgal P. K. Biocompatibility of choline salts as crosslinking agents for collagen based biomaterials. Chemical Communications 2010; 46: 294-296.

Wan Y., Creber K.A.M., Peppley B., Bui V.T. Synthesis, characterization and ionic conductive properties of Phosphorylated Chitosan membranes. Macromolecular Chemistry and Physics 2003; 204: 850-858.

Wandera S., Wickramasinghe S.R., Husson S.M. Stimuli-responsive membranes. Journal of Membrane Science 2010; 357: 6-35.

Waniphapichart P., Sungkum R., Taweepreda W., Nisoa M. Characteristics of chitosan membranes modified by argon plasmas. Surface & Coatings Technology 2009; 203: 2531-2535.

Xiong Y., Wang H., Wu C., Wang R. Preparation and characterization of conductive chitosan-ionic liquid composite membranes. Polymer Advanced Technologies 2011.

Yamagata M., Soeda K., Ikebe S., Yamazaki S., Ishikawa M. Chitosan-based gel electrolyte containing na ionic liquid for high-performance nanoqueous supercapacitors. Electrochimica Acta 2012; Article in Press.

Yin Y., Lv X., Tu H., Xu S. Zheng H. Preparation and swelling kinetics of pH-sensitive photocrosslinked hydrogel based on carboxymethyl chitosan. Journal of Polymer Research 2010; 17: 471-479.

Yoshizawa-Fujita M., Fujita K., Forsyth M., MacFarlane D. R. A new class of proton-conducting ionic plastic crystals based on organic cations and dihydrogen phosphate. Electrochemistry Communications 2007; 9: 1202–1205.

Zuleger S., Lippold B. C. Polymer particle erosion controlling drug release. I. Factors influencing drug release and characterization of the release mechanism. International Journal of Pharmaceutics 2001; 217: 139-152.

Appendix

Appendix A: Determination of IL molar fraction to be added to CS and CBC films.

In order to determine the exact number of NH_2, NH_3^+ and $COCH_3$ (from chitin) groups, the real degree of acetylation (DA) was calculated for chitosan of medium molecular weight (Sigma Aldrich, Portugal) by elemental analysis (data not shown). The DA of CS was 27%, which means that 73% of acetyl groups from chitin were deacetylated into NH_2 groups (DD =73%).

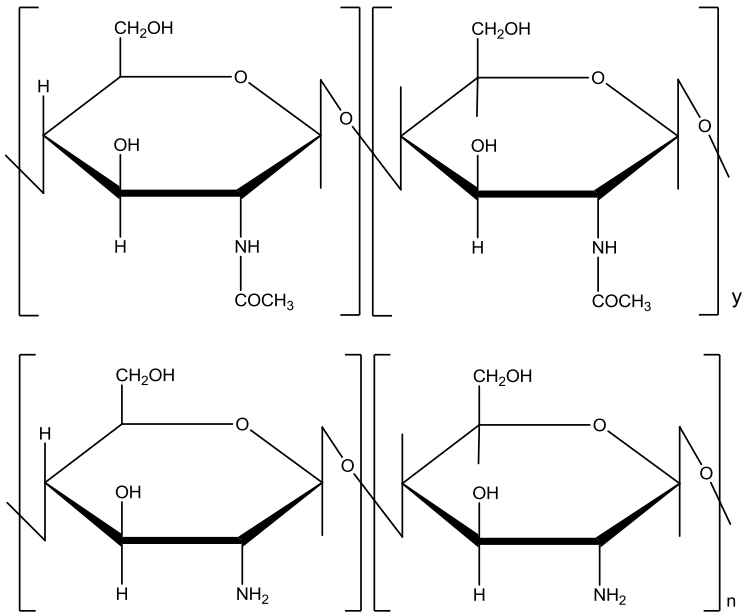

Monomers comprehended on CS's molecular structure: acetylated groups from chitin (y) and deacetylated groups (n).

This information permitted the calculation of the weight average molecular weight (M_w) of CS and consequently the number of moles of each referred groups.

$$M_n = (6 \times 12) + (4 \times 32) + 11 + 14 = 225\ g/mol$$

$$M_y = (8 \times 12) + (5 \times 32) + 13 + 14 = 283\ g/mol$$

$$\boldsymbol{Mw = (0,73\ x\ 225) + (0,27\ x\ 283) = 240,7\ g/mol}$$

$$\boldsymbol{\bar{M}\ (CS) = 145\ 000\ g/mol}$$

The number of monomer repetitions in 1 mole of CS is obtained by dividing its MW by the weight average molecular weight (M_w):

$$\frac{145000}{240,7} = 602,5\ monomers\ repetitions$$

Since the DD is 73%, it is possible to determinate the total amount of NH_2/NH_3^+ groups per 1 mole of CS.

$$602,5 \times 0,73 = 439,8\ NH_2/NH_3^+\ \ groups$$

The concentration of the prepared CS solution was 1% m/v. In this way the total number of moles of NH_2/NH_3^+ groups per gram of CS (DD=73%) is given by the following relationship:

$$n_{NH_2/NH_3^+} = \frac{1_{g\ CS}}{M_{w\ CS}} \times 73\%$$

$$\frac{1}{240,7} \times 0,73 = 3,03 \times 10^{-3}\ mol = 0,00303\ mmol\ of\ NH_2/NH_3^+\ groups$$

This value was used to calculate the amount of IL loaded into CS and CBC films. It was assumed that [Ch][Cl] or [Ch][DHP] would interact with polymeric chains by hydrogen bonding or ionic interactions, depending on the polymer and on its charges depending on the external conditions. The amount of IL loaded (in molar terms) was defined as 0, 25, 50 and 75% of the number of NH_2/NH_3^+ groups in the polymer.

Appendix B: Permeability measurements: water loss (g) vs. time (h).

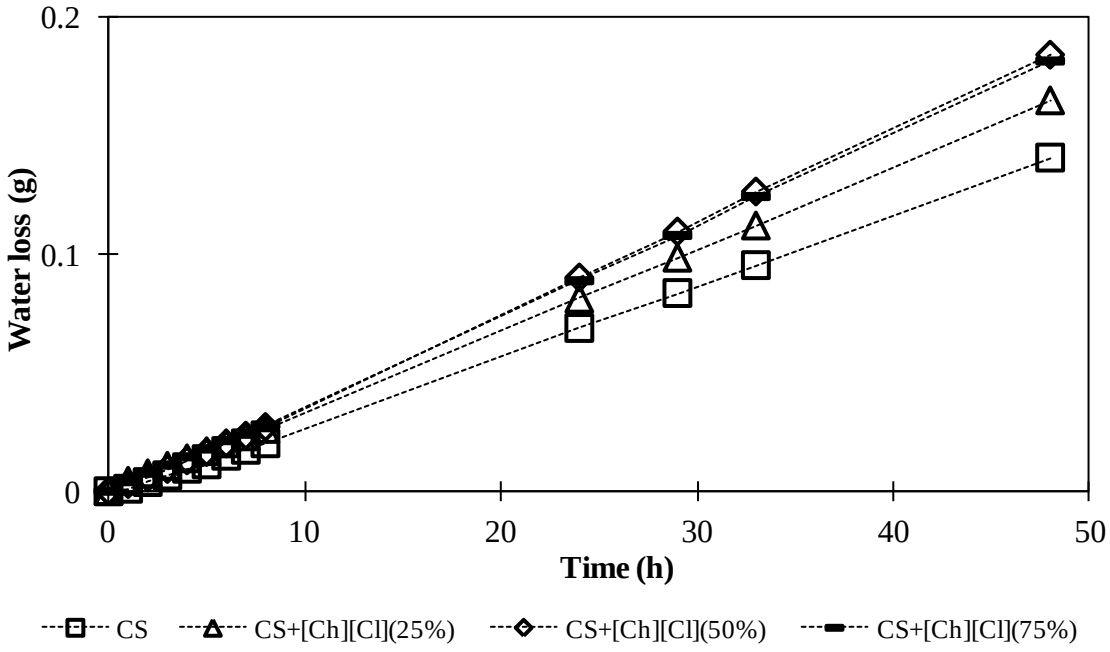

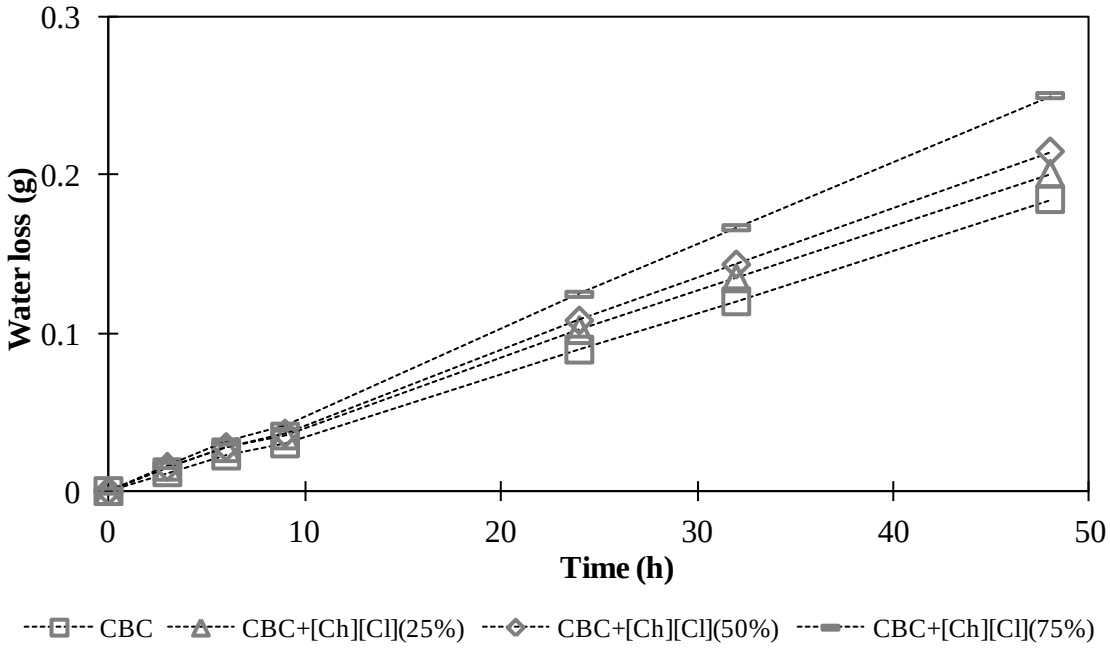

Appendix C: FTIR-ATR pos-swelling.

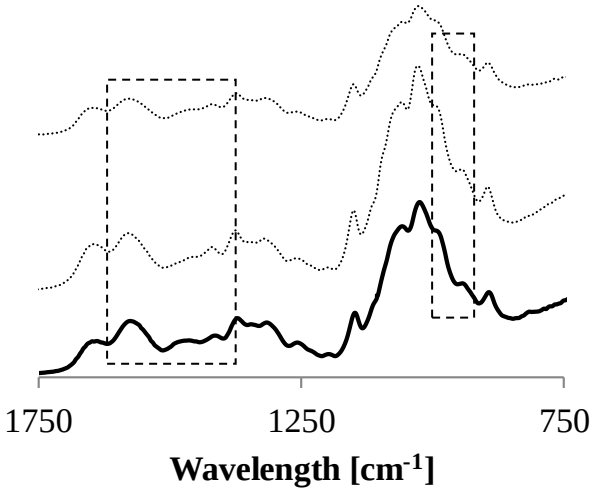

FTIR-ATR spectra of the CS obtained films loaded (darker lines) and non-loaded with choline chloride ([Ch][Cl]) (in the middle) and choline dihydrogen phosphate ([Ch][DHP]) (on top).

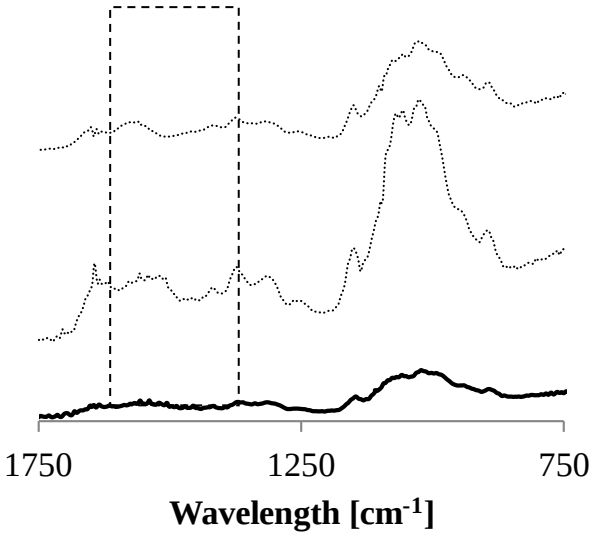

FTIR-ATR spectra of the CBC obtained films loaded (darker lines) and non-loaded with choline chloride ([Ch][Cl]) (in the middle) and choline dihydrogen phosphate ([Ch][DHP]) (on top).